Theses and Dissertations

December 2019

# Quantifying the Variability in Heavy Metal Concentrations in Produce Grown in Metals-Rich Soil

Harris Lowell Byers
*University of Wisconsin-Milwaukee*

Follow this and additional works at: https://dc.uwm.edu/etd

Part of the Agronomy and Crop Sciences Commons, Geochemistry Commons, and the Toxicology Commons

QUANTIFYING THE VARIABILITY IN HEAVY METAL CONCENTRATIONS IN

PRODUCE GROWN IN METALS-RICH SOIL


by

Harris Byers


A Dissertation Submitted in

Partial Fulfillment of the

Requirements for the Degree of


Doctor of Philosophy

in Geosciences


at

The University of Wisconsin-Milwaukee

December 2019

ABSTRACT

QUANTIFYING THE VARIABILITY IN HEAVY METAL CONCENTRATIONS IN
PRODUCE GROWN IN METALS-RICH SOIL

by

Harris Byers

The University of Wisconsin-Milwaukee, 2019
Under the Supervision of Professor Tim Grundl


Childhood Pb exposure is associated with a multitude of poor health outcomes. In food-insecure

areas, growing fresh produce in residential backyard gardens is one option for parents; however,

commonly grown crops are known to accumulate Pb in consumable tissues when grown in

metals-rich soils. A variety of produce representing a continuum of consumable tissues were

grown in soils collected from two residential vegetable gardens, a former metal foundry, and

commercial topsoil purchased from a local hardware store. The concentrations of heavy metals in

crop tissues were measured with custom wavelength dispersive X-ray Fluorescence (WD-XRF)

spectroscopy and portable energy dispersive X-ray Fluorescence (ED-XRF) spectroscopy

quantification routines. A general linear model was used to evaluate the factors contributing to

the accumulation of Pb in tissues as a surrogate evaluation of common best management

practices in urban agriculture. An exposure risk evaluation was completed based on the

concentration of Pb in consumable tissues to determine if consuming produce increased a child's

risk for Pb exposure. Due to the heterogeneous and anisotropic nature of urban soil, this work

demonstrates the difficulty of predicting Pb accumulation in crops based on Pb in the soil. It is

therefore recommended that direct monitoring of Pb in produce be used for a more accurate

prediction of child exposure to ingested Pb. Through direct measurements, the accumulation of

Pb in consumable tissues was the greatest in vegetables with a modified taproot (turnip, beetroot,

radish, carrot), with lesser concentrations in fruits (tomato, pepper), and produce grown on modified stems (potato). The accumulation of Pb varied between three cultivars of carrots of varying pigments; however, accumulation of Pb in beetroot did not vary between pigmented cultivars. Although several urban agriculture best management practices were confirmed in this study, children are at a potential increased risk for Pb exposure through consumption of produce grown in metals-rich residential soils.

To

my parents,

my wife,

and especially my boys

# TABLE OF CONTENTS

# LIST OF FIGURES

# LIST OF TABLES

# ACKNOWLEDGEMENTS

I must thank my advisor, Dr. Tim Grundl, for his patience and guidance in this project. He has challenged me to think more critically about scientific data and the value in rigorous evaluation of spectroscopy data. My committee (Drs. Lindsay McHenry, Shangping Xu, and Erik Gulbranson) has been critical in helping me design and implement this project. A special thanks to Dr. Lindsay McHenry for allowing me to use the X-ray lab during this project and for her willingness to allow me to use her instrumentation to analyze a matrix far afield from geologic sciences.

I am grateful to the community-based organizations who have helped me during this project by identifying residential vegetable gardens and coordinating soil and vegetable collections in their neighborhoods. This project would not have been possible without their assistance in recruiting residential property owners willing to donate their soil to this project.

I would like to thank Mr. Paul Engevold, the manager of the University of Wisconsin Milwaukee Department of Biological Science Greenhouse, for his assistance in growing vegetables in this study. I would like to thank Dr. Razia Azen and Dr. Rebecca Klaper for providing significant comments and suggestions throughout this Dissertation and to Dr. Erica Young for her guidance on plant physiology in Chapter 4 of this Dissertation. Although they are anonymous, I would like to thank the peer reviewers of Chapter 2 and Chapter 3 in their respective journals for their assistance in strengthening the manuscripts.

This work was supported in part by the Children's Health Environmental Core Center at the University of Wisconsin Milwaukee, which is funded through the National Institute of Environmental Health Sciences [grant number P30ES004184]. I specifically would like to

acknowledge the assistance from Dr. Jeanne Hewitt and Dr. David Petering for their coordination, support, and encouragement during this work.

I would like to thank my previous employer (Symbiont Science, Engineering and Construction, Inc.) and my current employer (Stantec Consulting Services Inc.) for their tuition assistance programs.

As a self-funded graduate student, I must thank my immediate family for their financial support and unending patience during this project. Completing this study would not have been possible without the support and nurturing of my wife, Dr. Rebecca Klaper. I am so blessed to have such a loving partner in life. You have supported, comforted, and encouraged me through this journey and have shared my hopes, thoughts, and dreams and I am grateful for our future together. I am grateful for the joyous energy of our boys Jacob and Benjamin, who were the inspiration of this project. Special thanks to my parents James and Nancy Byers for their encouragement during this journey and their lifelong dedication to supporting education. I can never repay your sacrifices working for decades in a cold warehouse to make sure I didn't have to.

This work is dedicated to all parents who strive every day to make difficult decisions in raising healthy children. I hope this work contributes to the ongoing efforts of researchers, regulators, health professionals, community-based organizations, parents, and others in reducing Pb exposure in our children.

# 1.0    INTRODUCTION

## 1.1    BACKGROUND AND PROJECT OBJECTIVES

Exposure to toxic heavy metals (e.g. Pb, As, Hg) or excess exposure to heavy metals needed in only trace amounts (e.g. Cu, Fe, Zn, Cr, and Mn) by the human body can result in metals poisoning. Because of their relatively low body mass, childhood heavy metal exposures are of particular concern. Although much remains unknown about long-term health outcomes from child exposure to many heavy metals, cognitive impairments associated with elevated blood lead levels (blood Pb concentration >10 $\mu$g dL$^{-1}$) in children are well documented, and emerging evidence suggests that long-term impacts from chronic low-level Pb exposure (blood Pb concentration $\leq$ 1$\mu$g dL$^{-1}$) are possible, leading to a multitude of poor health outcomes (Keller et al., 2017; Lane et al., 2008; Schnur & John, 2014). As child exposure to Pb remains a topic of great concern in environmental justice communities, further evaluation of potential Pb exposure through consumption of produce grown in urban soils is warranted.

Two identified sources of child ingestion of Pb are direct contact with lead-based paint and direct contact with metals-rich soil. Accepted intervention strategies inside the home to mitigate Pb exposure include removal or encapsulation of weathered Pb paint in combination with good housekeeping/cleaning procedures. Managing the risk of exposure to metals-rich soil is a near-impossible challenge because of the omnipresence Pb in urban soils from a multitude of possible sources [e.g. weathered paint (Clark et al., 2006 and 2008; Hall & Tinklenberg, 2003; Laidlaw et al., 2018); transportation/ lead-gasoline (Clark et al., 2006); compost (Murray et al., 2011a), leaching from infrastructure (Tom et al., 2014), anthropogenic industrial fill/spills (Afolayan, 2018; Clark et al., 2008), herbicides (Yokel & Delistraty, 2003), and mobilization/air

re-deposition of Pb-impacted soil/colloids from any of the abovementioned sources (Clark et al., 2008)].

As the popularity of urban agriculture grows in food-insecure areas, the potential exposure of children to metals-rich soil increases. Although child Pb exposure from direct contact with Pb-rich soil is considered to be the primary lead exposure pathway in urban agriculture, secondary exposure from chronic consumption of produce containing Pb could be a significant contributing factor (Chopra & Pathak, 2015; Ferri et al., 2015; Jolly et al., 2013), especially in high-risk populations, such as low-income, immigrant communities where exposure to Pb remains disproportionately high. However, there is very limited understanding on which crops common in urban agriculture have a propensity to uptake, transport, and accumulate Pb into consumable tissues.

The lack of understanding of plant uptake/accumulation of heavy metals is due to limited quantification methods, which are inconsistent between existing urban agriculture studies and often use complicated extraction and measurement procedures. As noted by many in the literature (e.g. Gallardo et al., 2016), X-Ray Fluorescence spectroscopy (XRF) is a promising technique in quantification of Pb and other heavy metals in produce tissues. Although prior reviews of this technology have identified several limiting factors (Marguí et al., 2009; Palmer et al., 2009; Singh et al., 2017), recent technological advancements in wavelength dispersive X-ray Fluorescence (WD-XRF) spectroscopy and portable energy dispersive X-ray Fluorescence (ED-XRF) spectroscopy suggest these quantification methods can be used to quantify Pb in foods down to single-digit $\mu g \ g^{-1}$ range. The use of XRF in urban agriculture remains limited because of the absence of commercially available reference materials, lack of standardization of sample

2

processing/handling/quantification methods, and misunderstanding of how matrix effects influence XRF measurements in a carbon matrix.

The overall objective of this project is to determine the variability in Pb concentrations in produce either grown in urban soils or purchased from a commercial source. Specifically, this project seeks to identify common crops with the propensity to uptake and transport Pb to consumable tissues and determine if gross plant physiology plays a role in Pb accumulation. Secondly, this project seeks to identify which commercially available produce and prepared foods could pose the greatest risk to Pb exposure. The overall project has four objectives centered around two hypotheses.

**Hypothesis 1. XRF methods can be developed to quantify heavy metals in soils and plants at limits of detection relevant to health-based regulatory limits.**

**Hypotheses 2. Heavy metal concentrations in produce will be the greatest in plants grown in soils with the greatest bio-available metal concentrations. Heavy metal concentrations will be greatest in modified taproots, decreasing in aboveground tissue groups. In addition, heavy metal concentrations will be greater in tissues rich in anthocyanin and carotenoids.**

**Objective 1: Develop procedures for handling and preparing soil for quantification of heavy metals with WD-XRF. Complete an inter-lab comparison of element concentrations using WD-XRF and ICP-MS to further characterize five commercial soil reference materials (SRMs) and develop custom measurement and calibration routines for quantification of heavy metals in prepared soil samples with WD-XRF using the target SRMs.** By adapting well established methods for preparation of rock samples (McHenry, 2009; McHenry et al., 2011), this project will develop methods for preparing competent soil samples

appropriate for WD-XRF quantification; use WD-XRF and ICP-MS to more fully characterize the target SRMs; and use the SRMs to develop custom calibration routines spanning the range of anticipated concentrations of heavy metals in soil.

**Objective 2: Standardize and develop procedures for produce tissue collection, handling, and preparation of homogeneous dried and non-dried samples for quantification of heavy metals with WD-XRF and ED-XRF. Develop reference materials suitable for use in developing custom calibration routines for quantification of heavy metals in prepared dried and non-dried plant samples with WD-XRF and ED-XRF.** This project will include pressing dried/powdered plant samples into competent pellets, which will be resilient to handling, infinitely thick with respect to the Cr Kα1 wavelength, and able to be analyzed by WD-XRF under vacuum without breakage. Homogenized non-dried samples can be analyzed with ED-XRF without leakage and will be infinitely thick with respect to the Pb Lβ1 wavelength. Calibration routines will be developed for WD-XRF and ED-XRF to quantify heavy metals in plant tissues in the single-digit μg g$^{-1}$ range.

**Objective 3: Quantify heavy metal concentrations in produce grown in metals-rich soil obtained from private properties in and near the City of Milwaukee.** Soil sources will include two vegetable gardens located at residential properties and an industrial property undergoing cleanup. The control soil will be commercial topsoil obtained from a local big-box commercial retailer. Crops to be grown in this study include cultivars of turnip (*Brassica rapa*), rutabaga (*Brassica napobrassica*), radish (*Raphanus sativus L.*), mustard (*Brassica juncea*), collards (*Brassica olerace*), tomato (*Solanum lycopersicum*), pepper (*Capsicum annuum*), okra (*Abelmoschus esculentus*), beetroot (*Beta vulgaris*), carrot (*Daucus carota sativus*), and potato

(*Solanum tuberosum*). A risk evaluation will be completed to determine if consumption of produce increases the risk for metals exposure in children.

**Objective 4: Quantify heavy metal concentrations in produce purchased from local commercial outlets.** This project will use XRF procedures developed in Objective 2 to quantify the concentrations of heavy metals in domestically-grown crops matching those in Objective 3 purchased from common grocery stores and in internationally-sourced foodstuffs purchased from grocery stores located near the neighborhoods where soil was collected during Objective 2. The concentrations of heavy metals in domestically-grown produce is expected to be less than the XRF method detection limit, and conversely, the concentrations of heavy metals in internationally-sourced foodstuffs is expected to be greater than the method detection limit.

## 1.2    EXPECTED SIGNIFICANCE OF THIS WORK

Prior urban agriculture studies have identified the potential risk from consumption of produce grown in metals rich soil. Although useful, this prior work has not included an in-depth evaluation of quantification methods and has not included an evaluation of crops grown in urban residential garden soils. This project bridges these gaps by leveraging a broad range of academic expertise, including urban geochemistry, XRF, and agronomy.

This project will determine if consumption of produce either grown in metals-rich soil or purchased from a commercial outlet contributes to the metals-burden of children. This project will ascertain if the risk posed by urban agriculture extends beyond direct contact with metals-rich soil. The results will be of particular importance to ongoing work by multiple federal/state/local agencies and community groups working to reduce the incidence of Pb poisoning in children and will be of particular importance to low-income minority communities already at high risk for Pb exposure where urban agriculture is prevalent. Because there is little

understanding about which crop types commonly grown in urban gardens have the greatest propensity to accumulate Pb and other heavy metals in consumable tissues, this work will add to the decision-making process for selecting crops most suitable for urban cultivation as a best practice to limit Pb exposure from produce consumption. Additionally, the influence of gross plant physiology (i.e. tissue groups, stress responses) on Pb transport is not well understood; therefore, this work seeks to identify differences in basic physiological constraints on Pb transport.

A second and equally novel goal of this project is to develop standardized methods for sample preparation and heavy metals quantification in crops with WD-XRF and ED-XRF. Prior urban agriculture studies have failed to achieve this goal because XRF quantification is too often treated as a "black box" and studies are blindly conducted without a rigorous understanding of X-ray physics or without deliberately controlling for matrix effects. This study will develop methods that can be directly used in food security studies for quantifying heavy metals in foods. Food security threats are often identified in retrospective studies limited to select food groups, select manufacturers/country of origin, and/or elements. However, with multiple new threats to food security identified each year, use of WD-XRF and portable ED-XRF spectrometry is a promising technique that could be used by regulators, researchers, and/or growers/manufacturers to identify security risks and prevent introduction of metals-rich produce into the commercial US food supply.

## 1.3    RELATIONSHIP OF THIS WORK TO PRESENT STATE OF KNOWLEDGE IN THE FIELD

### 1.3.1    Objective 1: Develop Routines for Quantification of Heavy Metals in Soil with XRF

Numerous geoscience/urban geochemistry investigations have used commercially available soil reference materials (SRM) available from the National Institute of Standards and Technology (NIST) as calibration reference materials or as quality control materials (Fernández et al., 2014; Kenna et al., 2011; McComb et al., 2014; Murray et al., 2011a; Sutton et al., 2012; Weindorf et al., 2012). NIST defines and provides Certified, Reference, and Information Values for element concentrations presented in SRM Certificates of Analysis. NIST certified values represent concentrations measured with the smallest measurement uncertainty and where sources of bias have been accounted for by NIST (May et al., 2000). Concentrations provided by NIST with larger measurement uncertainty are defined by NIST as reference values. Reported concentrations where uncertainty has not been evaluated are referred to by NIST as information values (May et al., 2000). Reference values or information values reported directly or as part of quality control for soil SRMs 2709, 2710, and 2711 have been provided previously by numerous investigators using XRF, ICP-MS, or ICP-OES. However, these three soil SRMs are no longer commercially available from NIST and have been replaced with SRM 2709a, SRM 2710a, and SRM 2711a, and along with SRM 2586 and SRM 2587, these five SRMs represent a continuum of heavy metal concentrations and are therefore considered representative of soils likely to be encountered in urban agriculture/urban geochemistry studies. However, characterization of these five soil SRMs remains sparse as very few reference values are available in the literature for the five available soil SRMs (Alvarez-Toral et al., 2013; Claverie et al., 2013; Eriksson et al., 2013; Fernández et al., 2014; Goix et al., 2011; Hoang et al., 2010; Milliard et al., 2011; Moon et al.,

2009; Paul et al., 2009). As the accuracy of XRF calibration routines is dependent on using fully characterized reference materials, the usefulness of these five SRMs in developing calibration routines for soil remains very limited until the SRMs are more fully characterized.

## 1.3.2    Objective 2: Develop Routines for Quantification of Heavy Metals in Produce with XRF

Because of the non-destructive nature of the analysis, XRF is emerging as a promising method for rapid quantification of heavy metals in produce. Recent work demonstrates that Pb and other heavy metals are taken up and translocated from the soil into consumable crop tissues (Clark et al., 2006; Ferri et al., 2015; Finster et al., 2004; Jolly et al., 2013; Lima et al., 2009; Nabulo et al., 2011; Rodriguez-Iruretagoiena et al., 2015; Sekara et al., 2005). Although human exposure and the resulting health impacts from direct contact with Pb-contaminated soil is considered to be the primary lead exposure pathway in urban agriculture, secondary exposure from chronic consumption of produce containing Pb could be a significant contributing factor (Chopra & Pathak, 2015; Ferri et al., 2015; Jolly et al., 2013), especially in high-risk populations, such as low-income, immigrant communities where exposure to Pb remains disproportionately high. Child exposure to Pb leads to a multitude of poor health outcomes (Keller et al., 2017; Lane et al., 2008; Schnur & John, 2014); therefore, further evaluation of Pb (and other heavy metals) exposure is paramount.

Established methods for measuring elements in plant tissues includes a combination of traditional wet chemistry methods such as atomic absorption spectrometry (AAS) (Bozym et al., 2015; Chopra & Pathak, 2015; Lima et al., 2009; Sekara et al., 2005; Song et al., 2012; Yadav et al., 2015), inductively coupled plasma-atomic emission spectrometry (ICP-AES) or inductively coupled plasma-mass spectrometry (ICP-MS) (Bešter et al., 2013; Finster et al., 2004; Murray et

al., 2011; Nabulo et al., 2011; Rodriguez-Iruretagoiena et al., 2015; Wiseman et al., 2013), wavelength dispersive XRF (WD-XRF) (Andersen et al., 2013; Figueiredo et al., 2016), bench-mounted energy-dispersive XRF (ED-XRF) (Anjos, et al., 2002; Gallardo et al., 2016; Jolly et al., 2013), and portable ED-XRF (Ferri et al., 2015; Gutiérrez-Ginés, et al., 2013; Sacristan et al., 2016; Towett et al., 2016). Recent work quantified heavy metals in with algae with portable ED-XRF using a fundamental parameter factory calibration algorithm for plastics (Bull et al., 2017; Turner et al., 2017).

Sample preparation for AAS or ICP-MS to quantify heavy metals in plants involves ashing plant material in a furnace or with concentrated hydrogen peroxide followed by digestion with acid ($HNO_3$, $HClO_4$, $H_2SO_4$) and/or microwave extraction using one or more concentrated acids. These sample preparation techniques are inherently dangerous and generate a significant hazardous waste stream. Comparatively, XRF sample preparation techniques preserve the sample matrix and minimize waste generation. As noted by many in the literature (e.g. Gallardo et al., 2016), XRF is a promising technique in quantification of Pb and other heavy metals in crop tissues. However, prior reviews of this technology have identified several limiting factors (Marguí et al., 2009; Palmer et al., 2009; Singh et al., 2017).

The greatest obstacles identified in prior studies using XRF to measure heavy metals are achieving a limit of detection within the range of regulatory thresholds and generating consistent results that can be confirmed with another quantification technology. Because of limited commercial availability of reference materials, prior studies involving XRF have not controlled for matrix effects by: neglecting to match the reference material matrix to sample matrix; by using a multitude of sample preparation techniques; or by utilizing XRF standard factory

9

calibrations optimized for non-carbon matrices. Further complicating prior XRF work is the quantitation of heavy metals based on the intensities of wavelengths with known peak overlaps.

Although Pb was identified as a constituent of concern in the 1970s, the USFDA only recently established an ingestion interim reference level (IRL) for Pb of 3 µg d$^{-1}$ for children and 12.5 µg d$^{-1}$ in adults. Surprisingly, USFDA has not established a food concentration standard for Pb; therefore, this project will rely on World Health Organization (WHO) food standards (WHO, 2018). The WHO has Pb standards for a variety of foods, and the calibration limits of detection developed in Objective 2 for Pb will be equal to the WHO Maximum Level for Pb in leafy vegetables of 0.3 µg g$^{-1}$ (on a dry weight basis).

### 1.3.3 Objective 3: Quantify Heavy Metal Concentrations in Crops Grown in Metals-Rich Urban Soils

Many heavy metals are found in plant tissues, some of which serve a metabolic function as summarized below (McBride, 1994; Taiz et al., 2014).

- Metabolically important nutrients obtained from the soil (lists incudes some non-heavy metals for comparison)
  - Macronutrients – N, K, Ca, Mg, P, S, Si
  - Micronutrients – Fe, Mo, Mn, B, Na
  - Toxic elements, but trace nutrient – Zn, Ni, Cu, V, Co, W, Cr, Cd
- Serve no metabolic function, but can be found in plants
  - As, Hg, Sb, Ag, Sc, P, U

Surprisingly, Pb was excluded from the list above. Although much remains unknown with respect to Pb, it serves no known metabolic function in plants, but instead triggers pathways in plants consistent with toxicity and stress responses.

**Source of Pb in Soil.** Managing the risk of exposure to metals-rich soil is a near-impossible challenge due to the omnipresence of Pb in urban soils from a multitude of possible sources [e.g. weathered paint (Clark et al., 2006, 2008; Hall & Tinklenberg, 2003; Laidlaw et al., 2018); transportation/ lead-gasoline (Clark et al., 2006); compost (Murray et al., 2011a), leaching from infrastructure (Tom et al., 2014), anthropogenic industrial fill/spills (Afolayan, 2018; Clark et al., 2008), herbicides (Yokel & Delistraty, 2003), and mobilization/air re-deposition of Pb-impacted soil/colloids from any of the abovementioned sources (Clark et al., 2008)].

**Solublization of Pb into Soil Solution.** The multitude of possible Pb sources, each with its own solubility, suggests that the generation of the Pb cation in soil originates from a multitude of sources with each source weathering at a different rate and under differing conditions. The one commonality between the solubility reactions is the generation of the $Pb^{+2}$ cation through acid dissolution or reductive dissolution of a Pb containing ligand (binder). Weathering can be redox driven (e.g. $PbO_2 + Mn^{+2} \rightarrow Pb^{+2} + MnO_4^-$) or acid dissolution of the parent material (e.g. cerrusite $+ 2H^+ \rightarrow Pb^{+2} + CO_2 + H_2O$) (Fetter, 2008; McBride, 1994). Although the process of weathering Pb paint in soil is not widely discussed in the literature, evidence from the art restoration literature (Monico et al., 2011) suggests weathering of Pb paint occurs through reduction of the binder (e.g. reduction of Cr in $PbCrO_4 \rightarrow Cr_2O_3 + Pb^{+2}$), which may be mediated by electron shuttling between organic or inorganic ligands in a process similar to the process in soil (Brose & James, 2010; Scott et al., 1998).

**Uptake of Pb into Roots and Root Transport.** Once released to soil solution, Pb enters the root hair through the apoplast pathway (Bovenkamp et al., 2013; Sancho et al., 2005) or by entry into the root hair via the symplast pathway using a transport protein to pass through the phospholipid bilayer (Edelstein & Ben-Hur, 2018; Tester & Leigh, 2001). $Pb^{+2}$ enters the

symplast pathway through the ATPase which is known to transport $Zn^{+2}$ and $Cd^{+2}$ (Bhargava, et al., 2012; Meyers et al., 2008; Patra et al., 2004).

The primary mechanism of heavy metal transport through the root is by root pressure and bulk flow of water driven by transpiration from aboveground biomass (Bhargava et al., 2012). Plants are able to restrict the movement of Pb once Pb enters the symplast pathway (e.g. sequestration in vacuole, precipitation), therefore, Pb predominantly moves through the root cortex via the apoplast pathway. Heavy metals traveling in the apoplast pathway can travel as far as the Casparian strip, but must pass through a membrane transport protein into the cytoplasm to continue transport to the stele and loading into the xylem for transport to aboveground tissues.

**Casparian Strip.** The Casparian strip is described in the literature as a "poorly ion-permeable secondary thickening in the cell" (Tester & Leigh, 2001) that serves as "a partial barrier" (Peralta-Videa et al., 2009; Sharma et al., 2015) for "Pb movement into the central cylinder tissue" (Peralta-Videa et al., 2009). Therefore, "Transport of metal ions through the Casparian strip occurs via an energy-requiring active transport system" (Edelstein & Ben-Hur, 2018). Although the description of the Casparian strip in the literature could use some refinement, SEM images have shown that the Casparian strip plays a significant role in restricting transport of heavy metals (ex Pb, Sb) into the stele (Meyers et al., 2008; Pierart et al., 2018).

**Loading to the Xylem and Transport to Aboveground Biomass.** Because Pb likely enters the cell using a transport protein designed for a divalent cation (e.g. $Zn^{+2}$), it is plausible Pb also uses a transporter designed for a divalent cation to be loaded into the xylem. Once in the xylem, heavy metals are available for movement via xylem sap and distribution to the aboveground biomass. The literature suggests that once in the xylem, heavy metals are often

bound to a ligand for transport to aboveground tissues, but remain present in a pH-dependent equilibrium between ion and ligand-bound forms (Clemens et al., 2002, Peralta-Videa et al., 2009). Once the Pb is transported through the xylem into aboveground tissues, the mobility of Pb to be transported/redistributed through the phloem is very limited (Sharma & Dubey, 2005).

**Modes of Plant Toxicity.** Pb toxicity in plants is expressed in the form of oxidative stress by formation of $H_2O_2$. Reactive oxygen species generated because of Pb exposure can alter membranes by oxidizing thiol groups of enzymes and peroxidation of the fatty acid portion of the phospholipid bilayer. Additionally, Pb will alter the structure and functions of enzymes by direct interaction with sulphydryl groups or substitution for essential elements (often divalent cations). Exposure to Pb is known to alter membranes of meristematic cells and the structure of chloroplasts (decreasing production of chlorophyll a and b). To mitigate this stress, plants increase the production of peroxidase triggered by nitric oxide, which is produced after metal exposure. Nitric oxide further upregulates superoxide dismutase and glutathione reductase. Plants are known to increase carotenoid and anthocyanin pigments to scavenge reactive oxygen species in leaf tissues. It follows therefore that vegetables rich in pigments would have greater capacity to mitigate heavy metal toxicity stress and therefore could have a greater propensity/capacity for Pb uptake and transport.

**Influence of Chelating Complexes**. Researchers in the early 1960s determined that ethylenediaminetetraacetic acid (EDTA) increases the solubility of heavy metals in soil (Shahid et al., 2012). Shahid et al. (2012) provides a useful table summarizing previous studies documenting variable responses in Pb concentrations in crop tissues with application of EDTA.

By adding EDTA to Pb-rich nutrient solution at a concentration of 0.25 μM, the concentration of Pb in shoot tissue of Brassica juncea (mustard) was 75-fold greater compared to

13

shoot tissue of plants grown in Pb-rich nutrient solution without EDTA (Vassil et al., 1998). In a Pb uptake study conducted using corn, researchers found that adding 2 g EDTA per kg of Pb impacted soil increased the concentration of Pb in corn shoot tissues from 40 $\mu g\ g^{-1}$ to 10,600 $\mu g\ g^{-1}$ (Huang & Cunningham, 1996). Interestingly, use of chelating complexes (EDTA) in a phytoextraction study involving beans (Phaseolus vulgaris) has shown that the EDTA-Pb complex is capable of transport through the symplast pathway from the cortex to the pericycle, at which point, the EDTA-Pb complex is loaded into the xylem and the metal-complex transported to the aboveground biomass. The results of this study suggest the EDTA-metal complex is biologically stable and capable of bypassing the major plant defense mechanisms associated with Pb removal. Fe-EDTA is an ingredient in some fertilizers and it is possible that gardeners are inadvertently increasing the plant bioavailability/mobility of Pb and other heavy metals through the use of common garden fertilizers.

**Evaluation of bioavailability assays**. The urban agriculture literature has not reached a consensus on the relationship between total Pb in soil and the concentration of Pb in crop tissues. The variability in Pb in produce is not linearly dependent on the total soil Pb. Clark et al. (2008) reported the concentration of Pb in produce varied by 3-orders of magnitude while the concentration of total Pb in soil varied at most by 50%.

Although the primary focus on this project is directly measuring Pb in plant tissues, relating those results to soil geochemistry is necessary. The most common extraction procedure used to estimate the bioavailability of heavy metals in midwestern garden soils is the Mehlich 3 procedure (e.g. Hosseiwwnpur & Motaghian, 2015; Minca et al., 2013). The Mehlich 3 procedure uses a mixture of weak acids and chelating agents (0.2N $CH_3COOH$ + 0.25N $NH_4NO_3$

+ 0.015N NH$_4$F + 0.013N HNO$_3$ + 0.001M EDTA) to mimic soil rhizosphere conditions at the

root hair (Mehlich, 1984).

**Accumulation of Pb in Produce.** Urban agriculture studies have noted that

concentrations of Pb in plant tissues decrease as much as 10-fold between each tissue group from

the roots → leaves → stems → fruits (Finster et al., 2004) with Pb concentrations in tissues

further summarized by (Sharma & Dubey, 2005) as root > leaf> stem > inflorescence > seed.

Fruiting bodies (e.g. tomatoes, strawberries, corn, apples) accumulate less Pb compared to

taproot crops (e.g. onions and carrots). However, concentrations of total Pb in produce grown in

similar soil could vary by as much as 3 orders of magnitude (Clark et al., 2008).

**Evaluation of Exposure Risk.** Estimates suggest that consumption of vegetables is a

secondary, less critical exposure route (Augustsson et al. 2015; Brown et al. 2016; Chopra and

Pathak 2015; Ferri et al. 2015; Jolly et al. 2013). However, much of the prior work did not

evaluate the accumulation of Pb in produce grown in soils with Pb concentrations representative

of soil from older neighborhoods (Attanayake et al. 2015; Entwistle et al. 2019; Mombo et al.

2016; Yousaf et al. 2016). Of work evaluating Pb accumulation in produce grown in soils close

to the range of Pb found in urban soils, the sample sizes and diversity of produce was limited

(Finster et al. 2004) or the source of Pb was associated with either an acidic spill (Lima et al.

2009b) or discharge from mining (Augustsson et al. 2015).Recent work has pointed out the

importance of food as an exposure route (Rai et al. 2019). Although commercial foods in the

United States are generally considered safe, work has identified Pb in commercially-sourced

spices, ethnic foods, folk medicines, and other foods (Dignam et al. 2019; Hore et al. 2019).

Further, now that the United States Food and Drug Administration (USFDA) has established an

Interim Reference Level (IRL) for Pb for children aimed at achieving the Center for Disease

Control's blood Pb reference value of 5 μg dL-1 (USFDA 2019), a quantitative evaluation of potential Pb exposure from consumption of home-grown produce is desperately warranted.

### 1.3.4 Objective 4: Quantify Heavy Metal Concentration in Produce Purchased from Grocery Stores

Heavy metal contamination identified in commercially available foods results in significant mass media coverage. Recalls are issued and offending brands pulled from grocery store shelves. This reactionary response is expected, but further highlights a possible risk of metals exposure posed by commercially-sourced foods. This potential exposure is of particular importance as vegetables are the third most common food purchased by supplemental nutritional assistance program households (Garasky et al., 2016). Under Objective 4, produce from grocery stores will be purchased and concentrations of heavy metals determined using methods described in Chapter 3. These samples will serve as the control for the study.

The FDA conducts limited annual sampling of commercially-available foods under the Total Diet Study Program; however, without numerical food quality standards for heavy metals, the interpretation of the annual sampling data is incomplete. Analysis of samples collected between 1991 and 2014 detected Pb in several fresh and canned vegetables/fruits; however, maximum concentrations were all less than 0.01 μg g$^{-1}$ (US Food and Drug Administration, 2007, 2013). The results of the FDA study will be used as a secondary control for this study.

### 1.4 EXPERIMENTAL METHODS

To achieve Objective 1, in Chapter 2, appropriate XRF reference materials were purchased with heavy metal (primarily Pb) concentrations similar in magnitude to previous urban geochemistry and urban agriculture studies (Clark et al., 2006, 2008; Defoe et al., 2014; Finster et al., 2004; Hu et al., 2014; Huang et al., 2012; McBride et al., 2014; Sharma et al., 2015). The

variability in element concentration in aliquots of each SRM was determined by WD-XRF using fused bead and pressed pellet sample preparation procedures and calibration routines described in McHenry (2009) and McHenry et al. (2011). Additional element concentrations were measured by three commercial laboratories (TestAmerica Laboratories, Inc., Pace Analytical Laboratories, Inc., and the Wisconsin State Lab of Hygiene) using well established wet-chemistry methods (USEPA, 1996, 2007). The results of the inter-laboratory comparison were used to develop custom WD-XRF measurement and calibration routines in the UWM Department of Geosciences X-Ray Laboratory.

The commutability of reference materials to samples is critical in minimizing measurement uncertainty and mitigating matrix effects (absorption/enhancement) but has often been overlooked in prior food studies (Byers et al., 2016). To achieve Objective 2, in Chapter 3, a library of custom dried plant-based reference materials was developed from easily obtainable commercial materials using methods similar to Figueiredo et al. (2016). Custom WD-XRF and ED-XRF measurement and quantification routines were developed using the reference materials and the routines validated with measurements of produce completed during work associated with Chapter 4.

To quantify accumulation of heavy metals in produce under Objective 3, in Chapter 4, a variety of crops representing a continuum of tissue groups were grown in soil collected from two residential properties, collected from a former metal foundry, and commercial topsoil purchased from a big-box retail outlet. Tissues were harvested and the concentrations of heavy metals determined using techniques described in Chapter 3. The risk to children from consuming produce grown in metals-rich soil was evaluated using commonly accepted exposure models.

To evaluate the presence of heavy metals in commercial produce under Objective 4, in Chapter 4, produce identical to that grown during Objective 3 was purchased from grocery stores and the concentrations of heavy metals were measured using techniques described in Chapter 3.

## 1.5    REFERENCES

Afolayan, A. O. (2018). Accumulation of Heavy Metals from Battery Waste in Topsoil, Surface Water, and Garden Grown Maize at Omilende Area, Olodo, Nigeria. Global Challenges, 2(3), 1700090. http://doi.org/10.1002/gch2.201700090

Alvarez-Toral, A., Fernandez, B., Malherbe, J., Claverie, F., Molloy, J. L., Pereiro, R., & Sanz-Medel, A. (2013). Isotope dilution mass spectrometry for quantitative elemental analysis of powdered samples by radiofrequency pulsed glow discharge time of flight mass spectrometry. Talanta, 115, 657–664. http://doi.org/10.1016/j.talanta.2013.06.024

Andersen, L. K., Morgan, T. J., Boulamanti, A. K., Álvarez, P., Vassilev, S. V., & Baxter, D. (2013). Quantitative X-ray fluorescence analysis of biomass: Objective evaluation of a typical commercial multi-element method on a WD-XRF spectrometer. Energy and Fuels, 27(12), 7439–7454. http://doi.org/10.1021/ef4015394

Anjos, M. J., Lopes, R. T., Jesus, E. F. O., Simabuco, S. M., & Cesareo, R. (2002). Quantitative determination of metals in radish using x-ray fluorescence spectrometry. X-Ray Spectrometry, 31(2), 120–123. http://doi.org/10.1002/xrs.567

Bešter, P. K., Lobnik, F., Eržen, I., Kastelec, D., & Zupan, M. (2013). Prediction of cadmium concentration in selected home-produced vegetables. Ecotoxicology and Environmental Safety, 96, 182–190. http://doi.org/10.1016/j.ecoenv.2013.06.011

Bhargava, A., Carmona, F. F., Bhargava, M., & Srivastava, S. (2012, August). Approaches for enhanced phytoextraction of heavy metals. Journal of Environmental Management. http://doi.org/10.1016/j.jenvman.2012.04.002

Bovenkamp, G. L., Prange, A., Schumacher, W., Ham, K., Smith, A. P., & Hormes, J. (2013). Lead uptake in diverse plant families: A study applying X-ray absorption near edge spectroscopy. Environmental Science and Technology, 47(9), 4375–4382. http://doi.org/10.1021/es302408m

Bozym, M., Florczak, I., Zdanowska, P., Wojdalski, J., & Klimkiewicz, M. (2015). An analysis of metal concentrations in food wastes for biogas production. Renewable Energy, 77, 467–472. http://doi.org/10.1016/j.renene.2014.11.010

Brose, D. A., & James, B. R. (2010). Oxidation-reduction transformations of chromium in aerobic soils and the role of electron-shuttling quinones. Environmental Science and Technology, 44(24), 9438–9444. http://doi.org/10.1021/es101859b

Bull, A., Brown, M. T., & Turner, A. (2017). Novel use of field-portable-XRF for the direct analysis of trace elements in marine macroalgae. Environmental Pollution, 220, 228–233. http://doi.org/10.1016/j.envpol.2016.09.049

Byers, H. L., McHenry, L. J., & Grundl, T. J. (2016). Forty-Nine Major and Trace Element Concentrations Measured in Soil Reference Materials NIST SRM 2586, 2587, 2709a, 2710a and 2711a Using ICP-MS and Wavelength Dispersive-XRF. Geostandards and Geoanalytical Research, 40(3), 433–445. http://doi.org/10.1111/j.1751-908X.2016.00376.x

Chantler, C. T., Olsen, K., Dragoset, R. A., Chang, J., Kishore, A. R., Kotochigova, S. A., & Zucker, D. S. (2005). X-Ray Form Factor, Attenuation and Scattering Tables (version 2.1). [Online]. Natl. Inst. Stand. Technol. Gaithersburg, MD. Retrieved from http://physics.nist.gov/ffast

Chopra, A. K., & Pathak, C. (2015). Accumulation of heavy metals in the vegetables grown in wastewater irrigated areas of Dehradun, India with reference to human health risk. Environmental Monitoring and Assessment, 187(7). http://doi.org/10.1007/s10661-015-4648-6

Clark, H. F., Brabander, D. J., & Erdil, R. M. (2006). Sources, Sinks, and Exposure Pathways of Lead in Urban Garden Soil. Journal of Environment Quality, 35(6), 2066. http://doi.org/10.2134/jeq2005.0464

Clark, H. F., Hausladen, D. M., & Brabander, D. J. (2008). Urban gardens: Lead exposure, recontamination mechanisms, and implications for remediation design. Environmental Research, 107(3), 312–319. http://doi.org/10.1016/j.envres.2008.03.003

Claverie, F., Malherbe, J., Bier, N., Molloy, J. L., & Long, S. E. (2013). Putting a spin on LA-ICP-MS analysis combined to isotope dilution. Analytical and Bioanalytical Chemistry, 405(7), 2289–2299. http://doi.org/10.1007/s00216-012-6645-8

Clemens, S., Palmgren, M. G., & Krämer, U. (2002, July). A long way ahead: Understanding and engineering plant metal accumulation. Trends in Plant Science. http://doi.org/10.1016/S1360-1385(02)02295-1

Cloquet, C., Rouxel, O., Carignan, J., & Libourel, G. (2005). Natural Cadmium Isotopic Variations in Eight Geological Reference Materials (NIST SRM 2711, BCR 176, GSS-1, GXR-1, GXR-2, GSD-12, Nod-P-1, Nod-A-1) and Anthropogenic Samples, Measured by MC-ICP-MS. Geostandards and Geoanalytical Research, 29(1), 95–106. http://doi.org/10.1111/j.1751-908X.2005.tb00658.x

Defoe, P. P., Hettiarachchi, G. M., Benedict, C., & Martin, S. (2014). Safety of Gardening on Lead- and Arsenic-Contaminated Urban Brownfields. Journal of Environment Quality, 43(6), 2064. http://doi.org/10.2134/jeq2014.03.0099

Edelstein, M., & Ben-Hur, M. (2018, April). Heavy metals and metalloids: Sources, risks and strategies to reduce their accumulation in horticultural crops. Scientia Horticulturae. http://doi.org/10.1016/j.scienta.2017.12.039

Eriksson, S. M., Mackey, E. A., Lindstrom, R. M., Lamaze, G. P., Grogan, K. P., & Brady, D. E. (2013). Delayed-neutron activation analysis at NIST. Journal of Radioanalytical and Nuclear Chemistry, 298(3), 1819–1822. http://doi.org/10.1007/s10967-013-2568-x

Fernández, B., Rodríguez-González, P., García Alonso, J. I., Malherbe, J., García-Fonseca, S., Pereiro, R., & Sanz-Medel, A. (2014). On-line double isotope dilution laser ablation inductively coupled plasma mass spectrometry for the quantitative analysis of solid materials. Analytica Chimica Acta, 851(C), 64–71. http://doi.org/10.1016/j.aca.2014.08.017

Ferri, R., Hashim, D., Smith, D. R., Guazzetti, S., Donna, F., Ferretti, E., … Lucchini, R. G. (2015). Metal contamination of home garden soils and cultivated vegetables in the province of Brescia, Italy: Implications for human exposure. Science of the Total Environment, 518–519, 507–517. http://doi.org/10.1016/j.scitotenv.2015.02.072

Fetter, C. W. (2008). Contaminant Hydrogeology (2nd ed.). Long Grove, IL: Waveland Press, Inc.

Figueiredo, A., Fernandes, T., Costa, I. M., Gonçalves, L., & Brito, J. (2016). Feasibility of wavelength dispersive X-ray fluorescence spectrometry for the determination of metal impurities in pharmaceutical products and dietary supplements in view of regulatory guidelines. Journal of Pharmaceutical and Biomedical Analysis, 122, 52–58. http://doi.org/10.1016/j.jpba.2016.01.028

Finster, M. E., Gray, K. A., & Binns, H. J. (2004). Lead levels of edibles grown in contaminated residential soils: A field survey. Science of the Total Environment. http://doi.org/10.1016/j.scitotenv.2003.08.009

Gallardo, H., Queralt, I., Tapias, J., Guerra, M., Carvalho, M. L., & Marguí, E. (2016). Possibilities of low-power X-ray fluorescence spectrometry methods for rapid multielemental analysis and imaging of vegetal foodstuffs. Journal of Food Composition and Analysis, 50, 1–9. http://doi.org/10.1016/j.jfca.2016.04.007

Garasky, S., Mbwana, K., Romualdo, A., Tenaglio, A., & Roy, M. (2016). Foods Typically Purchased by Supplemental Nutrition Assistance Program (SNAP) Households. Columbia, MD 21044. Retrieved from http://www.fns.usda.gov/research-and-analysis

Goix, S., Point, D., Oliva, P., Polve, M., Duprey, J. L., Mazurek, H., … Gardon, J. (2011). Influence of source distribution and geochemical composition of aerosols on children exposure in the large polymetallic mining region of the Bolivian Altiplano. Science of the Total Environment, 412–413, 170–184. http://doi.org/10.1016/j.scitotenv.2011.09.065

Gueguen, B., Rouxel, O., Ponzevera, E., Bekker, A., & Fouquet, Y. (2013). Nickel isotope variations in terrestrial silicate rocks and geological reference materials measured by MC-ICP-MS. Geostandards and Geoanalytical Research, 37(3), 297–317. http://doi.org/10.1111/j.1751-908X.2013.00209.x

Gutiérrez-Ginés, M. J., Pastor, J., & Hernández, A. J. (2013). Assessment of field portable X-ray fluorescence spectrometry for the in situ determination of heavy metals in soils and plants. Environmental Science: Processes & Impacts, 15(8), 1545. http://doi.org/10.1039/c3em00078h

Hall, G. S., & Tinklenberg, J. (2003). Determination of Ti, Zn, and Pb in lead-based house paints by EDXRF. Journal of Analytical Atomic Spectrometry, 18(7), 775–778. http://doi.org/10.1039/b300597f

Hoang, T. H., Bang, S., Kim, K. W., Nguyen, M. H., & Dang, D. M. (2010). Arsenic in groundwater and sediment in the Mekong River delta, Vietnam. Environmental Pollution, 158(8), 2648–2658. http://doi.org/10.1016/j.envpol.2010.05.001

Hosseiwwnpur, A. R., & Motaghian, H. (2015). Evaluating of many chemical extractants for assessment of Zn and Pb uptake by bean in polluted soils. Journal of Soil Science and Plant Nutrition, 15(1), 0–0. http://doi.org/10.4067/S0718-95162015005000003

Hu, W., Huang, B., Weindorf, D. C., & Chen, Y. (2014). Metals analysis of agricultural soils via portable x-ray fluorescence spectrometry. Bulletin of Environmental Contamination and Toxicology, 92(4), 420–426. http://doi.org/10.1007/s00128-014-1236-3

Huang, J., & Cunningham, S. (1996). Lead phytoextraction: Species variation in lead uptake and translocation. New Phytologist, 134(1), 75–84. http://doi.org/10.1111/j.1469-8137.1996.tb01147.x

Huang, Z. Y., Chen, T., Yu, J., Qin, D. P., & Chen, L. (2012). Lead contamination and its potential sources in vegetables and soils of Fujian, China. Environmental Geochemistry and Health, 34(1), 55–65. http://doi.org/10.1007/s10653-011-9390-6

Jolly, Y. N., Islam, A., & Akbar, S. (2013). Transfer of metals from soil to vegetables and possible health risk assessment. SpringerPlus, 2(1), 1–8. http://doi.org/10.1186/2193-1801-2-385

Keller, B., Faciano, A., Tsega, A., & Ehrlich, J. (2017). Epidemiologic Characteristics of Children with Blood Lead Levels ≥45 μg/dL. Journal of Pediatrics, 180, 229–234. http://doi.org/10.1016/j.jpeds.2016.09.017

Kenna, T. C., Nitsche, F. O., Herron, M. M., Mailloux, B. J., Peteet, D., Sritrairat, S., … Baumgarten, J. (2011). Evaluation and calibration of a Field Portable X-Ray Fluorescence spectrometer for quantitative analysis of siliciclastic soils and sediments. Journal of Analytical Atomic Spectrometry, 26(2), 395. http://doi.org/10.1039/c0ja00133c

Laidlaw, M. A. S., Alankarage, D. H., Reichman, S. M., Taylor, M. P., & Ball, A. S. (2018). Assessment of soil metal concentrations in residential and community vegetable gardens in Melbourne, Australia. Chemosphere, 199, 303–311. http://doi.org/10.1016/j.chemosphere.2018.02.044

Lane, S. D., Webster, N. J., Levandowski, B. A., Rubinstein, R. A., Keefe, R. H., Wojtowycz, M. A., … Aubry, R. H. (2008). Environmental Injustice: Childhood Lead Poisoning, Teen Pregnancy, and Tobacco. Journal of Adolescent Health, 42(1), 43–49. http://doi.org/10.1016/j.jadohealth.2007.06.017

Lima, F., Nascimento, C., Silva, F., Carvalho, V., & Filho, M. (2009). Lead concentration and allocation in vegetable crops grown in a soil contaminated by battery residues. Horticultura Brasileira, 27(3), 362–365.

Mäkinen, E., Korhonen, M., Viskari, E.-L., Haapamäki, S., Järvinen, M., & Lu, L. (2006). Comparison of Xrf and Faas Methods in Analysing Cca Contaminated Soils. Water, Air, & Soil Pollution, 171(1–4), 95–110. http://doi.org/10.1007/s11270-005-9017-6

Marguí, E., Queralt, I., & Hidalgo, M. (2009). Application of X-ray fluorescence spectrometry to determination and quantitation of metals in vegetal material. TrAC - Trends in Analytical Chemistry, 28(3), 362–372. http://doi.org/10.1016/j.trac.2008.11.011

Martynenko, A. (2014). True, Particle, and Bulk Density of Shrinkable Biomaterials: Evaluation from Drying Experiments. Drying Technology, 32(11), 1319–1325. http://doi.org/10.1080/07373937.2014.894522

May, W., Parris, R., Beck, C., Fassett, J., Greenberg, R., Guenther, F., … Others. (2000). Definitions of terms and modes used at NIST for value-assignment of reference materials for chemical measurements. NIST Special Publication.

McBride, M. B. (1994). Environmental Chemistry of Soils. New York: Oxford University Press, Inc.

McBride, M. B., Shayler, H. A., Spliethoff, H. M., Mitchell, R. G., Marquez-Bravo, L. G., Ferenz, G. S., … Bachman, S. (2014). Concentrations of lead, cadmium and barium in urban garden-grown vegetables: The impact of soil variables. Environmental Pollution, 194, 254–261. http://doi.org/10.1016/j.envpol.2014.07.036

McComb, J. Q., Rogers, C., Han, F. X., & Tchounwou, P. B. (2014). Rapid Screening of Heavy Metals and Trace Elements in Environmental Samples Using Portable X-Ray Fluorescence Spectrometer, A Comparative Study. Water, Air, & Soil Pollution, 225(12), 2169. http://doi.org/10.1007/s11270-014-2169-5

McHenry, L. J. (2009). Element mobility during zeolitic and argillic alteration of volcanic ash in a closed-basin lacustrine environment: Case study Olduvai Gorge, Tanzania. Chemical Geology, 265(3–4), 540–552. http://doi.org/10.1016/j.chemgeo.2009.05.019

McHenry, L. J., Chevrier, V., & Schörder, C. (2011). Jarosite in a Pleistocene East African saline-alkaline paleolacustrine deposit: Implications for Mars aqueous geochemistry. Journal of Geophysical Research E: Planets, 116(4). http://doi.org/10.1029/2010JE003680

Mehlich, A. (1984). Mehlich 3 soil test extractant: A modification of Mehlich 2 extractant. Communications in Soil Science and Plant Analysis, 15(12), 1409–1416. http://doi.org/10.1080/00103628409367568

Meyers, D. E. R., Auchterlonie, G. J., Webb, R. I., & Wood, B. (2008). Uptake and localisation of lead in the root system of Brassica juncea. Environmental Pollution, 153(2), 323–332. http://doi.org/10.1016/j.envpol.2007.08.029

Milliard, A., Durand-Jézéquel, M., & Larivière, D. (2011). Sequential automated fusion/extraction chromatography methodology for the dissolution of uranium in environmental samples for mass spectrometric determination. Analytica Chimica Acta, 684(1–2), 40–46. http://doi.org/10.1016/j.aca.2010.10.037

Minca, K. K., Basta, N., & Scheckel, K. G. (2013). Using the Mehlich-3 Soil Test as an Inexpensive Screening Tool to Estimate Total and Bioaccessible Lead in Urban Soils. Journal of Environmental Quality, 42(5), 1518–1526. http://doi.org/10.2134/jeq2012.0450

Monico, L., Van Der Snickt, G., Janssens, K., De Nolf, W., Miliani, C., Dik, J., … Cotte, M. (2011). Degradation process of lead chromate in paintings by Vincent van Gogh studied by means of synchrotron x-ray spectromicroscopy and related methods. 2. Original paint layer samples. Analytical Chemistry, 83(4), 1224–1231. http://doi.org/10.1021/ac1025122

Moon, J. H., Dung, H. M., Kim, S. H., & Chung, Y. S. (2009). Implementation of the k 0-NAA method by using k 0-IAEA software and the NAA#3 irradiation hole at the HANARO research reactor. Journal of Radioanalytical and Nuclear Chemistry, 280(3), 439–444. http://doi.org/10.1007/s10967-009-7474-x

Murray, H., Pinchin, T., & Macfie, S. (2011a). Compost application affects metal uptake in plants grown in urban garden soils and potential human health risk. Journal of Soils and Sediments, 11(5), 815–829. http://doi.org/10.1007/s11368-011-0359-y

Murray, H., Pinchin, T., & Macfie, S. (2011b). compost application affects update in plants grown in urban garden soils and potential human health risks. Journal of Soils and Sediments, 11(5), 815–829.

Nabulo, G., Black, C. R., & Young, S. D. (2011). Trace metal uptake by tropical vegetables grown on soil amended with urban sewage sludge. Environmental Pollution, 159(2), 368–376. http://doi.org/10.1016/j.envpol.2010.11.007

Palmer, P. T., Jacobs, R., Baker, P. E., Ferguson, K., & Webber, S. (2009). Use of field-portable XRF analyzers for rapid screening of toxic elements in fda-regulated products. Journal of Agricultural and Food Chemistry, 57(7), 2605–2613. http://doi.org/10.1021/jf803285h

Patra, M., Bhowmik, N., Bandopadhyay, B., & Sharma, A. (2004, December). Comparison of mercury, lead and arsenic with respect to genotoxic effects on plant systems and the development of genetic tolerance. Environmental and Experimental Botany. http://doi.org/10.1016/j.envexpbot.2004.02.009

Paul, R. L., MacKey, E. A., Zeisler, R., Spatz, R. O., & Tomlin, B. E. (2009). Determination of elements in SRM soil 2709a by neutron activation analysis. Journal of Radioanalytical and Nuclear Chemistry, 282(3), 945–950. http://doi.org/10.1007/s10967-009-0250-0

Peralta-Videa, J. R., Lopez, M. L., Narayan, M., Saupe, G., & Gardea-Torresdey, J. (2009, August). The biochemistry of environmental heavy metal uptake by plants: Implications for the food chain. International Journal of Biochemistry and Cell Biology. http://doi.org/10.1016/j.biocel.2009.03.005

Rodriguez-Iruretagoiena, A., Trebolazabala, J., Martinez-Arkarazo, I., Diego, A., & Madariaga, J. M. (2015). Metals and metalloids in fruits of tomatoes (Solanum lycopersicum) and their cultivation soils in the Basque Country: Concentrations and accumulation trends. Food Chemistry, 173, 1083–1089. http://doi.org/10.1016/j.foodchem.2014.10.133

Rodríguez-Ramírez, J., Méndez-Lagunas, L., López-Ortiz, A., & Torres, S. S. (2012). True Density and Apparent Density During the Drying Process for Vegetables and Fruits: A Review. Journal of Food Science. http://doi.org/10.1111/j.1750-3841.2012.02990.x

Sacristan, D., Rossel, R. A. V., & Recatala, L. (2016). Proximal sensing of Cu in soil and lettuce using portable X-ray fluorescence spectrometry. Geoderma, 265, 6–11. http://doi.org/10.1016/j.geoderma.2015.11.008

Sancho, D., Deban, L., Pardo, R., & Valladolid, D. (2005). Determination of zinc, cadmium, lead and copper in pellets and pulp of sugar beet. Journal of the Science of Food and Agriculture, 85(6), 1021–1025. http://doi.org/10.1002/jsfa.2046

Schnur, J., & John, R. M. (2014). Childhood lead poisoning and the new centers for disease control and prevention guidelines for lead exposure. Journal of the American Association of Nurse Practitioners. http://doi.org/10.1002/2327-6924.12112

Scott, D. T., Mcknight, D. M., Blunt-Harris, E. L., Kolesar, S. E., & Lovley, D. R. (1998). Quinone moieties act as electron acceptors in the reduction of humic substances by humics-reducing microorganisms. Environmental Science and Technology, 32(19), 2984–2989. http://doi.org/10.1021/es980272q

Sekara, A., Poniedzialek, M., Ciura, J., & Jedrszczyk, E. (2005). Cadmium and lead accumulation and distribution in the tissues of nine crops: Implications for phytoremediation. Polish Journal of Environmental Studies, 14(4), 509–516.

Shahid, M., Pinelli, E., & Dumat, C. (2012, June). Review of Pb availability and toxicity to plants in relation with metal speciation; role of synthetic and natural organic ligands. Journal of Hazardous Materials. http://doi.org/10.1016/j.jhazmat.2012.01.060

Sharma, K., Basta, N. T., & Grewal, P. S. (2015). Soil heavy metal contamination in residential neighborhoods in post-industrial cities and its potential human exposure risk. Urban Ecosystems, 18(1), 115–132. http://doi.org/10.1007/s11252-014-0395-7

Sharma, P., & Dubey, R. S. (2005). Lead Toxicity in Plants. Brazilian Journal of Plant Physiology, 14(1), 35–52.

Singh, V., Rai, P., Pathak, A., Tripathi, D., Singh, S., & Singh, J. (2017). Application of Wavelength-Dispersive X-Ray Fluorescence Spectrometry to Biological Samples. Spectroscopy, 32(7), 41–47.

Song, X., Hu, X., Ji, P., Li, Y., Chi, G., & Song, Y. (2012). Phytoremediation of cadmium-contaminated farmland soil by the hyperaccumulator beta vulgaris L. var. cicla. Bulletin of Environmental Contamination and Toxicology, 88(4), 623–626. http://doi.org/10.1007/s00128-012-0524-z

Sutton, M., Bibby, R. K., Eppich, G. R., Lee, S., Lindvall, R. E., Wilson, K., & Esser, B. K. (2012). Evaluation of historical beryllium abundance in soils, airborne particulates and facilities at Lawrence Livermore National Laboratory. Science of the Total Environment, 437, 373–383. http://doi.org/10.1016/j.scitotenv.2012.08.011

Taiz, L., Zeiger, E., Møller, I. M. (Ian M., & Murphy, A. S. (2014). Plant physiology and development (6th ed.). Oxford University Press, Inc. Retrieved from https://global.oup.com/ushe/product/plant-physiology-and-development-9781605352558?cc=ca&lang=en&q=sinauer

Tester, M., & Leigh, R. A. (2001). Partitioning of nutrient transport processes in roots. Journal of Experimental Botany, 52(Spec Issue), 445–57. http://doi.org/10.1093/jexbot/52.suppl_1.445

Thomsen, V. (2012). Spectral Background Radiation and the Background Equivalent Concentration in Elemental Spectrochemistry. Spectroscopy, 17(3), 28–36.

Thomsen, V., Schatzlein, D., & Mercuro, D. (2003). Limits of Detection in Spectroscopy. Spectroscopy, 18(12), 112–114. http://doi.org/Article

Tom, M., Fletcher, T. D., & McCarthy, D. T. (2014). Heavy metal contamination of vegetables irrigated by Urban stormwater: A matter of time? PLoS ONE, 9(11). http://doi.org/10.1371/journal.pone.0112441

Towett, E. K., Shepherd, K. D., & Drake, L. B. (2016). Plant elemental composition and portable X-ray fluorescence (pXRF) spectroscopy: Quantification under different analytical parameters. X-Ray Spectrometry, 45(2), 117–124. http://doi.org/10.1002/xrs.2678

25

Turner, A., Poon, H., Taylor, A., & Brown, M. T. (2017). In situ determination of trace elements in Fucus spp. by field-portable-XRF. Science of the Total Environment, 593–594, 227–235. http://doi.org/10.1016/j.scitotenv.2017.03.091

US Food and Drug Administration. Guidance for Industry: Lead in Candy Likely To Be Consumed Frequently by Small Children (2006). USA. Retrieved from https://www.fda.gov/Food/GuidanceRegulation/GuidanceDocumentsRegulatoryInformation/ucm077904.htm

US Food and Drug Administration. (2007). Total Diet Study Statistics on Element Results. College Park, Maryland 20740-3835. Retrieved from https://www.fda.gov/downloads/Food/FoodScienceResearch/TotalDietStudy/UCM243059.pdf

US Food and Drug Administration. (2013). Total Diet Study, Elements Results Summary Statistics, Market Baskets 2006 through 2013. College Park, Maryland 20740-3835. Retrieved from https://www.fda.gov/downloads/Food/FoodScienceResearch/TotalDietStudy/UCM184301.pdf

USEPA. (1996). Method 3050B - Acid digestion of sediments, sludges, and soils. 1996. http://doi.org/10.1117/12.528651

USEPA. (2007). Inductively Coupled Plasma-Mass Spectrometry EPA Method 6020A. In Test Methods for Evaluating Solid Waste (pp. 1–30). Retrieved from http://www.epa.gov/osw/hazard/testmethods/sw846/pdfs/6020a.pdf

USEPA. (2014). National functional guidelines for inorganic superfund data review. Retrieved from https://www.epa.gov/sites/production/files/2017-01/documents/national_functional_guidelines_for_inorganic_superfund_methods_data_review_01302017.pdf

Vassil, A. D., Kapulnik, Y., Raskin, I., & Salt, D. E. (1998). The Role of EDTA in Lead Transport and Accumulation by Indian Mustard 1. Plant Physiol (Vol. 117). http://doi.org/10.1104/pp.117.2.447

Weindorf, D. C., Zhu, Y., Chakraborty, S., Bakr, N., & Huang, B. (2012). Use of portable X-ray fluorescence spectrometry for environmental quality assessment of peri-urban agriculture. Environmental Monitoring and Assessment, 184(1), 217–227. http://doi.org/10.1007/s10661-011-1961-6

WHO. (2018). General Standard for Contaminants and Toxins in Food and Feed (CODEX STAN 193-1995), Pub. L. No. Codex STAN 193-1955 (2018). Retrieved from http://www.fao.org/input/download/standards/17/CXS_193e_2015.pdf

Wilson, S. A., Briggs, P. H., Mee, J. S., & Siems, D. F. (1994). Determination of thirty-two major and trace elements in three NIST soil SRMs using ICP-AES and WDXRF. Geostandards Newsletter, 18(1), 85–89.

Wiseman, C. L. S., Zereini, F., & Püttmann, W. (2013). Traffic-related trace element fate and uptake by plants cultivated in roadside soils in Toronto, Canada. Science of the Total Environment. http://doi.org/10.1016/j.scitotenv.2012.10.051

Yadav, R. K., Minhas, P. S., Lal, K., Chaturvedi, R. K., Yadav, G., & Verma, T. P. (2015). Accumulation of Metals in Soils, Groundwater and Edible Parts of Crops Grown Under Long-Term Irrigation with Sewage Mixed Industrial Effluents. Bulletin of Environmental Contamination and Toxicology. http://doi.org/10.1007/s00128-015-1547-z

Yokel, J., & Delistraty, D. A. (2003). Arsenic, lead, and other trace elements in soils contaminated with pesticide residues at the Hanford site (USA). Environmental Toxicology, 18(2), 104–114. http://doi.org/10.1002/tox.10106

## 2.0 FORTY-NINE MAJOR AND TRACE ELEMENT CONCENTRATIONS MEASURED IN NIST SOIL SRM 2586, SRM 2587, SRM 2709A, SRM 2710A, AND SRM 2711A USING ICP-MS AND WD-XRF.

### 2.1 INTRODUCTION

Numerous geoscience/urban geochemistry investigations have used commercially available NIST soil Standard Reference Material (SRM) as calibration standards or as quality control materials (Fernández et al., 2014; Kenna et al., 2011; McComb et al., 2014; Murray et al., 2011; Sutton et al., 2012; Weindorf, et al., 2012) NIST defines and provides Certified, Reference, and Information Values for element concentrations presented in SRM Certificates of Analysis. NIST certified values represent concentrations measured with the smallest measurement uncertainty and where sources of bias have been accounted for by NIST (May et al., 2000). Concentrations provided by NIST with larger measurement uncertainty are defined by NIST as reference values. Reported concentrations where uncertainty has not been evaluated are referred to by NIST as information values (May et al., 2000). Reference values or information values for the soil materials NIST SRM 2709, 2710 and 2711, reported either directly or as part of quality control exercises, have been provided previously by numerous investigators using XRF and/or ICP-MS (e.g., Wilson et al. 1994, Cloquet et al. 2005, Makinen et al. 2005, Murray et al. 2011, Weindorf et al. 2012, Gueguen et al. 2013). However, these three soil RMs are no longer commercially available and have been replaced by NIST SRM 2709a, 2710a and 2711a.

Along with SRM 2586 and SRM 2587, these five reference materials present a continuum of heavy metal concentrations and are considered representative of soils likely to be encountered in urban agriculture/urban geochemistry studies. However, characterization of these five soil RMs remains incomplete because very few reference values are available in the literature (Moon et al. 2009, Paul et al. 2009, Hoang et al. 2010, Goix et al. 2011, Milliard et al. 2011, Alvarez-Toral et al. 2013, Claverie et al. 2013, Eriksson et al. 2013, Fernandez et al. 2014). The purpose of this study is to further characterize the variability in element concentrations (strictly, the mass fractions) in the five NIST SRM soil materials and provide reference values for previously uncharacterized elements. This will contribute to reducing the measurement bias of custom calibration routines and improving the quality of control checks developed using these NIST reference materials.

## 2.2     EXPERIMENTAL

The commutability of reference materials to anticipated samples is critical in decreasing measurement uncertainty. This study was focused on soils with heavy metal (primarily Pb) concentrations similar in magnitude to previous urban geochemistry and urban agriculture studies (Finster et al. 2004, Clark et al. 2006, 2008, Huang et al. 2012, Defoe et al. 2014, Hu et al. 2014, McBride et al. 2014, Sharma et al. 2015). Therefore, five commercially available NIST soil reference materials encompassing a continuum in heavy metal concentrations, organic carbon and mineralogy likely to be found in urban soils were selected for characterization. These originated from (a) a fallow agricultural field in the San Joaquin Valley of California (NIST SRM 2709a); (b) the floodway of Silver Bow Creek in Montana near a brownfield property (NIST SRM 2710a); (c) an agricultural field located near a former smelting plant in Helena, MT

(NIST SRM 2011a); (d) an urban agricultural garden contaminated with lead-based paint (NIST SRM 2587); and (e) urban soils contaminated with lead-based paint (NIST SRM 2586).

Upon receipt of the NIST materials, each jar was shaken gently by hand for 30 s and aliquots of ca. 5 g were transferred from each jar to separate glass vials, which were then sealed with polyethylene caps. An aliquot of each NIST SRM soil sample was anonymized and submitted under chain of custody to the Wisconsin State Laboratory of Hygiene, Madison, Wisconsin (WSLH; a Wisconsin Department of Natural Resources certified laboratory) for ICP-MS analysis. Concurrently, two aliquots were used to prepare pressed pellets and fused beads for analysis by WD-XRF at the University of Wisconsin-Milwaukee Department of Geo- sciences XRF laboratory using two separate custom WD-XRF calibration routines. A fourth aliquot was used to determine the mass lost on ignition (LOI).

### 2.2.1 ICP-MS (WSLH)

National Institute for Science and Technology soil reference material samples were digested at the WSLH using a standard microwave digestion procedure that involved adding 8.0 ml of 16 mol l-1 HNO3 plus 2.0 ml of 12 mol l-1 HCl plus 2.5 ml of HF to 30-mg test portions of each RM. Digestions were measured in triplicate using a Thermo-Finnigan Element 2 magnetic-sector ICP-MS.

### 2.2.2 WD-XRF (Fused Bead Preparation)

Fused beads of each NIST soil RM were prepared using the protocol described in McHenry (2009) in which 1.000 g of soil was added to 1 g of oxidizer (ammonium nitrate) and 10.000 g of Claisse (Quebec, Canada) 50:50 lithium metaborate: lithium tetraborate flux containing 0.5% LiBr as a nonwetting agent. The material was fused at 1050 °C in a Claisse M4 programmable fusion system. Fused beads were measured three times with a Bruker AXS, Inc.

Pioneer S4 WD-XRF instrument using a custom measurement and calibration procedure based on eleven USGS sedimentary and igneous geological reference materials made in the same manner as samples prepared for this study, as described by McHenry (2009). The USGS geological reference materials used in this calibration routine are AGV-1, BCR-2, BHVO-2, BIR-1, DNC-1, DTS-2b, G-2, GSP-2, RGM-1, SGR-1 and STM-1. The custom routine was refined in the Pioneer S4 software by correcting for peak overlaps and adjusted for the use of the bromide nonwetting agent. Absorption and enhancement due to matrix effects were corrected in the Pioneer S4 software using fundamental parameters, and calibration materials with concentrations less than the limit of detection were removed from the calibration routine.

The intensities of eighteen major and trace elements in the reference materials were measured under vacuum using Ka1 lines except for Ba and Ce, which were measured using their La1 X-ray lines and concentrations determined through the custom fused bead calibration. To measure Na, K, Ca and Fe, the routine was optimized to count fluoresced X-rays for 10 s or until the statistical precision on counting values (determined as 3s based on a Poisson's law) was less than 0.3%. For Al and Si, fluoresced X-rays were counted for fixed times of 10 s and 4 s, respectively. To measure the concentrations of Mg and P, the routine counted fluoresced X-rays for 30 s or until the statistical precision (3s) was less than 0.3% and 1%, respectively. The remaining elements were measured for 10 s or until the statistical precision (3s) was < 5%. Depending on the element, the routine used a pentaerythrite (PET), lithium fluoride (LIF200) or multilayer (OVO-55) analyzer crystal, and either a flow or scintillation counter. Specific routine details for each element, including generator voltage, tube current, collimator, analyzer crystal, detector and peak overlap corrections, are provided in Table 2.1S.

### 2.2.3  WD-XRF (Pressed Pellet Preparation)

Pressed pellets of each NIST SRM soil were prepared by adding 10.0 g of material with four GeoQuant (Krupp Polysius Polab®) wax binder pills (1.25 g total) and combining in a tungsten carbide shatterbox for 30 s. Each prepared sample was placed in an Al sample cup and pressed at 25 t for 60 s in a 40 mm diameter pellet die hydraulic press as described in McHenry et al. (2011). Pressed pellets were measured three times using a Bruker AXS, Inc. Pioneer S4 WD-XRF for major and trace elements using a custom measurement and calibration routine developed using nine USGS sedimentary and igneous rock reference materials (AGV-2, BCR-2, BHVO-2, DNC-1, DTS-2b, GSP-2, QLO-1, SGR-1 and W-2A) made in the same manner as samples prepared for this study as described in McHenry et al. (2011). The custom calibration routine was refined in the Pioneer S4 software by correcting for peak overlaps, Rh Rayleigh and Compton peaks, and contamination of W and Co from the shatterbox. Calibration materials with concentrations less than the limit of detection were removed from the calibration routine.

The intensities of twenty-two elements in the NIST SRM materials were measured under vacuum using Ka1 lines, except for Ba and Ce, which were measured using La1 X- ray wavelengths and concentrations determined through the custom pressed pellet calibration. The routine was optimized to count fluoresced X-rays for 10 s or until the statistical precision (3s) was less than 5%. Depending on the element, the routine used a PET, LIF200 or OVO-55 crystal and either a flow or scintillation counter. Specific routine details for each element, including generator voltage, tube current, collimator, crystal, detector and peak overlap corrections, are provided in Table 2.2S.

### 2.2.4    Water Content and Loss on Ignition

Test portions, weighing 4 g, of each NIST SRM soil material were dried for 2 hr in an oven at 105 °C to estimate the water content of each soil. Each oven-dried NIST SRM soil sample was divided into three 1-g aliquots and, following McHenry (2009), each aliquot was combusted in a muffle furnace at 1050 °C for 15 min and the mean LOI calculated for each RM to estimate the mass of material lost during fused bead preparation.

### 2.2.5    Quality Control of WD-XRF Measurements

As noted by Thomsen et al. (2003), the limit of detection (LOD) is considered the smallest concentration of an element that produces a response that can be distinguished from the background. The limit of quantitation (LOQ) is considered the smallest concentration that can be measured with minimal bias and error. The LOD for each WD-XRF measurement was calculated by the Pioneer S4 software, and the LOQ of each WD-XRF measurement was estimated by multiplying the LOD by 3.3 as suggested by Thomsen et al. (2003). WD-XRF measurements less than the LOD are omitted from Tables 2.6–2.10. WD-XRF measurements greater than the LOD but less than the LOQ are denoted on Tables 2.6–2.10 with a 'J' data qualifier and are considered information values; likewise the 1s and RSD for these measurements are provided for information purposes only, and the measurements less than the LOQ are omitted from further evaluation in this data assessment study. In addition, the statistical precision on the intensity measurement for each WD-XRF measurement was calculated by the Pioneer S4 software based on Poisson's law, and if the statistical precision was greater than 12%, WD-XRF measurement results were omitted from Tables 2.1-2.10.

Due to contamination during sample preparation in the shatterbox, W and Co values cannot be reported for pressed pellet WD-XRF measurements. The flux used to make the fused beads contained 1% LiBr as a nonwetting agent, and due to a large peak overlap between Br and Rb, we are not able to report concentrations of Rb in fused bead WD-XRF pellets.

During the manufacturing process, NIST sieved each soil material through a 200-mesh screen; therefore, the maxi- mum particle size should be no more than 75 um. As WD- XRF X-ray penetration depths for the Mg, Al, Si, P, K, Ca and Ti Ka1 lines are less than 75 um, it is possible that the concentrations of these elements measured in this study using WD-XRF of pressed pellets are biased to elements concentrated in particles on the surface of the pellet and thus may not be representative of the bulk. Values for these measurands are reported in Tables 2.1–2.10 for information purposes only. The penetration depth for Na is only 4.1 um; therefore, these results for WD-XRF measurements of pressed pellets are not reported.

### 2.2.6    Data Reduction

Based on the triplicate measurements of each analyte by ICP-MS and WD-XRF, the mean concentration of each element, associated standard deviation (s) and the relative standard deviation (RSD; expressed as per cent) were calculated for each NIST SRM soil for each measurement technique. Major element concentrations are presented in Tables 2.1–2.5, and trace element concentrations are presented in Tables 2.6–2.10 along with corresponding NIST certified, information, and reference values and associated uncertainties reported by NIST.

To compare the concentrations measured in this study to concentrations reported by NIST and to other values reported in the literature, the relative difference (RD; expressed as a per cent) was calculated following USEPA (2007, 2014) as) as:

$$RD\ (\%)\ =\ \frac{(C1-C2)}{\frac{(C1+C2)}{2}}\ x\ 100 \tag{1}$$

where C1 and C2 are element concentrations in sample 1 and sample 2, respectively. Relative difference is a dimensionless statistical measurement commonly used to evaluate the precision of two measurements of inorganic elements (USEPA 2007, 2014). A RD of 0 indicates that the two measurements are equal, while a larger or smaller RD indicates an increasing difference between the two measurements. A positive RD indicates that C1 > C2; conversely, a negative RD indicates C1 < C2.

For the purpose of this investigation, we assumed that the NIST values are the correct values; therefore, we used RD as a measurement of bias. As recommended in USEPA (2014), we define a RD of ± 20% as the control limit. We acknowledge that many trace elements are difficult to measure; therefore, for our evaluation, we define a RD of ± 40% as the threshold limit. Element concentrations with RD values outside the threshold limit are provided for information purposes only.

The RD for each element for each NIST SRM soil comparing the NIST concentrations (C1) to the WSLH ICP-MS concentrations (C2) is illustrated on Figure 2.1. The RD for each element for each RM comparing the NIST concentrations (C1) with the fused bead WD-XRF concentrations (C2) is illustrated in Figure 2.2. The RDs comparing concentrations measured in this study by WSLH using ICP- MS (C2) to concentrations reported in the literature (C1) by Moon et al. (2009) and Paul et al. (2009), Hoang et al. (2010), Goix et al. (2011), Milliard et al. (2011), Alvarez- Toral et al. (2013), Claverie et al. (2013), Eriksson et al. (2013) and Fernandez et al. (2014) are shown in Figure 2.3.

## 2.3    RESULTS AND DISCUSSION

Excellent agreement was noted in the major and trace elements between measurements made in this investigation and the NIST certified, reference and information values (Figures 2.1

and 2.2). Measurement results from ICP-MS (at WSLH) seem to be uniformly lower compared with NIST values for NIST SRM 2710a, but no other bias is apparent in the WSLH measurements. As illustrated in Figure 2.1, 85% of WSLH measurements were within the control limit of ± 20% RD compared with NIST values and 99% of measurements were within the threshold limit of ± 40% RD compared with NIST values. In comparing the WD-XRF measurements of fused beads from our laboratory to NIST values, 97% of WD- XRF measurements were within the control limit of ± 20% RD and 100% of measurements were within the threshold limit of ± 40% RD. Elements with RD values outside the threshold limit are present in trace concentrations and are challenging to measure with reasonable precision. Therefore, we have great confidence in the values for the major and minor elements reported in this study.

Element concentrations measured in this study by ICP-MS by WSLH are in close agreement with concentrations reported in the literature (Figure 2.3). In comparing the WSLH ICP-MS measurements with literature values, 88% of WSLH measurements were within the control limit of ± 20% RD and 99% of measurements were within the threshold limit (± 40% RD). Therefore, we have great confidence in the values for the major and minor elements reported in this study.

For reference, the water contents in NIST SRM 2586, 2587, 2709a, 2710a and 2711a measured in this study were 1.6%, 1.1%, 2.7%, 1.8% and 2.1% m/m, respectively, and the mean LOI concentrations were 8.6%, 6.4%, 6.6%, 7.5% and 6.4% m/m, respectively. The respective standard deviations of the LOI measurements of NIST SRMs 2586, 2587, 2709a, 2710a and 2711a were 0.2%, 0.1%, 0.2%, 0.02% and 0.03% m/m.

Our future goal is to advance the use of portable ED-XRF in measuring concentrations of heavy metals in urban soil in situ. As demonstrated in recent work completed by Perroy et al. (2014) and Weindorf et al. (2012), portable ED-XRF is a promising tool for use in urban agriculture/geochemistry investigations. With the increased information provided in this investigation, the bias in custom calibration routines for portable ED-XRF spectrometers developed with the characterized NIST SRMs will be reduced.

## 2.4    CONCLUSIONS

Eighty-five per cent of ICP-MS measurements (made at the Wisconsin State Laboratory of Hygiene, Madison, Wisconsin) and 97% of WD-XRF measurements (made at the Department of Geosciences, University of Wisconsin– Milwaukee) generated in this data assessment exercise when compared with NIST certified, reference and information values fell within a control limit of ± 20% relative difference. This provides confidence in the values for the major and minor elements reported in this study. We have described the variability in concentrations of up to forty-nine elements (plus LOI) and have provided values for up to twenty-one elements previously uncharacterized by NIST in soil reference materials NIST SRM 2709a, 2710a, 2711a, 2586 and 2587. The additional characterization provided in this investigation will contribute to reducing measurement uncertainty in custom calibration routines and improving the quality of control checks developed using these NIST reference materials.

## 2.5    REFERENCES

Alvarez-Toral A, Fernandez B, Malherbe J, Claverie F, Molloy JL, Pereiro R and Sanz-Medel A (2013). Isotope dilution mass spectrometry for quantitative elemental analysis of powdered samples by radio frequency pulsed glow discharge time of flight mass spectrometry. Talanta, 115, 657–664.

Clark HF, Brabander DJ and Erdil RM (2006). Sources, Sinks, and Exposure Pathways of Lead in Urban Garden Soil. Journal of Environmental Quality, 35, 2066-2074.

Clark HF, Hausladen DM and Brabander DJ (2008). Urban gardens: Lead exposure, recontamination mechanisms, and implications for remediation design. Environmental Research, 107, 312– 319.

Claverie F, Malherbe J, Bier N, Molloy JL and Long SE (2013). Putting a spin on LA-ICP-MS analysis combined to isotope dilution. Anal Bioanal Chem, 405, 2289–2299.

Cloquet C, Rouxel O, Carignan J and Libourel G (2005). Natural Cadmium Isotopic Variations in Eight Geological Reference Materials (NIS T SRM 27 11, BCR 1 76, GSS-1, GXR-1, GXR-2, GSD-12, Nod-P -1, Nod-A-1) and Anthropogenic Samples, Measured by MC-ICP-MS. Geostandards and Geoanalytical Research, 29, 95-106.

Defoe PP, Hettiarachchi GM, Benedict C and Martin S (2014). Safety of Gardening on Lead and Arsenic Contaminated Urban Brownfields. Journal of Environmental Quality, 4, 2064-2078.

Eriksson SM, Mackey EA, Lindstrom RM, Lamaze GP, Grogan KP and Brady DE (2013). Delayed-neutron activation analysis at NIST. J Radioanal Nucl Chem, 298, 1819–1822.

Fernández B, Rodríguez-González P, Ignacio García Alonso J, Malherbe J, García-Fonseca S, Pereiro R and Sanz-Medel A (2014). On-line double isotope dilution laser ablation inductively coupled plasma mass spectrometry for the quantitative analysis of solid materials. Analytica Chimica Acta, 851, 64–71.

Finster ME, Gray KA and Binns HJ (2004). Lead levels of edibles grown in contaminated residential soils: a field survey. The Science of the Total Environment, 320, 245-257.

Goix S, Point D, Oliva P, Polve M, Duprey JL, Mazurek H, Guislain L, Huayta C, Barbieri FL and Gardon J (2011). Influence of source distribution and geochemical composition of aerosols on children exposure in the large polymetallic mining region of the Bolivian Altiplano. Science of the Total Environment, 412, 170–184.

Gueguen B, Rouxel O, Ponzevera E, Bekker A and Fouquet Y (2013). Nickel Isotope Variations in Terrestrial Silicate Rocks and Geological Reference Materials Measured by MC-ICP-MS. Geostandards and Geoanalytical Research, 37, 297–317.

Hoang TH, Bang S, Kim K-W, Nguyen MH and Dang DM (2010). Arsenic in groundwater and sediment in the Mekong River delta, Vietnam. Environmental Pollution, 158, 2648–2658.

Hu W, Huang B, Weindorf DC and Chen Y (2014). Metals Analysis of Agricultural Soils via Portable X-ray Fluorescence Spectrometry. Bull Environ Contam Toxicol, 92, 420–426.

Huang Z-Y, Chen T, Yu J, Qin D-P and Chen L (2012). Lead contamination and its potential sources in vegetables and soils of Fujian, China. Environ Geochem Health, 34, 55–65.

Kenna TC, Nitsche FO, Herron MM, Mailloux BJ, Peteet D, Sritrairat S, Sands E and Baumgarten J (2011). Evaluation and calibration of a Field Portable X-Ray Fluorescence spectrometer for quantitative analysis of siliciclastic soils and sediments. Journal of Analytical Atomic Spectrometry, 26, 395–405.

Makinen E, Korhonen M, Viskari E-L, Haapamaki S, Jarvinen M and Lu L (2005). Comparison of XRF and FAAS Methods in Analysinig CCA Contaminated Soils. Water, Air, and Soil Pollution, 171, 95-110.

May W, Parris R, Beck C, Fassett J, Greenberg R, Guenther F, Kramer G, Wise S, Gills T, Colbert J, Gettings R and MacDonald B (2000). Definitions of Terms and Modes Used at NIST for Value-Assignment of Reference Materials for Chemical Measurements. NIST Special Publication 260-136.

McBride MB, Shayler HA, Spliethoff HM, Mitchell RG, Marquez-Bravo LG, Ferenz GS, Russell-Anelli JM, Casey L and Bachman S (2014). Concentrations of lead, cadmium and barium in urban garden-grown vegetables: The impact of soil variables. Environmental Pollution, 194, 254-261.

McComb JQ, Rogers C, Han FX and Tchounwou PB (2014). Rapid Screening of Heavy Metals and Trace Elements in Environmental Samples Using Portable X-Ray Fluorescence Spectrometer, A Comparative Study. Water Air Soil Pollut, 225, 2169.

McHenry LJ, Chevrier V and Schröder C (2011). Jarosite in a Pleistocene East African saline-alkaline paleolacustrine deposit: Implications for Mars aqueous geochemistry. Journal of Geophysical Research, 116, E04002.

McHenry, LJ (2009). Element mobility during zeolitic and argillic alteration of volcanic ash in a closed-basin lacustrine environment: Case study Olduvai Gorge, Tanzania. Chemical Geology, 265, 540–552.

Milliard A, Durand-Jézéquel M and Larivière D (2011). Sequential automated fusion/extraction chromatography methodology for the dissolution of uranium in environmental samples for mass spectrometric determination. Analytica Chimica Acta, 684, 40–46.

Moon JH, Dung HM, Kim SH and Chung YS (2009). Implementation of the k0-NAA method by using k0-IAEA software and the NAA#3 irradiation hole at the HANARO research reactor. J. Radioanal Nucl Chem, 280, 439–444.

Murray H, Pinchin TA and Macfie SM (2011). Compost application affects metal uptake in plants grown in urban garden soils and potential human health risk. J. Soils Sediments, 11, 815-829.

Paul RL, Mackey EA, Zeisler R, Spatz RO and Tomlin BE (2009). Determination of elements in SRM soil 2709a by neutron activation analysis. J Radioanal Nucl Chem, 282, 945–950.

Perroy RL, Belby CS and Mertens CJ (2014). Mapping and modeling three dimensional lead contamination in the wetland sediments of a former trap-shooting range. Science of the Total Environment, 487, 72–81.

Sharma K, Basta NT and Grewal PS (2015). Soil heavy metal contamination in residential neighborhoods in post-industrial cities and its potential human exposure risk. Urban Ecosyst, 18, 115–132.

Sutton M, Bibby RK, Eppich GR, Lee S, Lindvall RE, Wilson K and Esser BK (2012). Evaluation of historical beryllium abundance in soils, airborne particulates and facilities at Lawrence Livermore National Laboratory. Science of the Total Environment, 437, 373–383.

Thomsen V, Schatzlein D and Mercuro D (2003). Limits of Detection in Spectroscopy. Spectroscopy, 18, 112-114.

Wang Z and Becker H (2013). Abundances of Sulfur, Selenium, Tellurium, Rhenium and Platinum-Group Elements in Eighteen Reference Materials by Isotope Dilution Sector-Field ICP-MS and Negative TIMS. Geostandards and Geoanalytical Research, 38, 189-209.

Weindorf DC, Zhu Y, Chakraborty S, Bakr N and Huang B (2012). Use of portable X-ray fluorescence spectrometry for environmental quality assessment of peri-urban agriculture. Environ Monit Assess, 184, 217–227.

Wilson SA, Briggs PH, Mee JS and Siems DF (1994). Determination of thirty-two major and trace elements in three NIST soil SRMs using ICP-AES and WDXRF. Geostandards Newsletter, 18, 85-89.

USEPA (2007). Method 6020a Inductively Coupled Plasma-Mass Spectrometry. In: U.S. Environmental Protection Agency's Office of Solid Waste, Test Methods for Evaluating Solid Waste, Physical/Chemical Methods, SF 846, 6010A-1 – 6010A-30.

USEPA (2014). National Functional Guidelines for Inorganic Superfund Data Review, USEPA-540-R-13-001.

Figure 2.1. Relative Difference between NIST and WSLH Measurements.
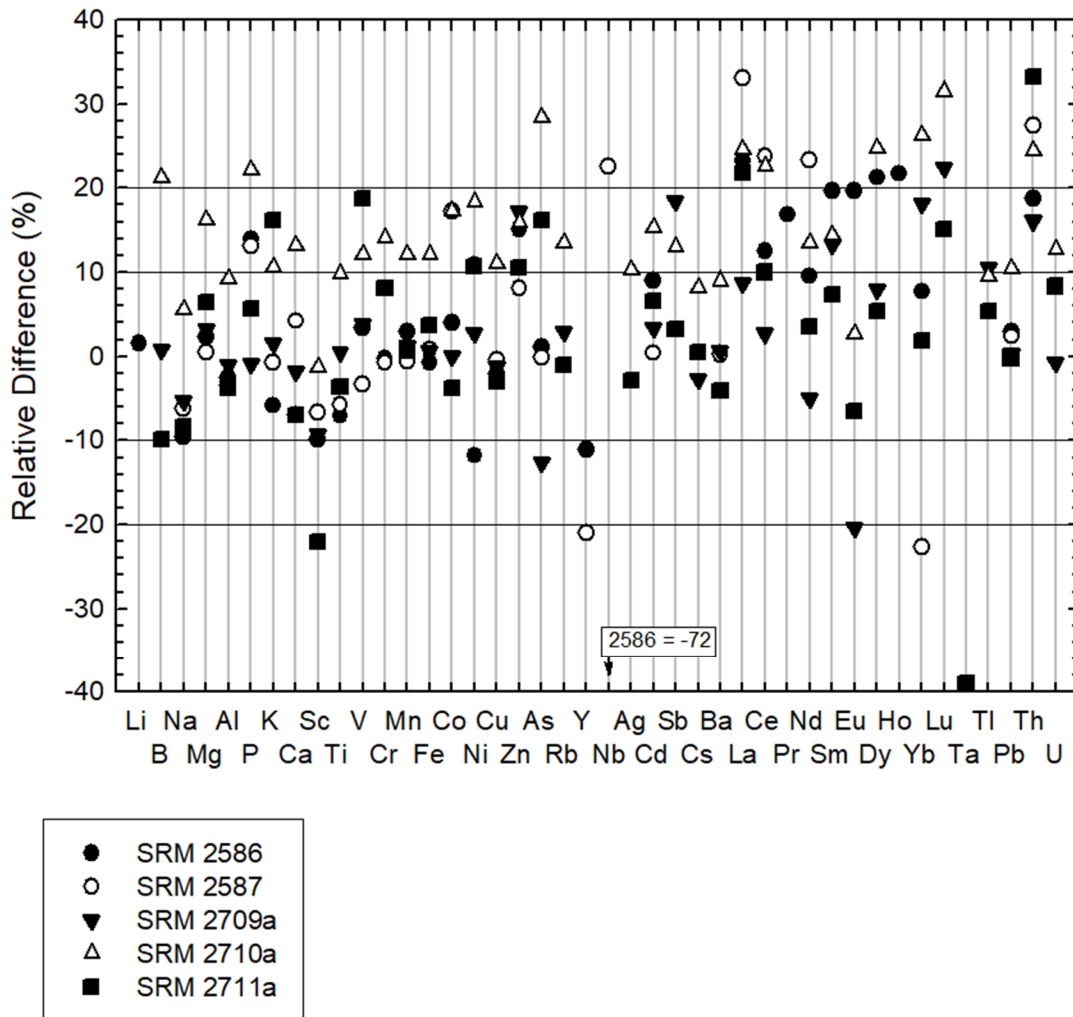


Note. Positive values indicate NIST values > WSLH measurements. Relative differences outside

the presented intervals are provided as text on the figure.

Figure 2.2. Relative Difference between NIST and Fused Bead WD-XRF Measurements.
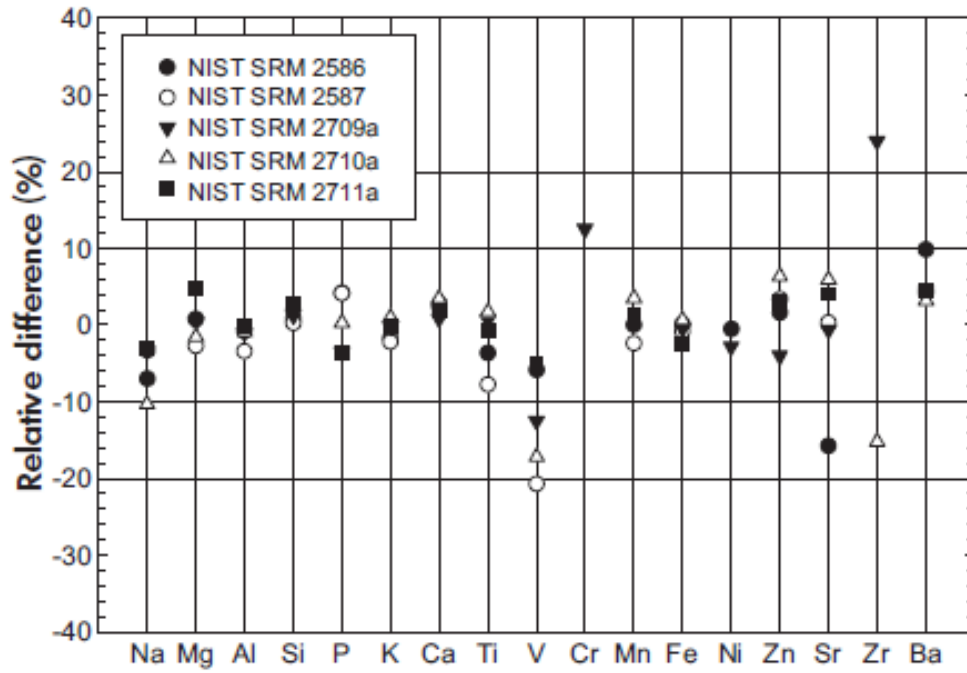


Note. Positive values indicate NIST values > Fused Bead WD-XRF measurements.

Figure 2.3. Relative Difference between WSLH and Literature Values.
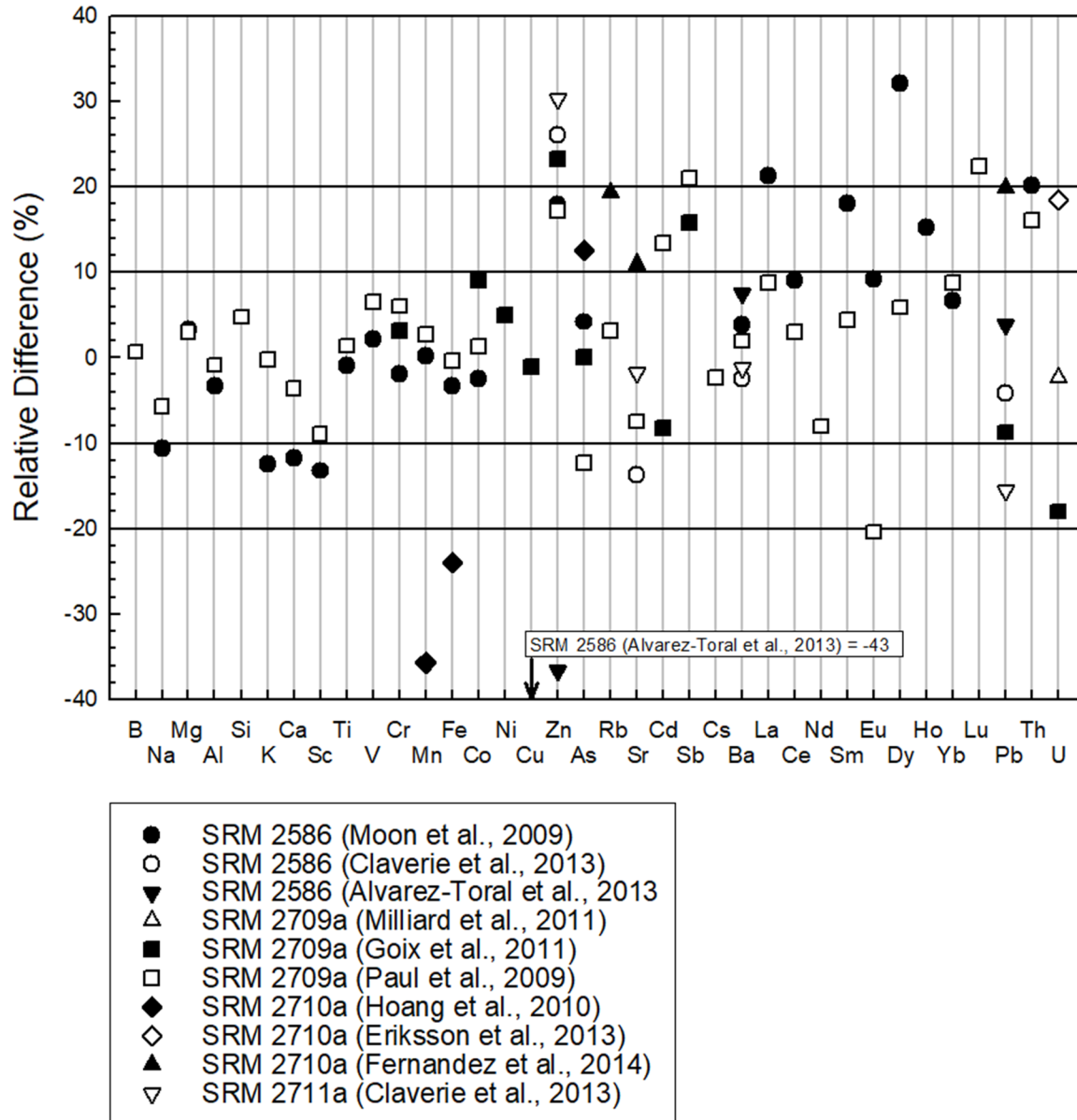


Note. Positive values indicate WSLH measurements > Literature Values.

Table 2.1. Element concentrations in NIST SRM 2586 determined using three measurement methods.

| | WD-XRF (FB) | | | WD-XRF (PP) | | | ICP-MS | | | NIST | |
|---|---|---|---|---|---|---|---|---|---|---|---|
| | g/100 g | 1 s ($\mu g\,g^{-1}$) | RSD | g/100 g | 1 s ($\mu g\,g^{-1}$) | RSD | g/100 g | 1 s ($\mu g\,g^{-1}$) | RSD | g/100 g | ± |
| Na | 0.50 | 113 | 2 | – | – | – | 0.52 | 63 | 1 | 0.468 | 730 |
| Mg | 1.69 | 0 | 0 | 2.48 | 265 | 1 | 1.67 | 51 | 0.3 | 1.707 | 840 |
| Al | 6.70 | 106 | 0.2 | 7.00 | 2570 | 2 | 6.83 | 2673 | 4 | 6.652 | 760 |
| Si | 28.94 | 546 | 0.2 | 28.72 | 6050 | 1 | – | – | – | 29.150 | 2100 |
| K | 0.99 | 48 | 0.4 | 1.01 | 115 | 1 | 1.03 | 1323 | 13 | 0.976 | 180 |
| Ca | 2.16 | 0 | 0 | 2.79 | 58 | 0.1 | 2.38 | 2695 | 11 | 2.218 | 540 |
| Fe | 5.16 | 162 | 0.3 | 5.96 | 58 | 0.1 | 5.20 | 918 | 2 | 5.161 | 890 |

Table 2.2. Element concentrations in NIST SRM 2587 determined using three measurement methods.

| | WD-XRF (FB) | | | WD-XRF (PP) | | | ICP-MS | | | NIST | |
|------|---------|------------------|-----|---------|------------------|-----|---------|------------------|-----|---------|------|
| | g/100 g | 1 s ($\mu$g g$^{-1}$) | RSD | g/100 g | 1 s ($\mu$g g$^{-1}$) | RSD | g/100 g | 1 s ($\mu$g g$^{-1}$) | RSD | g/100 g | $\pm$ |
| Na | 1.16 | 0 | 0 | – | – | – | 1.20 | 69 | 1 | 1.13 | 330 |
| Mg | 0.69 | 0 | 0 | 1.33 | 100 | 0.4 | 0.67 | 374 | 6 | 0.67 | 250 |
| Al | 6.07 | 140 | 0.2 | 6.33 | 208 | 0.2 | 6.07 | 3184 | 5 | 5.86 | 1700 |
| Si | 33.06 | 221 | 0.1 | 32.86 | 1966 | 0.3 | – | – | – | 33.13 | 2600 |
| K | 1.62 | 0 | 0 | 1.68 | 58 | 0.3 | 1.60 | 1801 | 11 | 1.58 | 550 |
| Ca | 0.91 | 41 | 0.4 | 1.32 | 0 | 0 | 0.89 | 728 | 8 | 0.93 | 200 |
| Fe | 2.84 | 107 | 0.4 | 3.11 | 100 | 0.2 | 2.79 | 1096 | 4 | 2.81 | 250 |

Table 2.3. Element concentrations in NIST SRM 2709a determined using three measurement methods.

| | WD-XRF (FB) | | | WD-XRF (PP) | | | ICP-MS | | | NIST | |
|---|---|---|---|---|---|---|---|---|---|---|---|
| | g/100 g | 1 s ($\mu g\ g^{-1}$) | RSD | g/100 g | 1 s ($\mu g\ g^{-1}$) | RSD | g/100 g | 1 s ($\mu g\ g^{-1}$) | RSD | g/100 g | ± |
| Na | 1.26 | 74 | 1 | – | – | – | 1.29 | 1150 | 9 | 1.22 | 300 |
| Mg | 1.45 | 60 | 0.4 | 2.52 | 208 | 0.4 | 1.41 | 1008 | 7 | 1.46 | 200 |
| Al | 7.44 | 360 | 0.4 | 7.76 | 3177 | 2 | 7.45 | 6528 | 9 | 7.37 | 1600 |
| Si | 29.93 | 1374 | 0.4 | 27.87 | 6372 | 1 | – | – | – | 30.30 | 4000 |
| K | 2.11 | 48 | 0.2 | 2.00 | 100 | 0.4 | 2.08 | 1611 | 8 | 2.11 | 600 |
| Ca | 1.89 | 0 | 0 | 2.52 | 153 | 0.4 | 1.94 | 1233 | 6 | 1.91 | 900 |
| Fe | 3.38 | 214 | 1 | 4.09 | 586 | 1 | 3.34 | 1026 | 3 | 3.36 | 700 |

Table 2.4. Element concentrations in NIST SRM 2710a determined using three measurement methods.

| | WD-XRF (FB) | | | WD-XRF (PP) | | | ICP-MS | | | NIST | |
|---|---|---|---|---|---|---|---|---|---|---|---|
| | g/100 g | 1 s ($\mu g\, g^{-1}$) | RSD | g/100 g | 1 s ($\mu g\, g^{-1}$) | RSD | g/100 g | 1 s ($\mu g\, g^{-1}$) | RSD | g/100 g | ± |
| Na | 0.99 | 43 | 0.4 | – | – | – | 0.85 | 872 | 10 | 0.89 | 190 |
| Mg | 0.75 | 35 | 0.4 | 0.87 | 0 | 0 | 0.62 | 500 | 8 | 0.73 | 380 |
| Al | 6.00 | 372 | 1 | 6.31 | 2747 | 2 | 5.43 | 4330 | 8 | 5.95 | 500 |
| Si | 30.31 | 1362 | 0.4 | 28.84 | 6523 | 1 | – | – | – | 31.10 | 4000 |
| K | 2.15 | 0 | 0 | 2.20 | 58 | 0.2 | 1.95 | 883 | 5 | 2.17 | 1300 |
| Ca | 0.93 | 41 | 0.4 | 1.48 | 58 | 0.3 | 0.84 | 734 | 9 | 0.96 | 450 |
| Fe | 4.29 | 331 | 1 | 4.72 | 473 | 1 | 3.83 | 3102 | 8 | 4.32 | 800 |

Table 2.5. Element concentrations in NIST SRM 2711a determined using three measurement methods.

| | WD-XRF (FB) | | | WD-XRF (PP) | | | ICP-MS | | | NIST | |
|---|---|---|---|---|---|---|---|---|---|---|---|
| | g/100 g | 1 s ($\mu$g g$^{-1}$) | RSD | g/100 g | 1 s ($\mu$g g$^{-1}$) | RSD | g/100 g | 1 s ($\mu$g g$^{-1}$) | RSD | g/100 g | ± |
| Na | 1.24 | 113 | 1 | – | – | – | 1.30 | 1169 | 9 | 1.20 | 100 |
| Mg | 1.02 | 0 | 0 | 1.66 | 173 | 1 | 1.00 | 340 | 3 | 1.07 | 600 |
| Al | 6.73 | 397 | 1 | 6.75 | 2512 | 2 | 6.98 | 4559 | 7 | 6.72 | 600 |
| Si | 30.55 | 742 | 0.2 | 28.78 | 7410 | 1 | – | – | – | 31.40 | 7000 |
| K | 2.53 | 0 | 0 | 2.58 | 115 | 0.4 | 2.15 | 7479 | 35 | 2.53 | 1000 |
| Ca | 2.37 | 0 | 0 | 2.76 | 58 | 0.1 | 2.59 | 2725 | 11 | 2.42 | 600 |
| Fe | 2.89 | 40 | 0.1 | 3.20 | 321 | 1 | 2.72 | 578 | 2 | 2.82 | 400 |

Table 2.6. Element concentrations in NIST SRM 2586 determined using three measurement methods.

| | WD-XRF (FB) | | | WD-XRF (PP) | | | ICP-MS | | | NIST | |
|---|---|---|---|---|---|---|---|---|---|---|---|
| | ($\mu$g g$^{-1}$) | (1 s) | RSD | ($\mu$g g$^{-1}$) | (1 s) | RSD | ($\mu$g g$^{-1}$) | (1 s) | RSD | ($\mu$g g$^{-1}$) | ± |
| Li | – | – | – | – | – | – | 24.61 | 1.87 | 8 | 25 | – |
| B | – | – | – | – | – | – | 50.93 | 0.00 | 0 | – | – |
| P | 960.1 | 0.0 | 0 | 1352.9 | 0.0 | 0 | 870.53 | 67.15 | 8 | 1001 | 77 |
| Sc | – | – | – | – | – | – | 26.49 | 0.74 | 3 | 24 | – |
| Ti | 6273.1 | 34.6 | 1 | 6872.5 | 115.5 | 2 | 6492.62 | 335.33 | 5 | 6050 | 660 |
| V | 169.6 | 1.1 | 1 | 205.3 | 18.8 | 9 | 154.76 | 3.80 | 2 | 160 | – |
| Cr | – | – | – | 356.0 | 9.8 | 3 | 301.73 | 11.79 | 4 | 301 | 45 |
| Mn | 1000.0 | 0.0 | 0 | 1033.3 | 57.7 | 6 | 971.20 | 6.33 | 1 | 1000 | 18 |
| Co | 28 J | 3.0 | 11 | – | – | – | 33.63 | 0.71 | 2 | 35 | – |
| Ni | 75.4 | 4.0 | 5 | 80.7 | 1.2 | 1 | 84.39 | 2.27 | 3 | 75 | – |
| Cu | – | – | – | 92.0 | 7.8 | 8 | 82.77 | 2.98 | 4 | 81 | – |
| Zn | 346.3 | 5.8 | 2 | 363.7 | 5.9 | 2 | 302.51 | 46.16 | 15 | 352 | 16 |
| Ga | – | – | – | 20.7 | 0.6 | 3 | – | – | – | 14 | – |
| As | – | – | – | – | – | – | 8.60 | 0.61 | 7 | 8.7 | 1.5 |
| Rb | – | – | – | 61.0 | 1.7 | 3 | 49.01 | 3.76 | 8 | – | – |
| Sr | 98.5 | 2.9 | 3 | 92.0 | 1.7 | 2 | – | – | – | 84.1 | 8 |
| Y | – | – | – | 27.0 | 1.0 | 4 | 23.46 | 1.11 | 5 | 21 | – |
| Zr | 277.9 | 4.6 | 2 | 287.7 | 1.5 | 1 | – | – | – | – | – |
| Nb | – | – | – | – | – | – | 12.74 | 0.33 | 3 | 6 | – |
| Mo | – | – | – | – | – | – | 1.11 | 0.25 | 23 | – | – |
| Ag | – | – | – | – | – | – | 0.55 | 0.09 | 17 | – | – |
| Cd | – | – | – | – | – | – | 2.48 | 0.23 | 9 | 2.71 | 0.54 |
| Sn | – | – | – | – | – | – | 13.29 | 0.05 | 0 | – | – |
| Sb | – | – | – | – | – | – | 3.07 | 0.11 | 3 | – | – |
| Cs | – | – | – | – | – | – | 1.93 | 0.16 | 9 | – | – |
| Ba | 374.4 | 34.8 | 9 | 491.3 | 16.5 | 3 | 411.72 | 15.61 | 4 | 413 | 18 |
| La | – | – | – | – | – | – | 23.52 | 0.40 | 2 | 29.7 | 4.8 |
| Ce | – | – | – | 66.3 | 29.2 | 44 | 51.17 | 2.08 | 4 | 58 | 8 |
| Pr | – | – | – | – | – | – | 6.17 | 0.18 | 3 | 7.3 | – |
| Nd | – | – | – | – | – | – | 24.00 | 0.84 | 4 | 26.4 | 2.9 |
| Sm | – | – | – | – | – | – | 5.01 | 0.27 | 5 | 6.1 | – |
| Eu | – | – | – | – | – | – | 1.23 | 0.03 | 3 | 1.5 | – |
| Dy | – | – | – | – | – | – | 4.36 | 0.21 | 5 | 5.4 | – |
| Ho | – | – | – | – | – | – | 0.88 | 0.02 | 3 | 1.1 | – |
| Yb | – | – | – | – | – | – | 2.44 | 0.09 | 4 | 2.64 | 0.51 |
| Lu | – | – | – | – | – | – | 0.35 | 0.01 | 3 | – | – |
| Ta | – | – | – | – | – | – | 0.85 | 0.00 | 0 | – | – |
| W | – | – | – | – | – | – | 1.24 | 0.28 | 22 | – | – |
| Tl | – | – | – | – | – | – | 0.35 | 0.01 | 2 | – | – |
| Pb | – | – | – | – | – | – | 419.48 | 14.41 | 3 | 432 | 17 |
| Th | – | – | – | – | – | – | 5.80 | 0.05 | 1 | 7 | – |
| U | – | – | – | – | – | – | 1.90 | 0.02 | 1 | – | – |

Note. Element concentrations qualified with a "J" are greater than the limit of detection, but less than the limit of quantitation. Shaded rows represent elements not characterized by NIST.

Table 2.7. Element concentrations in NIST SRM 2587 determined using three measurement methods.

| | WD-XRF (FB) | | | WD-XRF (PP) | | | ICP-MS | | | NIST | |
|---|---|---|---|---|---|---|---|---|---|---|---|
| | ($\mu g\,g^{-1}$) | (1 s) | RSD | ($\mu g\,g^{-1}$) | (1 s) | RSD | ($\mu g\,g^{-1}$) | (1 s) | RSD | ($\mu g\,g^{-1}$) | ± |
| Li | – | – | – | – | – | – | 34.19 | 2.83 | 8 | 32 | – |
| B | – | – | – | – | – | – | 66.84 | 3.32 | 5 | – | – |
| P | 931.0 | 25.2 | 3 | 1352.9 | 0.0 | 0 | 851.06 | 70.98 | 8 | 970 | 100 |
| Sc | – | – | – | – | – | – | 11.76 | 1.07 | 9 | 11 | – |
| Ti | 4235.4 | 34.6 | 1 | 4495.1 | 0.0 | 0 | 4153.97 | 185.30 | 4 | 3920 | 650 |
| V | 96.1 | 6.9 | 7 | 109.0 | 1.7 | 2 | 80.64 | 2.70 | 3 | 78 | – |
| Cr | – | – | – | 99.7 | 4.2 | 4 | 92.67 | 5.02 | 5 | 92 | 11 |
| Mn | 666.7 | 57.7 | 9 | 669.7 | 6.7 | 1 | 655.46 | 28.47 | 4 | 651 | 23 |
| Co | – | – | – | – | – | – | 11.78 | 0.32 | 3 | 14 | – |
| Ni | 43 J | 2.4 | 6 | 37.0 | 2.6 | 7 | 32.28 | 1.95 | 6 | 36 | – |
| Cu | – | – | – | 170.7 | 2.5 | 1 | 160.68 | 3.52 | 2 | 160 | – |
| Zn | 324.7 | 6.4 | 2 | 341.0 | 1.7 | 1 | 309.74 | 34.87 | 11 | 335.8 | 7.6 |
| Ga | – | – | – | 24.0 | 1.0 | 4 | – | – | – | 13 | – |
| As | – | – | – | – | – | – | 13.71 | 1.38 | 10 | 13.7 | 2.3 |
| Rb | – | – | – | 82.7 | 2.5 | 3 | 72.30 | 4.97 | 7 | – | – |
| Sr | 125.6 | 4.5 | 4 | 131.7 | 2.9 | 2 | – | – | – | 126 | 19 |
| Y | – | – | – | 28.0 | 0.0 | 0 | 18.51 | 1.16 | 6 | 15 | – |
| Zr | 296.0 | 4.4 | 1 | 269.0 | 0.0 | 0 | – | – | – | – | – |
| Nb | – | – | – | – | – | – | 11.17 | 0.32 | 3 | 14 | – |
| Mo | – | – | – | – | – | – | 1.64 | 0.20 | 12 | – | – |
| Cd | – | – | – | – | – | – | 1.91 | 0.14 | 7 | 1.92 | 0.23 |
| Sn | – | – | – | – | – | – | 17.10 | 5.73 | 33 | – | – |
| Sb | – | – | – | – | – | – | 2.10 | 0.34 | 16 | – | – |
| Cs | – | – | – | – | – | – | 3.10 | 0.30 | 10 | – | – |
| Ba | 544.3 | 12.7 | 2 | 650.3 | 1.2 | 0 | 566.81 | 25.03 | 4 | 568 | 12 |
| La | – | – | – | – | – | – | 20.77 | 1.42 | 7 | 29 | – |
| Ce | – | – | – | 82.7 | 4.0 | 5 | 44.89 | 2.81 | 6 | 57 | – |
| Pr | – | – | – | – | – | – | 5.09 | 0.27 | 5 | – | – |
| Nd | – | – | – | – | – | – | 19.77 | 1.18 | 6 | 25 | – |
| Sm | – | – | – | – | – | – | 3.95 | 0.19 | 5 | – | – |
| Eu | – | – | – | – | – | – | 1.03 | 0.06 | 6 | – | – |
| Dy | – | – | – | – | – | – | 3.38 | 0.26 | 8 | – | – |
| Ho | – | – | – | – | – | – | 0.68 | 0.04 | 6 | – | – |
| Yb | – | – | – | – | – | – | 2.01 | 0.10 | 5 | 1.6 | – |
| Lu | – | – | – | – | – | – | 0.29 | 0.02 | 7 | – | – |
| Tl | – | – | – | – | – | – | 0.48 | 0.03 | 7 | – | – |
| Pb | – | – | – | – | – | – | 3165.52 | 195.50 | 6 | 3242 | 57 |
| Th | – | – | – | – | – | – | 5.69 | 0.29 | 5 | 7.5 | – |
| U | – | – | – | – | – | – | 2.08 | 0.17 | 8 | – | – |

Note. Element concentrations qualified with a "J" are greater than the limit of detection, but less than the limit of quantitation. Shaded rows represent elements not characterized by NIST.

Table 2.8. Element concentrations in NIST SRM 2709a determined using three measurement methods.

| | WD-XRF (FB) | | | WD-XRF (PP) | | | ICP-MS | | | NIST | |
|---|---|---|---|---|---|---|---|---|---|---|---|
| | (µg g$^{-1}$) | (1 s) | RSD | (µg g$^{-1}$) | (1 s) | RSD | (µg g$^{-1}$) | (1 s) | RSD | (µg g$^{-1}$) | ± |
| Li | – | – | – | – | – | – | 51.88 | 0.74 | 1 | – | – |
| B | – | – | – | – | – | – | 73.42 | 2.14 | 3 | 74 | – |
| P | 712.8 | 25.2 | 4 | 1352.9 | 0.0 | 0 | 694.49 | 45.98 | 7 | 688 | 13 |
| Sc | – | – | – | – | – | – | 12.18 | 0.85 | 7 | 11.1 | 0.1 |
| Ti | 3336.3 | 34.6 | 1 | 3895.7 | 0.0 | 0 | 3344.09 | 102.09 | 3 | 3360 | 70 |
| V | 124.7 | 12.3 | 10 | 154.3 | 4.5 | 3 | 105.96 | 4.05 | 4 | 110 | 11 |
| Cr | 114.7 | 9.9 | 9 | 151.0 | 1.7 | 1 | 119.58 | 3.21 | 3 | 130 | 9 |
| Mn | 500 J | 0.0 | 0 | 593.3 | 7.6 | 1 | 522.47 | 4.74 | 1 | 529 | 18 |
| Co | – | – | – | – | – | – | 12.79 | 0.28 | 2 | 12.8 | 0.2 |
| Ni | 87.4 | 7.9 | 9 | 87.3 | 2.1 | 2 | 82.71 | 6.55 | 8 | 85 | 2 |
| Cu | – | – | – | 54.7 | 2.5 | 5 | 34.34 | 2.42 | 7 | 33.9 | 0.5 |
| Zn | 107.2 | 4.2 | 4 | 108.0 | 1.7 | 2 | 86.74 | 7.83 | 9 | 103 | 4 |
| Ga | – | – | – | 22.7 | 0.6 | 3 | – | – | – | – | – |
| As | – | – | – | – | – | – | 11.92 | 3.04 | 25 | 10.5 | 0.3 |
| Rb | – | – | – | 111.3 | 0.6 | 1 | 96.16 | 2.31 | 2 | 99 | 3 |
| Sr | 240.5 | 2.3 | 1 | 270.3 | 2.5 | 1 | – | – | – | 239 | 6 |
| Y | – | – | – | 27.3 | 0.6 | 2 | 15.34 | 0.62 | 4 | – | – |
| Zr | 153.2 | 4.0 | 3 | 170.3 | 1.2 | 1 | – | – | – | 195 | 46 |
| Nb | – | – | – | – | – | – | 8.61 | 0.09 | 1 | – | – |
| Mo | – | – | – | – | – | – | 1.30 | 0.36 | 27 | – | – |
| Ag | – | – | – | – | – | – | 0.31 | 0.08 | 25 | – | – |
| Cd | – | – | – | – | – | – | 0.36 | 0.03 | 8 | 0.371 | 0.002 |
| Sn | – | – | – | – | – | – | 1.87 | 0.78 | 42 | – | – |
| Sb | – | – | – | – | – | – | 1.29 | 0.49 | 38 | 1.55 | 0.06 |
| Cs | – | – | – | – | – | – | 5.14 | 0.21 | 4 | 5 | 0.1 |
| Ba | 936.6 | 5.4 | 1 | 1100.0 | 0.0 | 0 | 972.86 | 16.19 | 2 | 979 | 28 |
| La | – | – | – | – | – | – | 19.89 | 1.10 | 6 | 21.7 | 0.4 |
| Ce | – | – | – | 194.0 | 4.4 | 2 | 40.89 | 1.75 | 4 | 42 | 1 |
| Pr | – | – | – | – | – | – | 4.68 | 0.13 | 3 | – | – |
| Nd | – | – | – | – | – | – | 17.88 | 0.35 | 2 | 17 | – |
| Sm | – | – | – | – | – | – | 3.50 | 0.13 | 4 | 4 | – |
| Eu | – | – | – | – | – | – | 1.02 | 0.06 | 6 | 0.83 | 0.02 |
| Dy | – | – | – | – | – | – | 2.77 | 0.10 | 4 | 3 | – |
| Ho | – | – | – | – | – | – | 0.57 | 0.01 | 2 | – | – |
| Yb | – | – | – | – | – | – | 1.67 | 0.04 | 2 | 2 | – |
| Lu | – | – | – | – | – | – | 0.24 | 0.01 | 5 | 0.3 | – |
| Tl | – | – | – | – | – | – | 0.52 | 0.05 | 10 | 0.58 | 0.01 |
| Pb | – | – | – | – | – | – | 17.26 | 0.77 | 4 | 17.3 | 0.1 |
| Th | – | – | – | – | – | – | 9.28 | 0.28 | 3 | 10.9 | 0.2 |
| U | – | – | – | – | – | – | 3.17 | 0.14 | 4 | 3.15 | 0.05 |

Note. Element concentrations qualified with a "J" are greater than the limit of detection, but less than the limit of quantitation. Shaded rows represent elements not characterized by NIST.

Table 2.9. Element concentrations in NIST SRM 2710a determined using three measurement methods.

| | WD-XRF (FB) | | | WD-XRF (PP) | | | ICP-MS | | | NIST | |
|---|---|---|---|---|---|---|---|---|---|---|---|
| | ($\mu g\,g^{-1}$) | (1 s) | RSD | ($\mu g\,g^{-1}$) | (1 s) | RSD | ($\mu g\,g^{-1}$) | (1 s) | RSD | ($\mu g\,g^{-1}$) | ± |
| Li | – | – | – | – | – | – | 24.57 | 0.58 | 2 | – | – |
| B | – | – | – | – | – | – | 16.16 | 0.26 | 2 | 20 | – |
| P | 1047.4 | 0.0 | 0 | 1352.9 | 0.0 | 0 | 841.29 | 135.73 | 16 | 1050 | 40 |
| Sc | – | – | – | – | – | – | 10.03 | 0.80 | 8 | 9.9 | 0.1 |
| Ti | 3056.6 | 59.9 | 2 | 3416.3 | 0.0 | 0 | 2819.15 | 158.77 | 6 | 3110 | 70 |
| V | 97.4 | 14.8 | 15 | 112.3 | 2.5 | 2 | 72.69 | 3.84 | 5 | 82 | 9 |
| Cr | – | – | – | – | – | – | 19.98 | 1.00 | 5 | 23 | 6 |
| Mn | 2066.7 | 57.7 | 3 | 2200.0 | 0.0 | 0 | 1895.26 | 150.89 | 8 | 2140 | 60 |
| Co | – | – | – | – | – | – | 5.04 | 0.33 | 6 | 5.99 | 0.14 |
| Ni | – | – | – | 9 J | 1.5 | 18 | 6.66 | 1.57 | 24 | 8 | 1 |
| Cu | – | – | – | 3100.0 | 0.0 | 0 | 3062.89 | 412.13 | 13 | 3420 | 50 |
| Zn | 3923.2 | 33.3 | 1 | 4100.0 | 0.0 | 0 | 3567.00 | 631.33 | 18 | 4180 | 150 |
| Ga | – | – | – | 38.7 | 1.5 | 4 | – | – | – | – | – |
| As | – | – | – | – | – | – | 1157.05 | 29.31 | 3 | 1540 | 100 |
| Rb | – | – | – | 122.0 | 1.0 | 1 | 102.22 | 9.55 | 9 | 117 | 3 |
| Sr | 240.4 | 2.1 | 1 | 257.3 | 1.5 | 1 | – | – | – | 255 | 7 |
| Y | 27.6 | 1.2 | 4 | 29.0 | 0.0 | 0 | 13.27 | 1.10 | 8 | – | – |
| Zr | 232.9 | 4.9 | 2 | 233.7 | 2.1 | 1 | – | – | – | 200 | – |
| Nb | – | – | – | – | – | – | 11.32 | 0.79 | 7 | – | – |
| Mo | – | – | – | – | – | – | 7.61 | 0.61 | 8 | – | – |
| Ag | – | – | – | – | – | – | 36.11 | 3.21 | 9 | 40 | – |
| Cd | – | – | – | – | – | – | 10.55 | 1.76 | 17 | 12.3 | 0.3 |
| Sn | – | – | – | – | – | – | 8.89 | 1.03 | 12 | – | – |
| Sb | – | – | – | – | – | – | 46.12 | 5.44 | 12 | 52.5 | 1.6 |
| Cs | – | – | – | – | – | – | 7.61 | 0.88 | 12 | 8.25 | 0.11 |
| Ba | 767.3 | 25.4 | 3 | 941.0 | 11.8 | 1 | 724.21 | 54.64 | 8 | 792 | 36 |
| La | – | – | – | – | – | – | 23.92 | 2.77 | 12 | 30.6 | 1.2 |
| Ce | – | – | – | 148.0 | 9.5 | 6 | 47.86 | 4.63 | 10 | 60 | – |
| Pr | – | – | – | – | – | – | 5.22 | 0.45 | 9 | – | – |
| Nd | – | – | – | – | – | – | 19.22 | 1.72 | 9 | 22 | 2 |
| Sm | – | – | – | – | – | – | 3.46 | 0.27 | 8 | 4 | 0.2 |
| Eu | – | – | – | – | – | – | 0.80 | 0.11 | 14 | 0.82 | 0.01 |
| Dy | – | – | – | – | – | – | 2.34 | 0.22 | 9 | 3 | – |
| Ho | – | – | – | – | – | – | 0.48 | 0.04 | 9 | – | – |
| Yb | – | – | – | – | – | – | 1.54 | 0.17 | 11 | 2 | – |
| Lu | – | – | – | – | – | – | 0.23 | 0.02 | 11 | 0.31 | 0.01 |
| Tl | – | – | – | – | – | – | 1.38 | 0.18 | 13 | 1.52 | 0.02 |
| Pb | – | – | – | – | – | – | 4976.80 | 615.47 | 12 | 5520 | 30 |
| Th | – | – | – | – | – | – | 14.16 | 1.75 | 12 | 18.1 | 0.3 |
| U | – | – | – | – | – | – | 8.03 | 0.88 | 11 | 9.11 | 0.3 |

Note. Element concentrations qualified with a "J" are greater than the limit of detection, but less than the limit of quantitation. Shaded rows represent elements not characterized by NIST.

Table 2.10. Element concentrations in NIST SRM 2711a determined using three measurement methods.

| | WD-XRF (FB) | | | WD-XRF (PP) | | | ICP-MS | | | NIST | |
|---|---|---|---|---|---|---|---|---|---|---|---|
| | ($\mu g\,g^{-1}$) | (1 s) | RSD | ($\mu g\,g^{-1}$) | (1 s) | RSD | ($\mu g\,g^{-1}$) | (1 s) | RSD | ($\mu g\,g^{-1}$) | ± |
| Li | – | – | – | – | – | – | 29.05 | 1.47 | 5 | – | – |
| B | – | – | – | – | – | – | 55.22 | 9.41 | 17 | 50 | – |
| P | 872.8 | 0.0 | 0 | 1352.9 | 0.0 | 0 | 796.05 | 112.82 | 14 | 842 | 11 |
| Sc | – | – | – | – | – | – | 10.60 | 1.47 | 14 | 8.5 | 0.1 |
| Ti | 3196.5 | 34.6 | 1 | 3476.2 | 0.0 | 0 | 3287.54 | 195.65 | 6 | 3170 | 80 |
| V | 85.0 | 3.5 | 4 | 109.0 | 1.7 | 2 | 66.85 | 15.67 | 23 | 80.7 | 5.7 |
| Cr | – | – | – | 84.0 | 5.6 | 7 | 48.24 | 1.68 | 3 | 52.3 | 2.9 |
| Mn | 666.7 | 57.7 | 9 | 719.0 | 10.8 | 2 | 670.44 | 39.41 | 6 | 675 | 18 |
| Co | – | – | – | – | – | – | 10.27 | 1.38 | 13 | 9.89 | 0.18 |
| Ni | 18 J | 5.7 | 31 | 27 J | 1.5 | 6 | 19.50 | 1.60 | 8 | 21.7 | 0.7 |
| Cu | – | – | – | 151.7 | 4.0 | 3 | 144.31 | 20.14 | 14 | 140 | 2 |
| Zn | 401.7 | 5.8 | 1 | 418.3 | 7.6 | 2 | 372.74 | 96.70 | 26 | 414 | 11 |
| Ga | – | – | – | 24.7 | 0.6 | 2 | – | – | – | – | – |
| As | – | – | – | – | – | – | 90.96 | 8.63 | 9 | 107 | 5 |
| Rb | – | – | – | 136.0 | 3.0 | 2 | 121.29 | 12.95 | 11 | 120 | 3 |
| Sr | 232.4 | 2.0 | 1 | 256.0 | 1.7 | 1 | – | – | – | 242 | 10 |
| Y | 29.9 | 0.9 | 3 | 33.0 | 0.0 | 0 | – | – | – | – | – |
| Zr | 318.1 | 2.5 | 1 | 310.3 | 0.6 | 0 | – | – | – | – | – |
| Nb | – | – | – | – | – | – | 20.07 | 1.79 | 9 | – | – |
| Mo | – | – | – | – | – | – | 1.74 | 0.15 | 8 | – | – |
| Ag | – | – | – | – | – | – | 6.17 | 0.94 | 15 | 6 | – |
| Cd | – | – | – | – | – | – | 50.64 | 10.39 | 21 | 54.1 | 0.5 |
| Sn | – | – | – | – | – | – | 4.72 | 0.27 | 6 | – | – |
| Sb | – | – | – | – | – | – | 23.04 | 3.52 | 15 | 23.8 | 1.4 |
| Cs | – | – | – | – | – | – | 6.67 | 0.68 | 10 | 6.7 | 0.2 |
| Ba | 697.7 | 24.6 | 4 | 850.0 | 21.5 | 3 | 760.16 | 77.74 | 10 | 730 | 15 |
| La | – | – | – | – | – | – | 30.53 | 3.17 | 10 | 38 | 1 |
| Ce | – | – | – | 146.33 | 5.13 | 4 | 63.33 | 5.79 | 9 | 70 | – |
| Pr | – | – | – | – | – | – | 7.30 | 0.65 | 9 | – | – |
| Nd | – | – | – | – | – | – | 27.99 | 2.39 | 9 | 29 | 2 |
| Sm | – | – | – | – | – | – | 5.51 | 0.31 | 6 | 5.93 | 0.28 |
| Eu | – | – | – | – | – | – | 1.17 | 0.16 | 14 | 1.1 | 0.2 |
| Dy | – | – | – | – | – | – | 4.74 | 0.39 | 8 | 5 | – |
| Ho | – | – | – | – | – | – | 0.96 | 0.06 | 7 | – | – |
| Yb | – | – | – | – | – | – | 2.95 | 0.27 | 9 | 3 | – |
| Lu | – | – | – | – | – | – | 0.43 | 0.03 | 7 | 0.5 | – |
| Ta | – | – | – | – | – | – | 1.48 | 0.19 | 13 | 1 | – |
| W | – | – | – | – | – | – | 3.07 | 0.04 | 1 | – | – |
| Tl | – | – | – | – | – | – | 2.85 | 0.45 | 16 | 3 | – |
| Pb | – | – | – | – | – | – | 1402.88 | 225.33 | 16 | 1400 | 10 |
| Th | – | – | – | – | – | – | 10.72 | 1.35 | 13 | 15 | 1 |
| U | – | – | – | – | – | – | 2.77 | 0.35 | 13 | 3.01 | 0.12 |

Note. Element concentrations qualified with a "J" are greater than the limit of detection, but less than the limit of quantitation. Shaded rows represent elements not characterized by NIST.

Table 2.1S. Instrument setup and calibration routine details for WD-XRF fused bead analysis.

|  | Line | Generator Voltage (Kv) | Tube Current (mA) | Collimator (dg) | Analyzer Crystal | Detector | Peak Overlap Corrections |
|---|---|---|---|---|---|---|---|
| Al | Kα1 | 27 | 150 | 0.23 | PET | Flow Counter | Br Lα1 |
| Ba | Lα1 | 50 | 80 | 0.23 | Lif200 | Flow Counter | Ti Kα1 |
| Br | Lα1 | 27 | 150 | 0.23 | PET | Flow Counter | Al Kα1 |
| Ca | Kα1 | 50 | 81 | 0.46 | Lif200 | Flow Counter | *none* |
| Fe | Kα1 | 50 | 10 | 0.23 | Lif200 | Scintillation Counter | *none* |
| K | Kα1 | 50 | 81 | 0.46 | Lif200 | Flow Counter | *none* |
| Mg | Kα1 | 27 | 150 | 0.46 | OVO-55 | Flow Counter | Al Kα1 |
| Mn | Kα1 | 50 | 80 | 0.23 | Lif200 | Scintillation Counter | *none* |
| Na | Kα1 | 27 | 150 | 0.46 | OVO-55 | Flow Counter | *none* |
| Ni | Kα1 | 60 | 67 | 0.23 | Lif200 | Scintillation Counter | Fe Kβ1 |
| P | Kα1 | 27 | 150 | 0.46 | PET | Flow Counter | *none* |
| Si | Kα1 | 27 | 150 | 0.46 | PET | Flow Counter | Br Lγ2 |
| Sr | Kα1 | 60 | 66 | 0.23 | Lif200 | Scintillation Counter | Br Kβ2 |
| Ti | Kα1 | 50 | 80 | 0.23 | Lif200 | Flow Counter | *none* |
| V | Kα1 | 50 | 80 | 0.23 | Lif200 | Flow Counter | Ti Kβ1 |
| Y | Kα1 | 60 | 66 | 0.23 | Lif200 | Scintillation Counter | *none* |
| Zn | Kα1 | 60 | 66 | 0.23 | Lif200 | Scintillation Counter | *none* |
| Zr | Kα1 | 60 | 66 | 0.23 | Lif200 | Scintillation Counter | Sr Kβ1 |

Table 2.2S. Instrument setup and calibration routine details for WD-XRF pressed pellet analysis.

| | Line | Generator Voltage (Kv) | Tube Current (mA) | Collimator (dg) | Analyzer Crystal | Detector | Peak Overlap Corrections |
|---|---|---|---|---|---|---|---|
| Al | Kα1 | 27 | 150 | 0.23 | PET | Flow Counter | Br Lα1 |
| Ba | Lα1 | 50 | 80 | 0.23 | Lif200 | Flow Counter | Ti Kα1 |
| Br | Lα1 | 27 | 150 | 0.23 | PET | Flow Counter | Al Kα1 |
| Ca | Kα1 | 50 | 81 | 0.46 | Lif200 | Flow Counter | none |
| Ce | Lα1 | 50 | 80 | 0.23 | Lif200 | Flow Counter | Ba Lβ1 |
| Cr | Kα1 | 60 | 67 | 0.46 | Lif200 | Scintillation Counter | Fe Kα1 |
| Cu | Kα1 | 60 | 66 | 0.23 | Lif200 | Scintillation Counter | none |
| Fe | Kα1 | 50 | 10 | 0.23 | Lif200 | Scintillation Counter | Mn Kβ1 |
| Ga | Kα1 | 60 | 67 | 0.23 | Lif200 | Scintillation Counter | Rh Kα1/Compton, Ni Kβ5 |
| K | Kα1 | 50 | 81 | 0.46 | Lif200 | Flow Counter | none |
| Mg | Kα1 | 27 | 150 | 0.46 | OVO-55 | Flow Counter | Al Kα1 |
| Mn | Kα1 | 50 | 80 | 0.23 | Lif200 | Scintillation Counter | none |
| Ni | Kα1 | 60 | 67 | 0.23 | Lif200 | Scintillation Counter | Rh Kβ1/Rayleigh |
| P | Kα1 | 27 | 150 | 0.46 | PET | Flow Counter | none |
| Rb | Kα1 | 60 | 66 | 0.23 | Lif200 | Scintillation Counter | Rh Kα1/Rayleigh |
| Si | Kα1 | 27 | 150 | 0.46 | PET | Flow Counter | Br Lγ2 |
| Sr | Kα1 | 60 | 66 | 0.23 | Lif200 | Scintillation Counter | none |
| Ti | Kα1 | 50 | 80 | 0.23 | Lif200 | Flow Counter | none |
| V | Kα1 | 50 | 80 | 0.23 | Lif200 | Flow Counter | Ti Kβ1, Ba Lβ1 |
| Y | Kα1 | 60 | 66 | 0.23 | Lif200 | Scintillation Counter | none |
| Zn | Kα1 | 60 | 66 | 0.23 | Lif200 | Scintillation Counter | none |
| Zr | Kα1 | 60 | 66 | 0.23 | Lif200 | Scintillation Counter | Ba Kα2 |

# 3.0   XRF TECHNIQUES TO QUANTIFY HEAVY METALS IN VEGETABLES AT LOW DETECTION LIMITS

## 3.1   INTRODUCTION

For lithologic media, the quantification of elements using X-Ray Fluorescence (XRF) spectroscopy is well understood and methods of sample preparation, measurement methods, and calibration/quantification are well documented (e.g. Byers et al., 2016). In quantifying element concentrations using XRF, photons of energy are generated by an X-ray source (such as a compact Rh X-ray tube) and the photons pass through one or more primary filters to reduce the variability in source X-ray photon energy. Source photons then pass into a sample and transfer their energy to an inner-shell electron of an atom within the sample, which slightly displaces the electron from its preferred orbit leaving an unstable atom. An electron from an outer orbital then fills the vacancy in the lower orbital and at the same time releases energy in the form of a fluoresced secondary X-ray unique to the element and unique to the energy difference between orbitals. Element concentrations are determined by the rate at which fluoresced secondary X-rays are measured by a detector in the spectrometer.

Due to the non-destructive nature of the analysis, XRF is emerging as a promising method for rapid quantification of heavy metals in vegetables as recent work demonstrates that Pb and other heavy metals are taken up and translocated from the soil into consumable vegetable tissues (Clark et al., 2006; Ferri et al., 2015; Finster et al., 2004; Jolly et al., 2013; Lima et al., 2009; Nabulo et al., 2011; Rodriguez-Iruretagoiena et al., 2015; Sekara et al., 2005). Although

human exposure and the resulting health impacts from direct contact with Pb-contaminated soil is considered to be a primary pathway for Pb exposure in urban agriculture, secondary exposure from chronic consumption of vegetables containing Pb could be a significant contributing factor in total Pb exposure (Chopra & Pathak, 2015; Ferri et al., 2015; Jolly et al., 2013), especially in high-risk populations, such as low-income, immigrant communities where exposure to Pb remains disproportionately high. Child exposure to Pb leads to a multitude of poor health outcomes (Keller et al., 2017; Lane et al., 2008; Schnur & John, 2014); therefore, further evaluation of Pb (and other heavy metals) exposure is paramount.

Established methods for measuring elements in vegetable and herb tissues include a combination of traditional wet chemistry methods such as atomic absorption spectrometry (AAS) (Bozym et al., 2015; Chopra & Pathak, 2015; Lima et al., 2009; Sekara et al., 2005; Song et al., 2012; Yadav et al., 2015), inductively coupled plasma-atomic emission spectrometry (ICP-AES) or inductively coupled plasma-mass spectrometry (ICP-MS) (Bešter et al., 2013; Finster et al., 2004; Murray et al., 2011; Nabulo et al., 2011; Rodriguez-Iruretagoiena et al., 2015; Wiseman et al., 2013), wavelength dispersive XRF (WD-XRF) (Andersen et al., 2013; Figueiredo, et al., 2016), bench-mounted energy-dispersive XRF (ED-XRF) (Anjos et al., 2002; Gallardo et al., 2016; Jolly et al., 2013), and portable ED-XRF (Ferri et al., 2015; Gutiérrez-Ginés et al., 2013; Sacristan et al., 2016; Towett et al., 2016). Recent work quantified heavy metals in algae with portable ED-XRF using a fundamental parameter factory calibration for plastics (Bull et al., 2017; Turner et al., 2017).

Sample preparation for using AAS or ICP-MS to quantify heavy metals in plants involves ashing plant material in a furnace or with concentrated hydrogen peroxide followed by digestion with acid ($HNO_3$, $HCLO_4$, $H_2SO_4$) and/or microwave extraction using one or more concentrated

acids. These sample preparation techniques are inherently dangerous and generate a significant hazardous waste stream. Comparatively, XRF sample preparation techniques preserve the sample matrix and minimize waste generation. As noted by many in the literature (e.g. Gallardo et al., 2016), XRF is a promising technique in quantification of Pb and other heavy metals in vegetable tissues. However, prior reviews of this technology have identified several limiting factors (Marguí et al., 2009; Palmer et al., 2009; Singh et al., 2017). The greatest obstacles identified in prior studies using XRF to measure heavy metals are achieving a limit of detection within the range of regulatory thresholds and generating consistent results that can be confirmed with another quantification technology. Due to limited commercial availability of reference materials and treatment of XRF spectrometers as "black box", prior studies involving XRF have largely not controlled for matrix effects by: not matching the reference material matrix to sample matrix; using a multitude of sample preparation techniques; or using XRF standard factory calibrations optimized for non-carbon matrices. Further complicating prior XRF work is the quantitation of heavy metals based on the intensities of wavelengths with known peak overlaps. By addressing these inconsistencies and mitigating matrix effects, we hypothesize that WD-XRF and portable ED-XRF can be used to accurately and rapidly quantify heavy metals in vegetable samples with limits of detection applicable to health-based regulatory thresholds.

   Although the use of XRF in quantifying heavy metals in plant matrices has been reported previously, this work describes methods to systematically mitigate matrix effects through development of custom reference materials, building matrix-specific measurement and calibration routines, and confirming the efficacy of the XRF methods by comparison to ICP-MS analysis. Remarkably, no consumption standards exist in the United States for heavy metals in produce or cereals; therefore, this work relies on World Health Organization (WHO) food

standards (WHO, 2018). On a broader scale, food security threats are often identified in retrospective studies limited to select food groups, select manufacturers/countries of origin, and/or elements; however, with multiple new threats to food security identified each year, use of WD-XRF and portable ED-XRF spectrometry is a promising quality check that could be used at ports of entry by regulators, researchers, and/or growers/manufacturers to identify security risks prior to consumption/exposure.

## 3.2    EXPERIMENTAL

The single greatest source of bias in XRF measurements of vegetables is inter-element effects due to secondary absorption/enhancement of target wavelengths. Secondary absorption occurs when a fluoresced characteristic X-ray is absorbed by another atom in the matrix rather than returning to the detector, and if the absorbed energy is great enough, the atom will generate additional x-rays characteristic of the atom (direct secondary enhancement). Additional characteristic X-rays generated following secondary absorption can either return to the detector or be absorbed by additional atoms in the matrix and further generate characteristic x-rays (tertiary enhancement). Therefore, absorption/enhancement of characteristic X-rays can significantly alter the rate at which characteristic x-rays return to the detector such that element concentrations in the sample are not represented by the rate of characteristic x-rays. Mitigation of inter-element (matrix) effects therefore is central to all aspects of this experimental design.

The commutability of reference materials to samples is critical in minimizing measurement uncertainty (Byers et al., 2016) and mitigating matrix effects (absorption/enhancement), but has often been overlooked in prior food studies. Commutability is especially critical when using XRF to quantify heavy metal concentrations in homogenized dry and undried (raw) vegetables as the mass attenuation coefficient of the vegetable matrix is very

59

small compared to more common and readily available silicate-based soil reference materials, which were often used in previous food studies using XRF spectroscopy. Unfortunately, metals-rich plant-based reference materials are either no longer commercially available (eg. NIST SRM 1515, NIST SRM 1547, BCR-60, BCR-100, BCR-279) or represent a very limited continuum of metal concentrations (ex. NIST SRM 1570a, NIST SRM 1575a, BCR-129, BCR-414, BCR-482, BCR-670, ERM-CD281, IRMM-804).

Because fully developed and verified metals-rich plant-based reference materials are not readily available, custom dried plant-based reference materials were prepared from easily obtainable commercial materials using methods similar to (Figueiredo et al., 2016). Sample preparation techniques were developed for quantitation via WD-XRF and portable ED-XRF spectroscopy using the custom dried plant-based reference materials. Lastly, calibration routines were developed and confirmed with paired ICP-MS measurements of the reference materials. Paired XRF and ICP-MS measurements were taken for vegetables grown in garden soil collected from residential properties in the City of Milwaukee, Wisconsin to confirm the viability of the XRF measurement and calibration routines.

Similar wet plant-based reference materials were prepared as an analogue to raw vegetables in an effort to use portable ED-XRF for quantification of metals in the field. Sample preparation techniques for undried (raw) samples and calibration routines were established. Paired WD-XRF and portable ED-XRF measurements were obtained from vegetables grown in garden soil collected from residential properties in the City of Milwaukee to evaluate the viability of the wet plant-based portable ED-XRF measurement and calibration routines.

### 3.2.1 Dried Plant-Based XRF Measurement and Calibration Routines

**Preparation of Dry Plant-Based Reference Materials.** Twenty-one plastic jars containing 14 g of freeze-dried parsley were purchased from a retail source in Milwaukee, Wisconsin. The parsley was mixed in bulk and dried in an oven at 60 C for 48 h. The powdered parsley was powdered by hand and a 30 g (+/- 1 mg) aliquot of parsley power was added to a rotovap flask containing 200 ml of 18 μmho e-pure water and a pre-determined quantity of liquid ICP metals standard containing 100 mg L$^{-1}$ of Al, As, Cd, Cr, Co, Cu, Fe, Pb, Mg, Mn, Ni, K, Na, Zn and 600 mg L$^{-1}$ Y (Instrument Check Standard 7, SpecCerti Prep ®; Metuchen, NJ). The flask was swirled gently to hydrate the parsley and attached to a water-cooled rotovap (Heidolph Schwabach, Germany) operated at 80 °C and 80 RPM under vacuum to hydrate the parsley with the metals-rich solution while removing latent water. The rotovap process continued for 2 h or until the mixture was the consistency of a thick paste. The parsley was removed from the rotovap, dried in an oven at 60C for 48h. Dried material was milled in a tungsten carbide shatterbox for 30s to create a uniform homogeneous dry powder similar to (Marguí et al., 2009). The process was repeated in a step-wise fashion using varying volumes of metals standard to create a library of plant-based reference materials with nominal heavy metal (Al, As, Cd, Cr, Co, Cu, Fe, Pb, Mg, Mn, Ni, K, Na, and Zn) concentrations ranging from 0.5 μg g$^{-1}$ to 100 μg g$^{-1}$ dry weight and nominal Y concentrations ranging from 1 to 600 μg g$^{-1}$. A blank reference was created using the same process, but omitting the addition of the ICP Standard.

A 1g aliquot of each powdered reference material was digested by TestAmerica Laboratories, Inc. (Chicago, Illinois) using concentrated HNO3, HCl, and H2O2 per Method SW 846 3050B (USEPA, 1996). Heavy metal concentrations in the digestions were measured in triplicate at the UWM School of Freshwater Sciences using a high resolution ICP-MS (Thermo

Scientific Element 2) to confirm element concentrations in the reference materials. ICP-MS detection limits for heavy metals of concern are less than 0.1 μg g$^{-1}$.

**Preparation of Dry Pressed Pellets for XRF Analysis.** Preparation of typical powdered soil and rock samples for XRF analysis involves either fusing samples with a flux (such as lithium tetraborate) at high temperature or pressing powdered samples with a carbon-based binding agent under high pressure to create uniform pellets (Byers et al., 2016). Fusion or ashing is impractical; therefore, uniform pellets were created by pressing dried powdered plant samples at 25 t for 60 s in a 40 mm diameter hydraulic die press.

The variability in pellet thickness across the urban agriculture literature is large and is likely a source of bias. Because matrix attenuation is minimal in vegetable samples, source X-rays entering a vegetable sample can pass entirely through the sample and generate fluoresced X-rays from the entire sample thickness. Therefore, the depth of measurement (also referred to as escape depth) for each element wavelength becomes limited by the attenuation of the fluoresced secondary X-rays by the sample matrix, not by the attenuation of the source X-ray. For a given element wavelength, if the sample is thicker than the measurement depth, the net intensity of fluoresced X-rays is independent of sample thickness, and the pellet is considered "infinitely thick." If the sample is thinner than the measurement depth for a given element wavelength, the pellet is considered "infinitely thin." If a pellet is infinitely thin with respect to a given element wavelength, the net intensity of fluoresced X-rays is a function of sample thickness (mass) and subject to significant bias between samples unless samples are of uniform thickness. Additionally, vegetable samples considered infinitely thin could be subject to significant bias from characteristic fluoresced X-rays generated by the spectrometer shielding/housing passing backwards through the sample matrix and potentially generating secondary or tertiary

enhancement of characteristic X-rays from matrix elements or by passing through the matrix and being directly measured by the spectrometer detector.

The depth of measurement (or escape depth of fluoresced X-rays) is calculated based on the matrix density and mass attention coefficient for varying X-ray wavelengths of interest (Towett et al., 2016). Unfortunately, the mass attenuation coefficient for plant tissues is unknown and the density of dried vegetables is variable between tissues with reported values ranging from 1.1 g cm-3 to 1.7 g cm-3 (Martynenko, 2014; Rodríguez-Ramírez et al., 2012). We used a nominal density of 1.4 g cm-3 to represent a generic dried vegetable tissue and the mass attenuation coefficient of simple sugar+cellulose ($C_6H_{12}O_6C_6H_{10}O_5$) reported by the National Institute of Standards and Technology (Chantler et al., 2001) for varying wavelengths from 0 to 40 keV (Figure 3.1). With these conservative model factors, calculations indicate a dried plant-based sample 1.7 cm thick should be infinitely thick with respect to the Pb Lβ1 wavelength (12.614 keV). Based on the diameter of the pellet die used in this study, a 1.7 cm thick pellet would require approximately 30 g of dried plant material, which is too much powered material for the XRF pellet die to process. Further, as raw vegetables used in our larger study were 87% water on average, roughly 250 g of raw vegetable would be needed to create a single pellet; which is impractical. Knowing Cr is present inside the housing and shielding of the Pioneer S4 WD-XRF used in this study (Bruker AXS, Inc.), pellets had to be infinitely thick with respect to the CrKα1 wavelength (5.415 keV) to prevent bias in the measurements. To be conservative, 3.2 g of powdered sample per pellet were used and when pressed at 25 t for 60 s, resulted in a pellet approximately 1.9 mm thick. Pellets prepared in this manner are competent, resilient to handling, maintain integrity when stored long-term in a desiccator, and can be analyzed by WD-XRF spectrometry under vacuum without breakage.

Selecting appropriate wavelengths for quantification of heavy metals with XRF is critical to minimize bias and error in measurement routines. Lighter weight elements are commonly quantified based on Kα wavelengths, and due to the keV limitations of the Rh X-ray tube, elements heavier than La are commonly quantified based on Lα wavelengths. However, as shown on Figure 3.2a, the Pb Lα1 wavelength overlaps the As Kα1 wavelength. Therefore, to mitigate the peak overlap with As, we used the Lβ1 wavelength for quantification of Pb.

The potential for absorption and enhancement in the matrix was evaluated for each element of interest using data provided by (Hubbell & Seltzer, 2004). Enhancement of the Pb Lβ1 wavelength is not expected from elements in the parsley matrix, from elements contained in the ICP Standard, or from elements in the shielding/housing. However, as illustrated on Figure 3.1S, absorption and secondary or tertiary enhancement of Ka1 wavelengths of Zn, Ni, Fe, Cr, Cu, Co, Mn, and As is possible from elements in the parsley matrix, elements contained in the ICP Standard, and/or elements in the spectrometer shielding/housing.

Using multiple metal foils, we assessed the measurement depth of each element wavelength of interest and possible matrix effects as described in Section 2.1.4 to confirm we had adequately controlled for possible bias associated with pellet thickness and matrix effects.

**Development of a Dried Plant-Based WD-XRF Measurement and Calibration Routine.** A custom measurement routine was developed in the Bruker AXS, Inc. Pioneer S4 WD-XRF Spectra Plus software to measure the intensities under vacuum of Pb using the Pb Lβ1 wavelength and Cr, Ni, and Y using Kα1 wavelengths. Specific analytical details for each element are provided on Table 3.1S.

Each pellet in the reference material library was analyzed with the WD-XRF measurement routine. Custom calibration routines for each element were developed by

64

comparing net X-ray intensities to known dry weight element concentrations based on element concentrations in each reference material (including the "blank") as determined by ICP-MS. The routine corrected for rhodium Rayleigh and Compton peaks, matrix effects, and possible contamination of tungsten and cobalt from the shatterbox. Reference materials with element concentrations less than the limit of detection determined by the Pioneer S4 software were omitted from the calibration routines. The goodness of fit, root mean square error, calibration range, the LOD determined by the Pioneer S4 software, and the LOQ calculated per (Thomsen et al., 2003) are listed in Table 3.1. The coefficient of determination ($r^2$) of each calibration is no less than 0.999 with corresponding single-digit root mean square errors.

**Confirmation of the Dry Plant-Based WD-XRF Measurement and Calibration Routine.** Common garden vegetables were grown in pots of metals-rich soil sourced from residential vegetable gardens in the City of Milwaukee, Wisconsin. The vegetables were harvested, scrubbed vigorously under running water, peeled (root vegetables only), chopped, dried in an oven at 60 ºC for 48h, milled in a tungsten shatterbox for 30 s, and a 3.20 g aliquot of each sample was pressed at 25 t for 60 s in a 40 mm diameter pellet hydraulic die press. Each sample was analyzed by WD-XRF using the routine described previously and concentrations determined from calibration curves.

Infinite thickness calculations were confirmed using the vegetable pellets by comparing the change in net WD-XRF intensities measurements with and without the presence of a metal foil placed behind dried pressed vegetable samples. The four separate metal foils used in this evaluation include two 99% pure foils of (1) 0.2 mm Cu and (2) 1 mm Pb and two alloy foils of (3) 0.3 mm "nickel-silver" (consisting of 65% Cu, 18% Ni, and 17% Zn) and (4) 0.4 mm stainless steel foil containing Cr and Mn.

After measurement with WD-XRF, 23 vegetable pressed pellets representing the range of measured Pb concentrations were broken into 1g aliquots and digested by TestAmerica Laboratories, Inc. using Method SW 846 3050B (USEPA, 1996). Heavy metal concentrations in the digestions were measured in triplicate at the UWM School of Freshwater Sciences using a high resolution ICP-MS (Thermo Scientific Element 2) and concentrations converted to dry weight for comparison between the two analytical techniques. The paired relationships between ICP-MS and WD-XRF measurements of Pb in vegetables are illustrated on Figure 3.3a.

**Development of a Dried Plant-Based Portable ED-XRF Measurement and Calibration Routine.** The WD-XRF used in this study is a bench-mounted spectrometer, which limits the usefulness of this technology in real-time quantification of heavy metals in remote locations, such as agricultural fields, gardens, or ports of entry. Portable hand-held ED-XRF is a promising technology for rapid quantification of elements and shows particular promise in the areas of food security/food quality. However, older ED-XRF spectrometers often measured intensities of elements from peaks with known overlaps and relied on default factory calibrations. Recently developed instrumentation allows the entire X-Ray spectrum to be captured, stored, and custom calibrations developed based on distinctive element wavelengths. Methods for developing and confirming measurement and calibration routines for quantification of heavy metals in dried pressed pellets with portable ED-XRF are identical to the methods described previously in developing and confirming routines for WD-XRF. In addition to confirming the infinite thickness calculations using metals foils, the influence of measurement time on accuracy and the influence of multi-metal primary filters on detection limits were evaluated.

The dried pressed pellet reference materials used in the WD-XRF measurement routine were placed on the stage of a Bruker Tracer portable ED-XRF spectrometer and the fluoresced XRF spectra captured using the Bruker S1PXF software program. Fluoresced X-rays were measured with a silicon drift detector for 120 seconds in air at 40 keV and 40 uA and used a removable multi-metal primary filter consisting of 25 μm Cu, 25 μm Ti, and 25 μm Al (Cu/Ti/Al filter). The average valid photon count rate was 16,815 photons per second with a resolution of 20.04 eV per channel at full height width for the Mn Kα 1 wavelength. The X-ray source of the spectrometer is a Rh-tube oriented at a 53-degree angle with respect to the sample. As the entire spectrum from 0 to 40 keV was captured by the software, routines were developed to quantify Cr, Mn, Ni, Cu, Zn, Pb, Y, and Cd. The captured spectra for the 10 μg g$^{-1}$ reference material and the net Pb Lβ1 wavelength intensities for six reference materials are illustrated on Figure 3.2. Calibration routines were developed by comparing net X-ray intensities to known dry weight element concentrations using the Bruker Microsoft Excel plugin (S1CalProcess). The peak overlap corrections, goodness of fit, root mean square error, calibration range, the LOD calculated using the background equivalent concentration approach (Thomsen, 2012) and the LOQ calculated (Thomsen et al., 2003) for each element are summarized on Table 3.2. The r$^2$ of each calibration is no less than 0.97 with corresponding single-digit root mean square errors.

To confirm that the infinite thickness observations made with WD-XRF remained valid for portable ED-XRF, the same reference materials were analyzed for 120 seconds and net intensities determined. A piece of 1 mm 99% pure Pb foil was placed behind the pellet and the analysis repeated. The Pb foil was removed and a 0.025 mm piece of 99.9% pure Mo foil was placed behind the pellet and the analysis repeated a third time. The associated intensities

increased with the presence of a metal foil, confirming the pressed pellets are infinitely thin with respect to the Pb Lβ1 and Mo Kα1 wavelengths.

Prior studies have counted fluoresced X-rays in plant material from 30 to 240 seconds (Bull et al., 2017; Gutiérrez-Ginés et al., 2013; Sacristan et al., 2016), or did not specify count times. To optimize the portable ED-XRF measurement routine and to quantify the improvement in the accuracy with an increase of time, four dried plant-based reference materials were analyzed by ED-XRF as described previously by varying measurement times from 5 s to 300 s. The resulting Pb concentrations were compared to the known Pb concentrations and the relative percent differences between each data pair calculated as described in Byers et al. (2016) (Figure 3.2S). The relative difference neared + 10% at 120s and only marginal improvements were noted with longer measurement time, therefore 120 seconds was selected as the default measurement time for the portable ED-XRF measurement routine.

Primary multi-metal filters have been designed by ED-XRF manufacturers to reduce variability in the energy of source X-ray photons and reduce background radiation. As illustrated on Figure 3.2a, the Pb Lβ1 peak is located on the shoulder of the inelastic Compton radiation peak originating from the Rh tube. Normally, XRF measurements are normalized to this inelastic scatter (18.5-19.5 keV); however, normalization requires additional steps in the calibration. Therefore, the ED-XRF measurement and calibration steps outlined above were repeated using an alternative removable multi-metal primary filter consisting of 25 μm Ti, 50 μm Fe, and 25 μm Mo (Ti/Fe/Mo) designed to reduce the overall Compton radiation. The average valid photon count rate was 2,931 photons per second with a resolution of 19.98 eV per channel at full height width for the Mn Kα1 wavelength. The peak overlap corrections, goodness of fit, root mean square error, calibration range, the LOD calculated using the background equivalent

concentration approach (Thomsen, 2012) and the LOQ calculated (Thomsen et al., 2003) for each element summarized on Table 3.2S. Although the calibration goodness of fit parameters with the Ti/Fe/Mo multi-metal primary filter are reasonable ($r^2$ values near one with single digits RMSE values), there is a small loss of fit in lower wavelengths.

**Confirmation of the Dry Plant-Based Portable ED-XRF Measurement and Calibration Routine.** The researchers grew common garden vegetables as described in Section 2.1.4 and samples prepared as described in Section 2.1.3. Each sample was analyzed by portable ED-XRF using the primary filter as described above. After measurement with the ED-XRF, 27 vegetable pressed pellets representing the range of measured Pb concentrations were broken into 1g aliquots and analyzed using ICP-MS as described in Section 2.1.3. The paired relationships between ICP-MS and ED-XRF measurements for Pb are illustrated on Figure 3.3b.

To determine if changing primary multi-metal filters improved the applicability of the calibration to vegetable samples with respect to Pb, 35 additional samples of vegetables grown by the researchers were prepared as dried pressed pellets and analyzed with ED-XRF equipped with the Ti/Fe/Mo multi-metal primary filter. Concentrations were compared to measurements made using WD-XRF; the paired relationships between WD-XRF and ED-XRF measurements for Pb are illustrated on Figure 3.3c. Although the calibrations for Pb using either primary filter is acceptable, the viability of the calibration routine to actual samples is better with the Cu/Ti/Al filter.

### 3.2.2    Wet Plant-Based ED-XRF Measurement and Calibration Routines

**Preparation of Wet Plant-Based Reference Materials.** A major limitation to the use of portable ED-XRF in urban agriculture and food security applications is the lack of commercially available metals-rich raw (undried) plant-based reference materials. In developing undried

69

reference materials analogous to raw vegetables, additional commercially sourced dried parsley was mixed with the liquid ICP metals standard and processed in a roto-vap as described previously to create a second library of eleven dried/homogenized parsley-based reference materials with Pb concentrations ranging from 0.5 µg g$^{-1}$ to 100 µg g$^{-1}$ on a dry-weight basis as confirmed by WD-XRF. The mean water content of vegetables grown in metals-rich soil used in this study is 87% with a standard deviation of 4%. To prepare a reference library analogous to raw vegetables, a 1.50 g aliquot of dried reference material was added to a glass vial containing 8.50 g of e-Pure water. The mixture was gently stirred, the jar lid tightly secured, and the mixture allowed to rest for 12h. The process was repeated in a step-wise fashion to create a library of "wet" plant-based reference materials with Pb concentrations ranging from 0.0 µg g$^{-1}$ to 15 µg g$^{-1}$ wet weight. A blank reference was created using the same process. A second set of reference materials was created with 65% water for comparison purposes.

**Development of Wet Plant-Based Portable ED-XRF Measurement and Calibration Routine.** The 65% and 85% water content plant-based reference material sets were packed into single open-ended 32 mm diameter (10 ml volume) XRF sample cups (Premier Lab Supply; Port St. Lucie, FL) and secured with 4.0-micron polypropylene film (Premier Lab Supply). Each sample cup was analyzed via portable ED-XRF for 120 seconds using the Bruker S1PXF software program as described previously using the Cu/Ti/Al primary filter. The average valid photon count rates for reference materials with 65% and 85% water were 34,684 and 35,324 photons per second, respectively, with resolutions of 20.02 eV per channel at full height width for the Mn Kα wavelength. The measurement routine measured fluoresced X-rays for 120 seconds at 40 keV and 40 uA.

Calibration routines were developed to quantify Cr, Ni, Pb and Y. Custom calibration routines for each set of reference material were developed in Microsoft Excel using the Bruker plugin (S1CalProcess). The goodness of fit, root mean square error, calibration range, the LOD calculated using the background equivalent concentration approach (Thomsen, 2012) and the LOQ calculated (Thomsen et al., 2003) for each element is summarized on Table 3.3 for both water contents. The goodness of fit parameters for each element using the 85% water content reference set are less than those using the 65% water content reference set. Although the LOD and LOQ values for each element are similar between the two water contents, when converted from wet weight concentrations to dry weight concentrations, the calibration developed with 85% water content is weaker by comparison.

**Confirmation of the Wet ED-XRF Measurement and Calibration Routine**. Common garden vegetables were grown by the researchers in pots of metals rich soil sourced from residential vegetable gardens in the City of Milwaukee, Wisconsin. The vegetables were harvested, scrubbed vigorously under running water, and peeled (if necessary). Each vegetable tissue sample was coarsely homogenized in a food processor for 10 seconds. An aliquot of the homogenized slurry was poured into a 32 mm XRF sample cup and the sample cup secured with 4-micron polypropylene film. The sample cup was placed on the stage of a Bruker Tracer portable ED-XRF spectrometer and the fluoresced XRF spectra captured and analyzed as described in Section 2.2.2. The concentration of heavy metals was calculated based on the 85% water calibration routine. After analysis, the wet sample was dried and pressed pellets prepared as described in section 2.1.2 and analyzed using the dried WD-XRF measurement routine.

To confirm the measurement depth of raw vegetables with portable ED-XRF, 67 vegetables grown in soil collected from residential vegetable gardens in Milwaukee, WI were

coarsely homogenized, packed into sample holders, X-rays counted for 120 seconds, and net intensities determined. A piece of 1mm 99% pure Pb foil was placed behind the sample holder and the analysis repeated. The Pb foil was removed and a 0.025 mm piece of 99% pure Mo foil was placed behind the sample holder and the analysis repeated a third time. Based on the change in peak intensities, the samples are considered infinitely thick for the Pb Lβ1 wavelength, but not the Mo Kα1 wavelength.

### 3.2.3    Data Evaluation

The $r^2$ statistic is commonly used in bivariate calibration regressions to explain the amount of variability in the dependent variable (concentration) that can be explained by the independent variable (peak intensity). In XRF spectroscopy, researchers strive to maximize the $r^2$ value as close to 1 as possible. Further, the XRF calibration routines are also evaluated with root mean square error (RMSE) values, which is the standard deviation of the calibration regression residuals. Most importantly, the RMSE can be interpreted in terms of measurement units of the dependent variable, which in this study is element concentration expressed in $\mu g\ g^{-1}$. Therefore, in refining calibration routines, the $r^2$ values were maximized and RMSE values minimized.

RMSE values were further used to evaluate the minimum element concentration quantifiable by each calibration. If the RMSE is less than the calculated LOQ, then the LOQ represents the smallest concentration that can be quantified by a calibration routine. However, if the RMSE is greater than the LOQ, then the RMSE represents the smallest concentration that can be quantified by the calibration routine. This approach allows for a greater certainty in the calibration and is more rigorous compared to the more common approach where the calibration range assumed to be represented by the range in concentration of calibration reference materials.

## 3.3 RESULTS AND DISCUSSION

### 3.3.1 Dried Plant-Based WD-XRF Measurement and Calibration Routines

**Evaluation of Measurement Depth and the Infinite Thickness Assumption.** Dried pressed pellets of vegetables of consistent mass considered infinitely thick with respect to CrK$\alpha$1 and considered infinitely thin with respect to Pb L$\beta$1 were analyzed and the measurement depths confirmed with metal foils as described previously. Net intensities of the Pb L$\beta$1 wavelength increased 4 orders of magnitude when the Pb foil was placed behind samples, thus confirming the pressed pellet samples are infinitely thin at 12.614 keV. Similarly, the net intensities of the Cu K$\alpha$1 fluoresced X-rays increased one order of magnitude confirming samples remained infinitely thin at 8.046 keV. When the "nickel-silver" foil was added behind the sample, the mean Ni K$\alpha$1 net intensity increased by 11 counts per second, which is a statistically significant increase (t< 0.001; 16 df) and equal to an increase of 77 $\mu$g g$^{-1}$. The mean net intensity of the Mn K$\alpha$1 wavelength increased by 0.05 counts per second when the stainless steel foil was added, which is a statistically significant increase based on a matched-pair analysis (t< 0.01; 15 df), although the mean increase is equal to an increase of only 1 $\mu$g g$^{-1}$. The Cr K$\alpha$1 (5.415 keV) net intensities and corresponding concentrations did not increase (t> 0.5; 15 df) when the stainless steel foil was added behind samples. This empirical evaluation matches the calculations of infinite thickness illustrated on Figure 3.1, and by controlling for matrix effects, confirms that the dried vegetable pressed pellets used in this study are appropriate for use in measuring elements with fluoresced wavelengths less than 5.451 keV. Potential enhancement from absorption of characteristic x-rays generated in the housing is controlled.

Researchers are cautioned to evaluate multiple thicknesses of sample to quantify the impact thickness will have on measurement results for a particular element of interest. For

example, although the concentration of Mn increased by 1 µg g$^{-1}$ by adding foil behind the pellet, this increase may be within acceptable bias tolerances in some applications, especially if the target element is not present in the shielding and housing of the spectrometer or not subject to influence from absorption/enhancement by matrix elements.

**Evaluation of the Dry Plant-Based WD-XRF Measurement and Calibration Routine for Pb.** Measurements indicate Pb is not present in the housing of the WD-XRF, therefore, although the pellets are infinitely thin for the Pb Lβ1 wavelength, the housing of the WD-XRF is not a direct source of bias in these measurements. The RMSE value of the Pb WD-XRF calibration routine is greater than the LOD, but less than the LOQ; therefore, the calibration range for Pb varies between 1 and 96 µg g$^{-1}$ (Table 3.1). Although RMSE and LOQ values from calibrations developed by others are not widely available in the literature, the LOD value for Pb in this study is one or more orders of magnitude less than values reported previously (Andersen et al., 2013, Gutierrez-Gines et al., 2013, Gallardo et al., 2016), and more importantly, the LOD (0.3 µg g$^{-1}$) is equal to the Maximum Level for Pb in leafy vegetables (on a dry weight basis) and only 0.1 µg g$^{-1}$ greater than the Maximum Level for Pb in cereal (WHO, 2018).

The appropriateness of the WD-XRF calibration routine for Pb developed in this study to actual vegetable samples was further confirmed with paired ICP-MS measurements. The slope of the bivariate regression between 23 WD-XRF and ICP-MS measurements of vegetables grown in metals-rich soil is 1.08 with an r$^2$ value of 0.96 providing additional support in the accuracy of WD-XRF measurements (Figure 3.3a).

**Evaluation of the Dry Plant-Based WD-XRF Measurement and Calibration Routine for Cr, Ni, and Y.** ICP-MS measurements confirmed the presence of Cr and Ni in the parsley used in this study. However, as RMSE values are less than LOQs and the XRF software

calculated LODs are less than the Cr and Ni concentrations in the blank, the Cr and Ni calibrations are considered satisfactory for the element concentrations represented by the reference materials (Table 3.1). Although RMSE and LOQ values for calibrations are largely absent from the literature, our LOD values for these elements are lower than those previously achieved (Ni and Cu; Gutiérrez-Ginés et al., 2013 and Cu; Otaka et al., 2014).

The concentrations of Y were minor in the vegetable samples; therefore, our evaluation of the WD-XRF routine with ICP-MS was not possible. However, measurements indicate Y is not present in the housing of the WD-XRF, therefore, although the pellets are infinitely thin for the Y Kα1 wavelength, the housing of the WD-XRF is not a direct source of bias in these measurements. Unfortunately, the concentrations of Cr and Ni are greater than the WD-XRF LOQs for only eight confirmation samples; therefore, our evaluation of the WD-XRF routine with ICP-MS is limited. Potential bias from absorption/enhancement due to the matrix and further enhanced by XRF shielding containing mixed metals is critical when evaluating transition metals in a carbon matrix. For instance, because the pressed pellets are infinitely thick for Cr Kα1, the presence of Cr in the housing/shielding of the XRF are not considered direct sources of bias in measurements. However, fluoresced Fe Kα1 X-rays from the shielding could be absorbed by Cr in the matrix and enhance fluorescence of Cr Kα1 X-rays. In addition, measurable quantities of Ni are present in the WD-XRF housing/shielding and the pellets are considered infinitely thin for Ni; therefore, characteristic Ni Kα1 X-rays generated by the XRF housing could return to the detector and serve as a source of direct bias. Or, Ni Kα1 characteristic X-rays generated by the shielding could be absorbed by Fe in the sample matrix, which could in turn enhance the generation of Cr Kα1 wavelengths. Therefore, researchers cannot ignore increased matrix enhancement due to the influence of shielding. To mitigate this potential source of bias,

the same shielding/housing must be used for all samples so that critical enhancement influences can be controlled during development of the calibration routine.

### 3.3.2    Dried Plant-Based ED-XRF Measurement and Calibration Routines

**Evaluation of Measurement Depth and the Infinite Thickness Assumption.** This study focuses on the most common heavy metals, therefore optimization of ED-XRF calibration focused primarily on the spectrum between Cr Kα1 (5.415 keV) and Pb Lβ1 (12.614 keV) with less interest in the Y Kα1 (14.958 keV) to Cd Kα1 (23.173 keV) range.

Measurement depths of the dried pellets with portable ED-XRF were evaluated with metal foils as described previously. Similar to WD-XRF measurements, the Pb Lβ1 and Mo Kα1 intensities measured by ED-XRF increased significantly with the presence of the associated metal foil. Therefore, the pressed pellets are infinitely thin with respect to the Pb Lβ1 and Mo Kα1.

**Evaluation of the Dry Plant-Based ED-XRF Measurement and Calibration Routine for Pb.** The RMSE, LOD, and LOQ values for the portable ED-XRF calibration for Pb with the Cu/Ti/Al multi-metal primary filter (Table 3.2) are nearly identical to the values for the WD-XRF calibration routine. Even more promising is the calibration accuracy that was achieved with the portable ED-XRF even though measurement count times are 5 times less than WD-XRF. Further, the confirmation of ED-XRF measurements with 27 paired ICP-MS measurements suggest the ED-XRF calibration routine with the Cu/Ti/Al multi-metal primary filter is accurate (regression $r^2$ = 0.97; slope = 1.02) with no apparent bias (Figure 3.3b).

The variation between the measured concentrations and known concentrations using four reference materials decreases sharply when portable ED-XRF measurement times are increased,

with very little difference in RD values in measurements lasting 120 seconds or longer (Figure 3.2S). Therefore 120 seconds analysis time is considered sufficient.

To reduce the Compton peak, the calibration and verification process summarized above was repeated using the a Ti/Fe/Mo multi-metal primary filter. Although the valid photon count rates reduced significantly with the second primary filter, the RMSE, LOD, and LOQ values (Table 3.2S) did not increase significantly compared to the first filter. However, the confirmation of Pb ED-XRF measurements with 35 paired WD-XRF measurements of vegetable samples indicate the ED-XRF calibration routine with the Ti/Fe/Mo multi-metal primary filter is weak (regression $r^2 = 0.91$; slope = 1.39) with an unexplainable positive bias (Figure 3.3c). Although the Ti/Fe/Mo primary filter decreased background radiation, use of the Cu/Ti/Al primary filter is preferable for quantification of Pb in vegetables.

**Evaluation of the Dry Plant-Based ED-XRF Measurement and Calibration Routine for Additional Heavy Metals.** Although Pb is the primary metal of interest in this study, the ED-XRF captured a wide spectrum range allowing for quantification of several metals. The relatively small RMSE and LOQ values suggest these elements can be accurately measured with ED-XRF down to the single-digit $\mu g \; g^{-1}$ range (Table 3.2).

### 3.3.3    Wet Plant-Based Portable ED-XRF Measurement and Calibration Routines

**Evaluation of Measurement Depth and the Infinite Thickness Assumption.** Based on a matched-pair statistical analysis, adding Pb foil behind the sample cups did not increase the net intensity of the Pb L$\beta$1 wavelength ($p < 0.08$, DF=67) suggesting the coarsely homogenized wet (raw) samples packed into sample cups are infinitely thick for wavelengths less than 12.614 keV. However, adding Mo foil behind the sample cups significantly increased the net intensities of the

77

Mo Kα1 wavelength (p< 0.001; DF=66) confirming that samples are infinitely thin for wavelengths greater than 17.480 keV.

The RMSE, LOD, and LOQ values on a wet weight basis from the 85% water calibration of Cr, Ni, Pb, and Y (Table 3.3) are similar to values from the dry pressed pellets indicating X-ray attenuation by the presence of water is minimal. However, when converted to a dry weight basis the portable ED-XRF RMSE, LOD, and LOQ values from the wet plant-based calibration routine are comparatively large. Although the water in the reference materials does not significantly attenuate fluoresced X-rays, the water present in the matrix dilutes the quantity of heavy metals per unit volume of sample to a point where ED-XRF measurements of wet vegetables are not useful from a regulatory perspective unless the element concentrations are sufficiently large. Very few vegetables grown in this study had heavy metal concentrations greater than LOQs, therefore evaluation of the 85% water ED-XRF calibrations with confirmation samples was not possible.

Increasing the sample analysis time is the most common way to increase the precision and accuracy of XRF measurements and lower XRF detection limits. A supplemental ED-XRF calibration was developed using the 85% water content reference set by increasing the count time from 120s to 300s; calibration details are summarized on Table 3.3S. By increasing the measurement time, the relatively small RMSE values from the calibrations converted to dry-weight concentrations based on water content suggests Cr, Ni, and Pb can be accurately measured with ED-XRF down to the single-digit $\mu g\ g^{-1}$ range in raw samples (Table 3.3S). Although we were unable to empirically measure the LOD and LOQ using 300 s measurement time, increasing sample analysis time by a factor of 4 should reduce the detection limit by a factor of 2. If this relationship holds true for raw vegetable samples, based on the LOD at 120 s

(Table 3.3), we expect the LOD for Pb with 300 s measurement time to decrease to near 1 μg g$^{-1}$ (wet weight), which would be equivalent to approximately 7 μg g$^{-1}$ on a dry weight basis.

The mean water content of 261 vegetable samples used in this study is 87% with a standard deviation of 4%, therefore, using the 65% water content calibration would be inappropriate to quantify heavy metals in our raw vegetables. However, this work suggests that if the water content of food samples is not more than 65% (for example grains or cereals), portable ED-XRF spectrometry could detect Pb in raw samples at concentrations as low as 1 μg g$^{-1}$ dry weight (Table 3.3) with 120s count time. Further, this suggests that portable ED-XRF is a viable technology for use in element quantification in prepared foods with low water contents.

## 3.4   CONCLUSIONS

This work has shown that by managing matrix effects, XRF can be a useful tool in quantification of Pb and other heavy metals in vegetables. In our case, practical limits existed on the preparation of samples of sufficient thickness to retain all source and characteristic X-rays. Therefore, in addition to measuring samples and reference materials under the same conditions (ex. energy, current, filter, count time, atmosphere), the most critical factors we managed in developing measurement routines for quantification of heavy metals in plant tissues with WD-XRF and portable ED-XRF were:

1.   Developing reference materials with commutability to samples and maintaining consistency with sample preparation/handling (ex. drying time, milling time, sample mass),

2.   Selecting proper wavelengths to eliminate peak overlaps and controlling for possible enhancement from within the matrix or from characteristic X-rays generated by the shielding/housing,

79

3. Analyzing samples for long enough to maximize accuracy and precision, and

4. Confirming the viability of new routines to actual samples through paired analysis of samples with another quantification technology to provide additional assurance in the measurement and calibration routines.

As we hypothesized, by addressing these critical factors, this study demonstrates that WD-XRF and portable ED-XRF can be used to accurately and rapidly quantify heavy metals in vegetable samples with limits of detection achieving regulatory thresholds. Although the most robust calibration was obtained with WD-XRF, this technology is limited to fixed laboratory-based instruments. Slight compromise in the precision and accuracy of measurements with portable ED-XRF is offset by the portability and ease of use of this technology outside of a traditional laboratory setting.

Quantification of heavy metals in wet coarsely-homogenized raw (undried) vegetable tissues was performed; however, RMSE and LODs on a dry-weight basis are strongly influenced by measurement time and water content which currently limits this technology. However, the technology is very promising for analysis of coarsely homogenized wet (raw) foodstuffs with lower water contents, such as grains and legumes and could easily be adopted for prepared foods.

## 3.5 REFERENCES

Andersen, L. K., Morgan, T. J., Boulamanti, A. K., Álvarez, P., Vassilev, S. V., & Baxter, D. (2013). Quantitative X-ray fluorescence analysis of biomass: Objective evaluation of a typical commercial multi-element method on a WD-XRF spectrometer. Energy and Fuels, 27(12), 7439–7454. http://doi.org/10.1021/ef4015394

Anjos, M. J., Lopes, R. T., Jesus, E. F. O., Simabuco, S. M., & Cesareo, R. (2002). Quantitative determination of metals in radish using x-ray fluorescence spectrometry. X-Ray Spectrometry, 31(2), 120–123. http://doi.org/10.1002/xrs.567

Bešter, P. K., Lobnik, F., Eržen, I., Kastelec, D., & Zupan, M. (2013). Prediction of cadmium concentration in selected home-produced vegetables. Ecotoxicology and Environmental Safety, 96, 182–190. http://doi.org/10.1016/j.ecoenv.2013.06.011

Bozym, M., Florczak, I., Zdanowska, P., Wojdalski, J., & Klimkiewicz, M. (2015). An analysis of metal concentrations in food wastes for biogas production. Renewable Energy, 77, 467–472. http://doi.org/10.1016/j.renene.2014.11.010

Bull, A., Brown, M. T., & Turner, A. (2017). Novel use of field-portable-XRF for the direct analysis of trace elements in marine macroalgae. Environmental Pollution, 220, 228–233. http://doi.org/10.1016/j.envpol.2016.09.049

Byers, H. L., McHenry, L. J., & Grundl, T. J. (2016). Forty-Nine Major and Trace Element Concentrations Measured in Soil Reference Materials NIST SRM 2586, 2587, 2709a, 2710a and 2711a Using ICP-MS and Wavelength Dispersive-XRF. Geostandards and Geoanalytical Research, 40(3), 433–445. http://doi.org/10.1111/j.1751-908X.2016.00376.x

Chantler, C. T., Olsen, K., Dragoset, R. A., Chang, J., Kishore, A. R., Kotochigova, S. A., & Zucker, D. S. (2001). X-Ray Form Factor, Attenuation, and Scattering Tables. Washington, DC: National Institute of Standards and Technology, U.S. Department of Commerce. Retrieved from https://www.nist.gov/pml/x-ray-form-factor-attenuation-and-scattering-tables

Chopra, A. K., & Pathak, C. (2015). Accumulation of heavy metals in the vegetables grown in wastewater irrigated areas of Dehradun, India with reference to human health risk. Environmental Monitoring and Assessment, 187(7). http://doi.org/10.1007/s10661-015-4648-6

Clark, H. F., Brabander, D. J., & Erdil, R. M. (2006). Sources, Sinks, and Exposure Pathways of Lead in Urban Garden Soil. Journal of Environment Quality, 35(6), 2066. http://doi.org/10.2134/jeq2005.0464

Ferri, R., Hashim, D., Smith, D. R., Guazzetti, S., Donna, F., Ferretti, E., … Lucchini, R. G. (2015). Metal contamination of home garden soils and cultivated vegetables in the province of Brescia, Italy: Implications for human exposure. Science of the Total Environment, 518–519, 507–517. http://doi.org/10.1016/j.scitotenv.2015.02.072

Figueiredo, A., Fernandes, T., Costa, I. M., Gonçalves, L., & Brito, J. (2016). Feasibility of wavelength dispersive X-ray fluorescence spectrometry for the determination of metal impurities in pharmaceutical products and dietary supplements in view of regulatory guidelines. Journal of Pharmaceutical and Biomedical Analysis, 122, 52–58. http://doi.org/10.1016/j.jpba.2016.01.028

Finster, M. E., Gray, K. A., & Binns, H. J. (2004). Lead levels of edibles grown in contaminated residential soils: A field survey. Science of the Total Environment. http://doi.org/10.1016/j.scitotenv.2003.08.009

Gallardo, H., Queralt, I., Tapias, J., Guerra, M., Carvalho, M. L., & Marguí, E. (2016). Possibilities of low-power X-ray fluorescence spectrometry methods for rapid multielemental analysis and imaging of vegetal foodstuffs. Journal of Food Composition and Analysis, 50, 1–9. http://doi.org/10.1016/j.jfca.2016.04.007

Gutiérrez-Ginés, M. J., Pastor, J., & Hernández, A. J. (2013). Assessment of field portable X-ray fluorescence spectrometry for the in situ determination of heavy metals in soils and plants. Environmental Science: Processes & Impacts, 15(8), 1545. http://doi.org/10.1039/c3em00078h

Hubbell, J. H., & Seltzer, S. M. (2004). X-Ray Mass Attenuation Coefficients. Gaithersburg, MD. http://doi.org/https://dx.doi.org/10.18434/T4D01F

Jolly, Y. N., Islam, A., & Akbar, S. (2013). Transfer of metals from soil to vegetables and possible health risk assessment. SpringerPlus, 2(1), 1–8. http://doi.org/10.1186/2193-1801-2-385

Keller, B., Faciano, A., Tsega, A., & Ehrlich, J. (2017). Epidemiologic Characteristics of Children with Blood Lead Levels ≥45 μg/dL. Journal of Pediatrics, 180, 229–234. http://doi.org/10.1016/j.jpeds.2016.09.017

Lane, S. D., Webster, N. J., Levandowski, B. A., Rubinstein, R. A., Keefe, R. H., Wojtowycz, M. A., Aubry, R. H. (2008). Environmental Injustice: Childhood Lead Poisoning, Teen Pregnancy, and Tobacco. Journal of Adolescent Health, 42(1), 43–49. http://doi.org/10.1016/j.jadohealth.2007.06.017

Lima, F., Nascimento, C., Silva, F., Carvalho, V., & Filho, M. (2009). Lead concentration and allocation in vegetable crops grown in a soil contaminated by battery residues. Horticultura Brasileira, 27(3), 362–365.

Marguí, E., Queralt, I., & Hidalgo, M. (2009). Application of X-ray fluorescence spectrometry to determination and quantitation of metals in vegetal material. TrAC - Trends in Analytical Chemistry, 28(3), 362–372. http://doi.org/10.1016/j.trac.2008.11.011

Martynenko, A. (2014). True, Particle, and Bulk Density of Shrinkable Biomaterials: Evaluation from Drying Experiments. Drying Technology, 32(11), 1319–1325. http://doi.org/10.1080/07373937.2014.894522

Murray, H., Pinchin, T., & Macfie, S. (2011). compost application affects update in plants grown in urban garden soils and potential human health risks. Journal of Soils and Sediments, 11(5), 815–829.

Nabulo, G., Black, C. R., & Young, S. D. (2011). Trace metal uptake by tropical vegetables grown on soil amended with urban sewage sludge. Environmental Pollution, 159(2), 368–376. http://doi.org/10.1016/j.envpol.2010.11.007

Otaka, A., Hokura, A., & Nakai, I. (2014). Determination of trace elements in soybean by X-ray fluorescence analysis and its application to identification of their production areas. Food Chemistry, 147, 318–326. http://doi.org/10.1016/j.foodchem.2013.09.142

Palmer, P. T., Jacobs, R., Baker, P. E., Ferguson, K., & Webber, S. (2009). Use of field-portable XRF analyzers for rapid screening of toxic elements in fda-regulated products. Journal of Agricultural and Food Chemistry, 57(7), 2605–2613. http://doi.org/10.1021/jf803285h

Rodriguez-Iruretagoiena, A., Trebolazabala, J., Martinez-Arkarazo, I., Diego, A., & Madariaga, J. M. (2015). Metals and metalloids in fruits of tomatoes (Solanum lycopersicum) and their cultivation soils in the Basque Country: Concentrations and accumulation trends. Food Chemistry, 173, 1083–1089. http://doi.org/10.1016/j.foodchem.2014.10.133

Rodríguez-Ramírez, J., Méndez-Lagunas, L., López-Ortiz, A., & Torres, S. S. (2012). True Density and Apparent Density During the Drying Process for Vegetables and Fruits: A Review. Journal of Food Science. http://doi.org/10.1111/j.1750-3841.2012.02990.x

Sacristan, D., Rossel, R. A. V., & Recatala, L. (2016). Proximal sensing of Cu in soil and lettuce using portable X-ray fluorescence spectrometry. Geoderma, 265, 6–11. http://doi.org/10.1016/j.geoderma.2015.11.008

Schnur, J., & John, R. M. (2014). Childhood lead poisoning and the new centers for disease control and prevention guidelines for lead exposure. Journal of the American Association of Nurse Practitioners. http://doi.org/10.1002/2327-6924.12112

Sekara, A., Poniedzialek, M., Ciura, J., & Jedrszczyk, E. (2005). Cadmium and lead accumulation and distribution in the tissues of nine crops: Implications for phytoremediation. Polish Journal of Environmental Studies, 14(4), 509–516.

Singh, V., Rai, P., Pathak, A., Tripathi, D., Singh, S., & Singh, J. (2017). Application of Wavelength-Dispersive X-Ray Fluorescence Spectrometry to Biological Samples. Spectroscopy, 32(7), 41–47.

Song, X., Hu, X., Ji, P., Li, Y., Chi, G., & Song, Y. (2012). Phytoremediation of cadmium-contaminated farmland soil by the hyperaccumulator beta vulgaris L. var. cicla. Bulletin of Environmental Contamination and Toxicology, 88(4), 623–626. http://doi.org/10.1007/s00128-012-0524-z

Thomsen, V. (2012). Spectral Background Radiation and the Background Equivalent Concentration in Elemental Spectrochemistry. Spectroscopy, 17(3), 28–36.

Thomsen, V., Schatzlein, D., & Mercuro, D. (2003). Limits of Detection in Spectroscopy. Spectroscopy, 18(12), 112–114. http://doi.org/Article

Towett, E. K., Shepherd, K. D., & Drake, L. B. (2016). Plant elemental composition and portable X-ray fluorescence (pXRF) spectroscopy: Quantification under different analytical parameters. X-Ray Spectrometry, 45(2), 117–124. http://doi.org/10.1002/xrs.2678

Turner, A., Poon, H., Taylor, A., & Brown, M. T. (2017). In situ determination of trace elements in Fucus spp. by field-portable-XRF. Science of the Total Environment, 593–594, 227–235. http://doi.org/10.1016/j.scitotenv.2017.03.091

USEPA. (1996). Method 3050B - Acid digestion of sediments, sludges, and soils. 1996. http://doi.org/10.1117/12.528651

WHO. (2018). General Standard for Contaminants and Toxins in Food and Feed (CODEX STAN 193-1995), Pub. L. No. Codex STAN 193-1955 (2018). Retrieved from http://www.fao.org/input/download/standards/17/CXS_193e_2015.pdf

Wiseman, C. L. S., Zereini, F., & Püttmann, W. (2013). Traffic-related trace element fate and uptake by plants cultivated in roadside soils in Toronto, Canada. Science of the Total Environment. http://doi.org/10.1016/j.scitotenv.2012.10.051

Yadav, R. K., Minhas, P. S., Lal, K., Chaturvedi, R. K., Yadav, G., & Verma, T. P. (2015). Accumulation of Metals in Soils, Groundwater and Edible Parts of Crops Grown Under Long-Term Irrigation with Sewage Mixed Industrial Effluents. Bulletin of Environmental Contamination and Toxicology. http://doi.org/10.1007/s00128-015-1547-z

Figure 3.1. Calculated XRF measurement depth curve for a pressed pellet consisting of Cellulose + Sugar ($C_6H_{10}O_5C_6H_{12}O_6$).
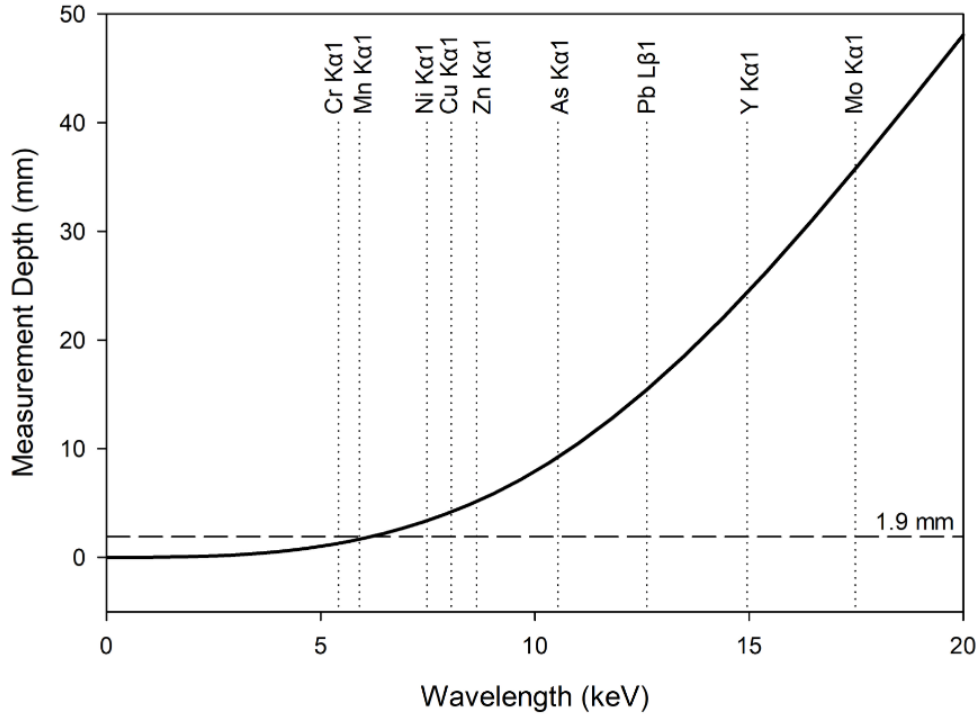


Note. Element wavelengths of interest are identified for reference. For a given pellet thickness, wavelengths to the left of the solid curved black line are considered infinitely thick, while wavelengths to the right are not. Pellets used in this study were 1.9 mm thick, which is indicated with a horizontal dashed line for reference.

85

Figure 3.2.a. ED-XRF spectrum with the Cu/Ti/Al primary filter of the 10 µg g$^{-1}$ pressed pellet reference material with element wavelengths and Compton/Raleigh peaks identified.
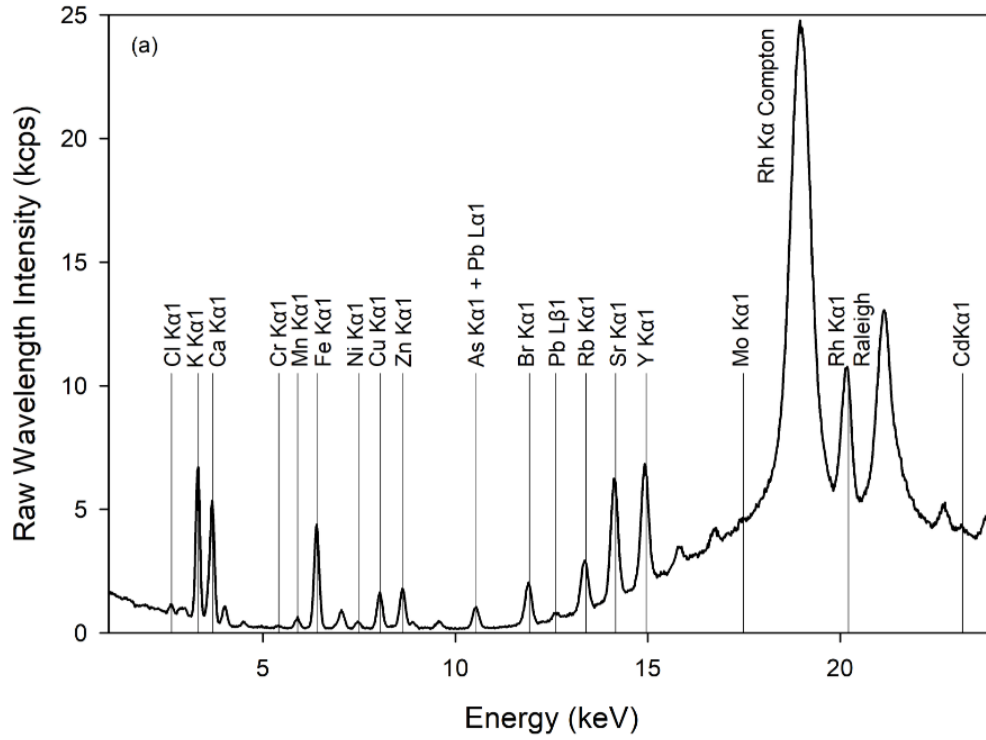
Figure 3.2.b. the ED-XRF spectra of at the Pb L$\beta$1 wavelength for pellet reference materials with nominal Pb concentrations of 0 (heavy line), 5, 10, 20, 50, and 100 $\mu$g g$^{-1}$ (successively higher peaks).
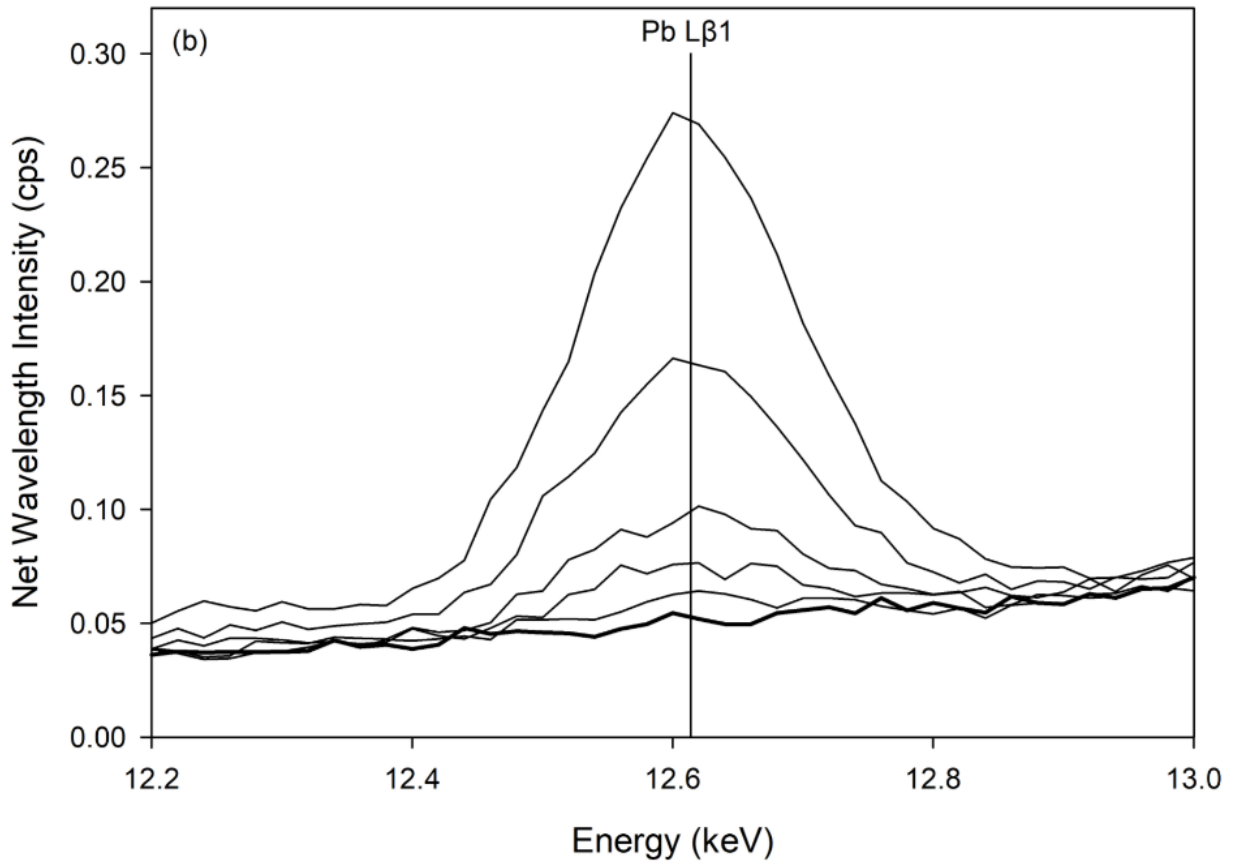
Figure 3.3. Paired confirmation Pb measurements of dried vegetable samples using (a) WD-XRF and ICP-MS, (b) ED-XRF (with the Cu/Ti/Al primary filter) and ICP-MS, and (c) ED-XRF (with the Ti/Fe/Mo primary filter) and WD-XRF.
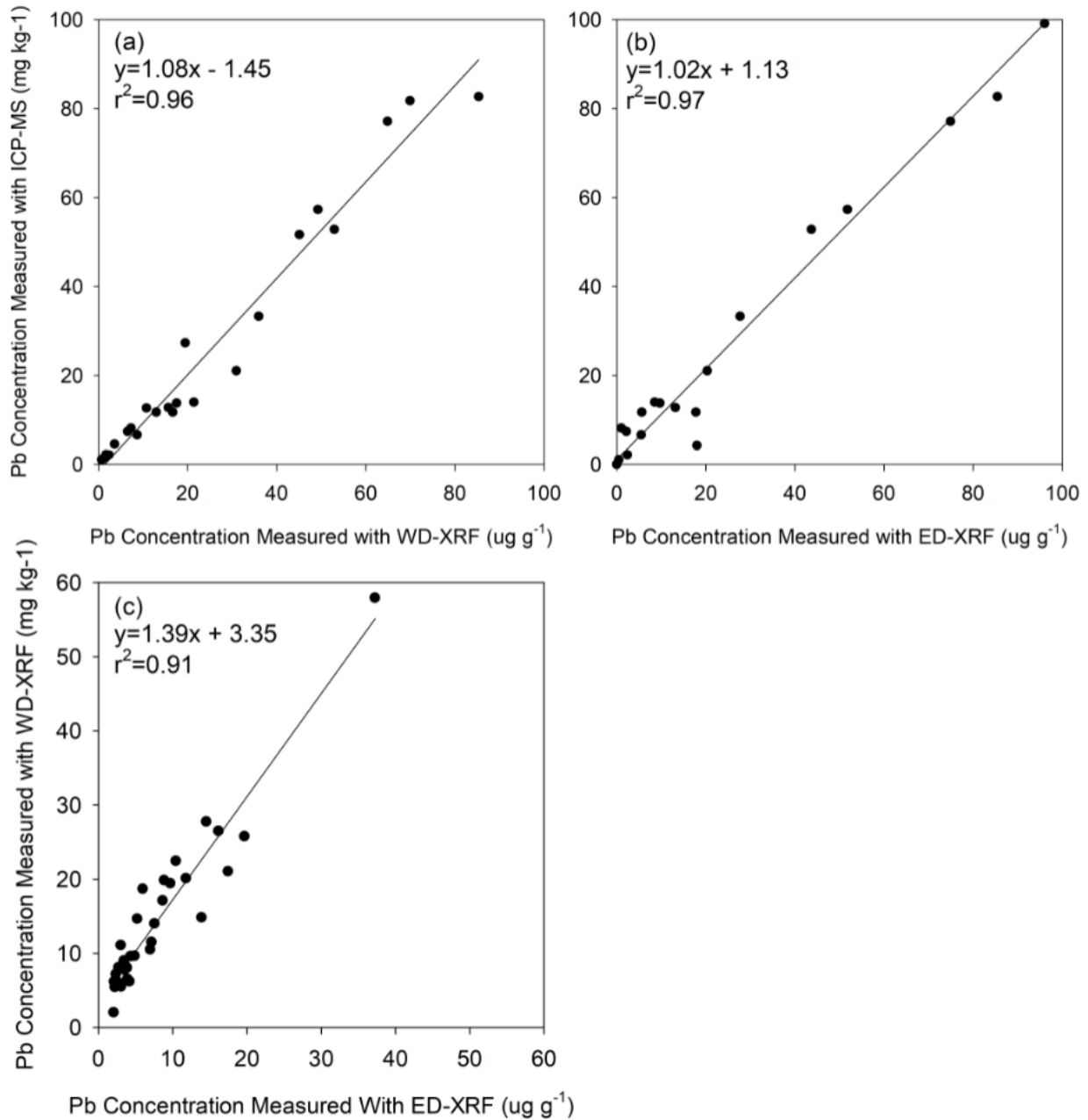


Note. The regression equation for each line and the coefficient of determination ($r^2$) are provided.

Table 3.1. Goodness of fit parameters for WD-XRF calibrations of pressed pellets for Cr, Ni, Pb, and Y.

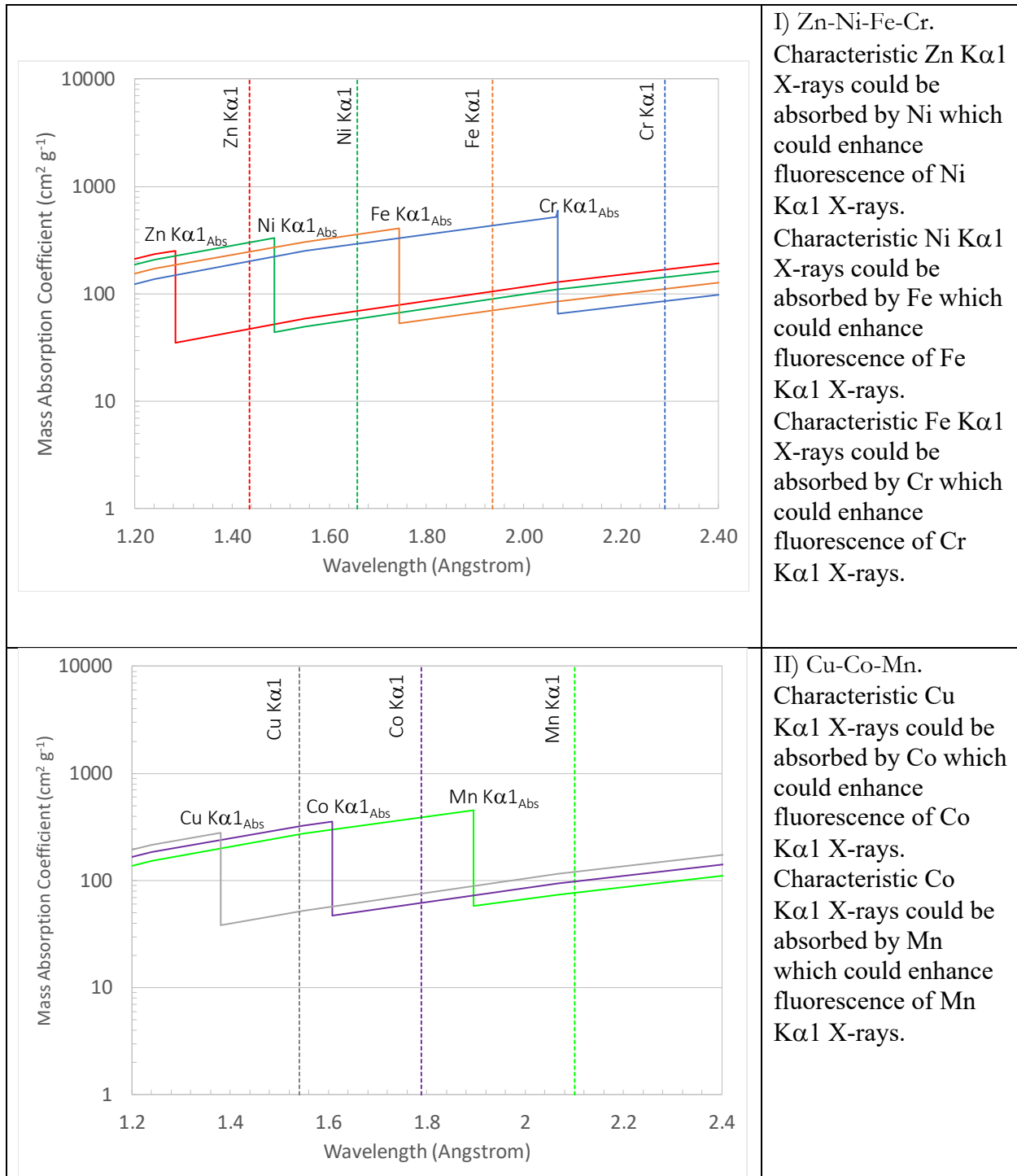| | Calibration $r^2$ | RMSE ($\mu g\ g^{-1}$) | Range in Reference Materials ($\mu g\ g^{-1}$) | | LOD ($\mu g\ g^{-1}$) | LOQ ($\mu g\ g^{-1}$) |
|---|---|---|---|---|---|---|
| Cr | 0.99 | 1.2 | 3.1 | 105 | 0.6 | 2.0 |
| Ni | 0.99 | 0.9 | 6.6 | 111 | 0.4 | 1.3 |
| Pb | 0.99 | 0.7 | 0.1 | 96 | 0.3 | 1.0 |
| Y | 0.99 | 1.0 | 0.5 | 600 | 0.3 | 1.0 |

Note. The Root Mean Square Error (RMSE) of the calibration, range in reference materials, Limit of Detection (LOD), and Limit of Quantitation (LOQ) are expressed in $\mu g\ g^{-1}$, dry weight. The K$\alpha$1 wavelengths were used for each calibration, except for Pb which used the L$\beta$1 wavelength.

Table 3.2. Goodness of fit parameters for ED-XRF calibrations of pressed pellets with the Cu/Ti/Al primary filter.

|  | Peak Overlap Corrections | Calibration $r^2$ | RMSE ($\mu g\ g^{-1}$) | Range in Reference Materials ($\mu g\ g^{-1}$) | | LOD ($\mu g\ g^{-1}$) | LOQ ($\mu g\ g^{-1}$) |
|---|---|---|---|---|---|---|---|
| Cr | Fe Kα1 | 0.99 | 3.0 | 3.1 | 105 | 2.3 | 7.5 |
| Mn | *none* | 0.97 | 7.1 | 66.2 | 176 | 3.7 | 12.1 |
| Ni | *none* | 0.99 | 3.7 | 6.6 | 111 | 1.4 | 4.5 |
| Cu | *none* | 0.99 | 3.7 | 27.1 | 129 | 1.6 | 5.3 |
| Zn | *none* | 0.99 | 4.6 | 40.6 | 181 | 0.2 | 0.7 |
| As | Pb Lα1 | 1.00 | 3.3 | 0.5 | 131 | 0.3 | 0.9 |
| Pb | *none* | 1.00 | 0.9 | 0.1 | 96 | 0.3 | 1.1 |
| Y | *none* | 0.99 | 17.8 | 0.5 | 600 | 1.5 | 4.9 |
| Cd | *none* | 0.94 | 11.2 | 0.6 | 119 | 0.2 | 0.6 |

Note. The Root Mean Square Error (RMSE) of the calibration, range in reference materials, Limit of Detection (LOD), and Limit of Quantitation (LOQ) are expressed in $\mu g\ g^{-1}$, dry weight. The Kα1 wavelengths were used for each calibration, except for Pb which used the Lβ1 wavelength. Peak overlap corrections used in refining the calibration routines are summarized.

Table 3.3. Goodness of fit parameters for ED-XRF calibrations with the Cu/Ti/Al primary filter for plant-based reference materials consisting of 85 percent (%) and 65% water.

| | Calibration $r^2$ | Concentration ($\mu g\ g^{-1}$, wet weight) | | | | | Water Content | Concentration ($\mu g\ g^{-1}$, dry weight) | | |
|---|---|---|---|---|---|---|---|---|---|---|
| | | RMSE | Range in Reference Materials | | LOD | LOQ | | RMSE | LOD | LOQ |
| Cr | 0.70 | 3 | 0.3 | 17 | 3 | 11 | | 21 | 23 | 76 |
| Ni | 0.94 | 1 | 0.2 | 17 | 4 | 12 | 85% | 9 | 23 | 77 |
| Pb | 0.86 | 2 | 0.0 | 15 | 2 | 7 | | 12 | 13 | 44 |
| Y | 0.90 | 10 | 0.2 | 96 | 1 | 2 | | 66 | 4 | 14 |
| Cr | 0.97 | 2 | 1 | 41 | 4 | 13 | | 7 | 12 | 38 |
| Ni | 0.99 | 1 | 0.4 | 42 | 2 | 6 | 65% | 3 | 5 | 17 |
| Pb | 1.00 | 1 | 0.0 | 36 | 0.4 | 1 | | 3 | 1 | 4 |
| Y | 0.95 | 17 | 0.4 | 234 | 4 | 14 | | 48 | 12 | 41 |

Note. The Root Mean Square Error of the calibration (RMSE), Limit of Detection (LOD), and Limit of Quantitation (LOQ) were measured in $\mu g\ g^{-1}$ wet weight with ED-XRF, and these values converted to dry weight concentrations based on water content. The K$\alpha$1 wavelengths were used for each calibration, except for Pb which used the L$\beta$1 wavelength.

Figure 3.1S. Possible secondary or tertiary enhancement due to absorption of characteristic X-rays in mixtures of (I) Zn, Ni, Fe, Cr; (II) Cu, Co, Mn; and (III) Br, As.



I) Zn-Ni-Fe-Cr. Characteristic Zn K$\alpha$1 X-rays could be absorbed by Ni which could enhance fluorescence of Ni K$\alpha$1 X-rays. Characteristic Ni K$\alpha$1 X-rays could be absorbed by Fe which could enhance fluorescence of Fe K$\alpha$1 X-rays. Characteristic Fe K$\alpha$1 X-rays could be absorbed by Cr which could enhance fluorescence of Cr K$\alpha$1 X-rays.

II) Cu-Co-Mn. Characteristic Cu K$\alpha$1 X-rays could be absorbed by Co which could enhance fluorescence of Co K$\alpha$1 X-rays. Characteristic Co K$\alpha$1 X-rays could be absorbed by Mn which could enhance fluorescence of Mn K$\alpha$1 X-rays.

www.manaraa.com

III) Br-As-Pb. Characteristic Br K$\alpha$1 X-rays could be absorbed by As which could enhance fluorescence of As K$\alpha$1 X-rays. Br is present in the matrix used in this study. No enhancement of Pb from Br is expected. However, notice the overlap of the Pb L$\alpha$1 X-rays with As K$\alpha$1 X-rays; therefore, the Pb Lb1 wavelength is used in this study for quantification of Pb.

Figure 3.2S. Relative percent difference between ED-XRF measurements (with a Cu/Ti/Al

primary filter) of Pb and known values for four reference materials.
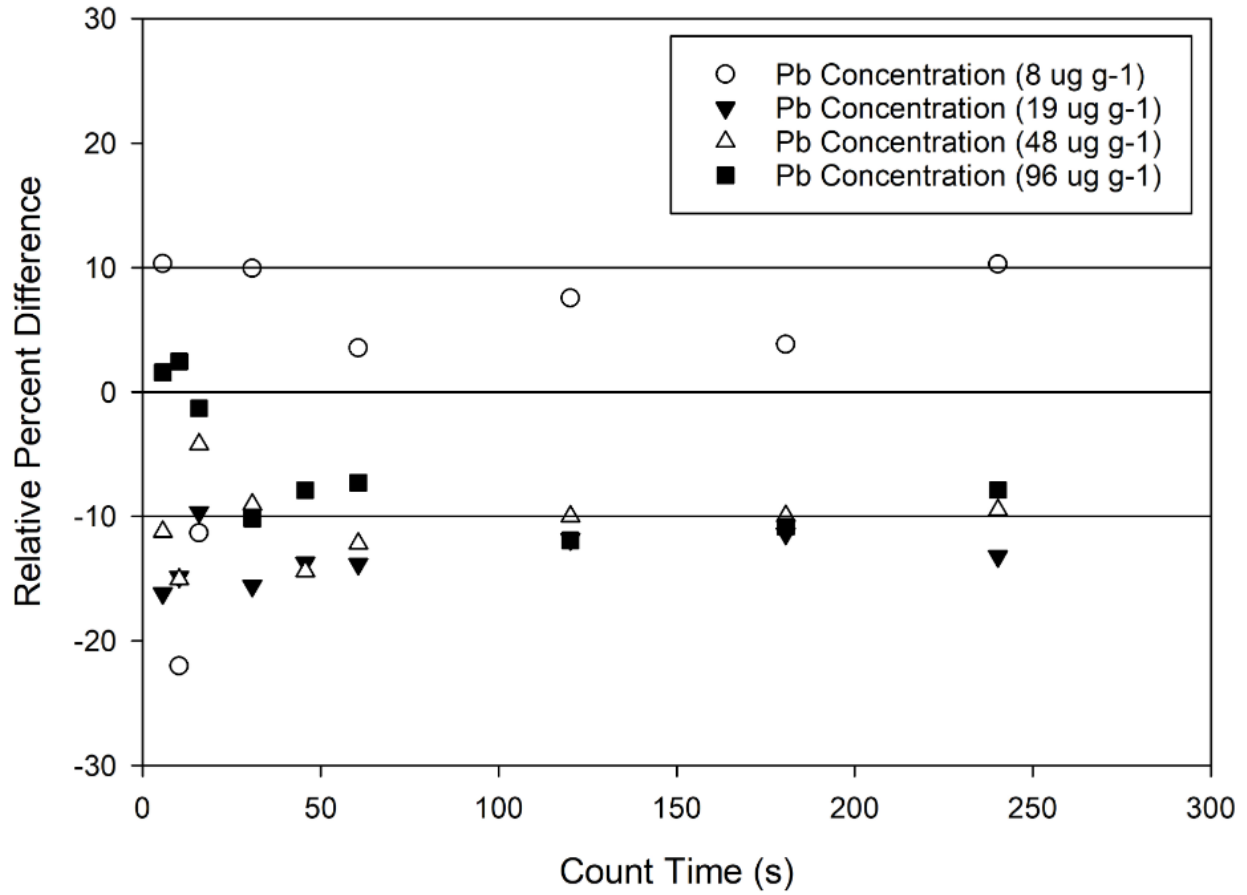


Note. Positive values indicate the expected concentration is greater than the measured

concentration.

Table 3.1S. WD-XRF measurement routine specifications.

| | Line | Background (Kv) | Line (Kv) | Background (Kv) | Measurement Time (Peak) | Measurement Time (Background | Generator Voltage (Kv) |
|---|---|---|---|---|---|---|---|
| Cr | Kα1 | 5.36847 | 5.415 | 5.48878 | 30s | 10s | 60 |
| Ni | Kα1 | 7.37114 | 7.480 | 7.58034 | 30s | 10s | 60 |
| Pb | Lβ1 | 12.29548 | 12.614 | 12.94036 | 300s | 300s | 60 |
| Y | Kα1 | 14.45286 | 14.958 | 15.47622 | 30s | 10s | 60 |

| | Tube Current (mA) | Sample Rotation (rev/s) | Collimator Mask | Collimator (dg) | Analyzer Crystal | Detector | Peak Overlap Corrections |
|---|---|---|---|---|---|---|---|
| Cr | 67 | 0.5 | 34mm | 0.46 | Lif200 | Scintillation Counter | *none* |
| Ni | 67 | 0.5 | 34mm | 0.46 | Lif200 | Scintillation Counter | *none* |
| Pb | 67 | 0.5 | 34mm | 0.46 | Lif200 | Scintillation Counter | *none* |
| Y | 67 | 0.5 | 34mm | 0.46 | Lif200 | Scintillation Counter | *none* |

Table 3.2S. Goodness of fit parameters for ED-XRF calibrations with the Ti/Fe/Mo primary filter of pressed pellets.

|  | Peak Overlap Corrections | Calibration $r^2$ | RMSE ($\mu g\ g^{-1}$) | Calibration Range ($\mu g\ g^{-1}$) | | LOD ($\mu g\ g^{-1}$) | LOQ ($\mu g\ g^{-1}$) |
|---|---|---|---|---|---|---|---|
| Cr | Fe Kα1 | 0.84 | 15.6 | 3.1 | 105 | 0.9 | 3.0 |
| Mn | *none* | 0.88 | 14.4 | 66.2 | 176 | 5.8 | 19.0 |
| Ni | *none* | 1.00 | 1.5 | 6.6 | 111 | 3.3 | 10.8 |
| Cu | *none* | 0.93 | 9.9 | 27.1 | 129 | 1.4 | 4.6 |
| Zn | *none* | 0.96 | 9.7 | 40.6 | 181 | 1.2 | 4.0 |
| As | Pb Lα1 | 1.00 | 1.5 | 0.5 | 131 | 1.1 | 3.6 |
| Pb | *none* | 1.00 | 1.4 | 0.1 | 96 | 0.9 | 2.9 |
| Y | *none* | 1.00 | 0.8 | 0.0 | 600 | 0.1 | 0.4 |
| Cd | *none* | 0.99 | 3.9 | 0.6 | 119 | 10.0 | 32.9 |

Note. The Root Mean Square Error (RMSE) of the calibration, range in reference materials, Limit of Detection (LOD), and Limit of Quantitation (LOQ) are expressed in $\mu g\ g^{-1}$, dry weight. The Kα1 wavelengths were used for each calibration, except for Pb which used the Lβ1 wavelength. Peak overlap corrections used in refining the calibration routines are included.

Table 3.3S. Goodness of fit parameters for ED-XRF calibrations with the Cu/Ti/Al primary filter for plant-based reference materials consisting of 85 percent (%) with 300 s count time.

| | Calibration $r^2$ | Concentration ($\mu g\ g^{-1}$, wet weight) | | | Water Content | Concentration ($\mu g\ g^{-1}$, dry weight) |
| | | RMSE | Range in Reference Materials | | | RMSE |
|---|---|---|---|---|---|---|
| Cr | 0.96 | 1.1 | 0.3 | 17 | | 7 |
| Ni | 0.99 | 0.4 | 0.2 | 17 | 85% | 2.5 |
| Pb | 0.99 | 0.2 | 0.0 | 15 | | 1.1 |
| Y | 0.99 | 3.8 | 0.2 | 96 | | 25 |

Note. The Root Mean Square Error (RMSE) of the calibration was measured in $\mu g\ g^{-1}$ (wet weight) and these values converted to dry weight based on water content. The Kα1 wavelengths were used for each calibration, except for Pb which used the Lβ1 wavelength.

# 4.0 ACCUMULATION OF PB IN 9 COMMON CROPS GROWN IN METALS-RICH RESIDENTIAL GARDEN SOILS AND SOIL FROM A FORMER METAL FOUNDRY

## 4.1 INTRODUCTION

Growing produce in urban centers is actively encouraged to increase food security and strengthen communities (Ghose and Pettygrove 2014; Pettygrove and Ghose 2018). However, for community members with limited mobility and/or financial resources, few options exist for growing produce other than to use in-place soils at residential properties, which could result in produce cultivation in metals-rich soils. A multitude of poor health outcomes in children are associated with Pb exposure (Amato et al. 2013; Keller et al. 2017; Lane et al. 2008; Magzamen et al. 2015; Sampson and Winter 2018; Schnur and John 2014), and although much progress has been made since the 1970s in reducing blood Pb in children (Dignam et al. 2019), Pb exposure continues to be a critical environmental justice issue in minority/low-income neighborhoods (Whitehead and Buchanan 2019).

Blood lead concentrations in children have been shown to be strongly associated with the concentration of Pb in soil (Laidlaw et al. 2016; Zahran et al. 2015) and the presumption is that ingestion of soil+dust is the most significant exposure route in children. The concentration of Pb in urban soils is known to be highly variable (Clark et al. 2006, 2008; Defoe et al. 2014; Finster et al. 2004; Huang et al. 2012; McBride et al. 2014; Perroy et al. 2014; Sharma et al. 2015) and the sources of Pb in urban soils represent a broad continuum of historic land uses/spills/releases. Several studies have broadly attributed the primary sources of Pb in urban soils to weathering paint (Clark et al. 2006, 2008; Laidlaw et al. 2018); transportation (Clark et al. 2006); stormwater or river water used for irrigation (Ratul et al. 2018; Tom et al. 2014); soil

98

amendments (Murray et al. 2011b); or anthropogenic fill, such as foundry sand and industrial waste/debris. More localized spills/releases associated with industry/mining (Augustsson et al. 2015; Mombo et al. 2016; Pizarro et al. 2016; Yuan et al. 2019) and the use of fertilizers/pesticides (Reboredo et al. 2019) are also acknowledged inputs of Pb to agricultural soils.

In the context of urban agriculture, the mobility, toxicity, and bioavailability of Pb in soil (especially anthrosols) is a function of the solubility of the Pb source and the availability of the $Pb^{+2}$ cation (or very rarely as $Pb_4(OH_4)^{+4}$ ), which is strongly regulated in soil by pH, cation exchange capacity, and the presence of organic and nonorganic ligands. Common crops grown in metals-rich soils have the potential to accumulate Pb in consumable tissues (Clark et al. 2006; Ferri et al. 2015; Finster et al. 2004; Jolly et al. 2013; Lima et al. 2009a; Nabulo et al. 2011; Rodriguez-Iruretagoiena et al. 2015; Sekara et al. 2005; Yousaf et al. 2016). Accumulation of Pb in consumable produce is strongly associated with crop type, with more commonly studied modified taproot crops (e.g. carrots) tending to accumulate more Pb than fruit crops (e.g. tomatoes, beans); however, very little is known about the potential for Pb accumulation in beetroots and in potatoes grown in metals-rich soils. In addition, although parents are encouraged to feed children brightly colored produce, little is known about the role pigments may play in accumulating Pb in select root crop cultivars. Several best management practices have been recommended to reduce the potential for Pb exposure (Abdel-Rahman et al. 2018; Brown et al. 2016; Mombo et al. 2016); however, as the risk for Pb exposure cannot be eliminated, continued evaluation of best management practices in the context of home-grown produce grown in residential soils is warranted. Therefore, a study growing a wide variety of produce in soils

collected from urban sources, including existing residential vegetable gardens, is warranted so that a more realistic evaluation of exposure risk can be completed.

Estimates suggest that consumption of vegetables is a secondary, less critical exposure route (Augustsson et al. 2015; Brown et al. 2016; Chopra and Pathak 2015; Ferri et al. 2015; Jolly et al. 2013). However, much of the prior work did not evaluate the accumulation of Pb in produce grown in soils with Pb concentrations representative of soil from older neighborhoods (Attanayake et al. 2015; Entwistle et al. 2019; Mombo et al. 2016; Yousaf et al. 2016). Of work evaluating Pb accumulation in produce grown in soils close to the range of Pb found in urban soils, the sample sizes and diversity of produce was limited (Finster et al. 2004) or the source of Pb was associated with an acidic spill (Lima et al. 2009b) or discharge from mining (Augustsson et al. 2015).

Recent work summarizing the literature has pointed out the importance of food as an exposure route (Rai et al. 2019). Although commercial foods in the United States are generally considered safe, work has identified Pb in commercially-sourced spices, ethnic foods, folk medicines, and other foods (Dignam et al. 2019; Hore et al. 2019). Further, the United States Food and Drug Administration (USFDA) recently establishing an Interim Reference Level (IRL) for Pb for children aimed at achieving the Center for Disease Control's blood lead reference value of 5 $\mu$g dL$^{-1}$ (USFDA 2019) and for adults; therefore, further evaluation of potential Pb exposure from consumption of home-grown produce is desperately warranted. Additionally, previous studies that used X-Ray fluorescence (XRF) spectroscopy to measure Pb in produce failed to reach limits of detection less than 1 $\mu$g g$^{-1}$ due to several key factors (Marguí et al. 2009; Palmer et al. 2009; Singh et al. 2017). This study seeks to address inconsistencies in using

100

XRF for quantification of Pb in produce and demonstrate the usefulness of this analytical technique in evaluating the risk for Pb exposure though ingestion of produce.

This study addresses these limitations by: (1) using newly-developed XRF sample preparation techniques and quantification routines to measure Pb in a variety of common crops grown in a range of Pb-rich residential and former industrial urban soils, (2) evaluating factors predicting the accumulation of Pb in consumable crop tissues, and (3) assessing the potential Pb exposure to a child through consumption of produce grown in metals-rich soil in the context of other exposure vectors.

## 4.2 METHODS

**Identification of Project Area.** Minority (non-white) children less than 3 years of age, living in older homes, from low-income families, are at the greatest risk for Pb poisoning (Amato et al. 2013; City of Milwaukee 2017). The Pb poisoning rate of children in the City of Milwaukee, and in particular those living in Census Tract 90, is nearly ten-times the rate of the United States (Table 4.1). Demographics from Census Tract 90 characterize the target area as a high-density, low-income, minority, environmental justice community, which is supported by a recent study of the overall area by Pettygrove and Ghose (2018). Therefore, using soils from vegetable gardens collected from occupied residential properties in Census Tract 90 is considered a practical way to evaluate the risk for Pb exposure through consumption of produce grown at residential properties. As estimated by Dignam et al. (2019), upwards of 23 million homes in the US are estimated to pose a risk for Pb exposure due to Pb-bearing paint; therefore, the applicability of the results of this study extend far beyond the project area.

**Acquisition of Metals-Rich Soil.** Soil samples were collected from 14 owner-occupied properties in Census Tract 90 with active vegetable gardens. The concentrations of heavy metals

in these soil samples were determined for screening purposes using WD-XRF using procedures and custom calibrations as described in Byers et al. (2016). Owners of two of the properties were willing to donate their garden soil to this study. The garden at Residence 1 was located adjacent to a painted garage constructed prior to 1978 and visible white paint chips were present in the garden soil. The total Pb in soil from Residence 1 ranged from 1,300 to 13,400 $\mu g \ g^{-1}$, with a mean of $5,950 \pm 4,922 \ \mu g \ g^{-1}$. The garden at Residence 2 was located adjacent to a retaining wall and a painted wood deck constructed prior to 1978 and visible brown paint chips were present in the garden soil. The total Pb in soil from Residence 2 ranged from 1,800 to 6,300 $\mu g \ g^{-1}$, with a mean of $5,017 \pm 1,608 \ \mu g \ g^{-1}$. Although the concentrations of Pb in the two garden soils are significantly greater than health-based direct contact soil standards set by the Wisconsin Department of Natural Resources (WDNR, the state environmental regulatory agency), the concentrations are considered representative of the variability of Pb in soils in cultivated vegetable gardens located at residential properties under similar circumstances and are within ranges of Pb concentrations in urban soils identified by others (e.g. Augustsson et al. 2015; Finster et al. 2004; Obrycki et al. 2017) and similar to previous soil studies in Milwaukee (Brinkmann 1994). Soil from each vegetable garden was dug by hand using a stainless-steel shovel, transported to the University of Wisconsin – Milwaukee (UWM) greenhouse, and placed into lined 5-gallon plastic horticulture pots.

To evaluate a possible exposure scenario under "guerilla gardening" practices, soil was collected from an abandoned former metal foundry undergoing cleanup/remediation, transported, and placed in lined horticulture pots at the UWM greenhouse. The total Pb in soil from the Former Foundry ranged from 724 to 2,900 $\mu g \ g^{-1}$, with a mean of $1,825 \pm 556 \ \mu g \ g^{-1}$.

A common best management practice to increase the safety of urban agriculture is to replace urban soil with commercial topsoil. To simulate this practice, bags of Scotts® Premium Topsoil (The Scotts Company LLC; Marysville, Ohio) were purchased, and placed in lined horticulture pots at the UWM greenhouse. The total Pb concentration in commercial topsoil ranged from 4 to 5 $\mu g \ g^{-1}$, with a mean of $4.5 \pm 0.4 \ \mu g \ g^{-1}$.

**Cultivation of Produce.** Produce was selected for this study to represent a variety of consumable tissue types common in urban gardens. Cultivars were selected to represent a variety of pigments. Produce grown in this study includes the following: carrot (Daucus carota subsp. sativus var. 'Scarlet Nantes'); beetroot (Beta vulgaris L. var. 'Detroit'; var. 'Chioggia'; and var. 'Albino'); turnip (Brassica rapa var. 'Purple Top White Globe'); radish (Raphanus sativus var. 'Champion'); potato (Solanum tuberosum L. var. 'Yukon Gold'); tomato (Solanum lycopersicum L.var. 'Better Boy'); sweet pepper (Capsicum annuum L. var. 'Sweet Banana'). Vegetable seeds packaged by W. Atlee Burpee & Co. (Warminster, PA), seedlings (tomato and sweet pepper), and seed potatoes were purchased from a big-box home-improvement retailer located in the City of Milwaukee, Wisconsin. Seeds of heirloom beetroot cultivars (var. 'Bulls Blood' and var. 'Albino') and carrot cultivars (var. 'Pusa Asita Black' and var. 'Lunar White') were purchased from Baker Creek Heirloom Seeds (Mansfield, MO). Common produce names will be used, except for denoting cultivars. Beetroots will be referred to by their cultivar variety name. Carrots will be referred to by color whereby var. Scarlet Nantes will be referred to as "orange," var. Lunar White will be referred to as "white" and var. Pusa Asita Black will be referred to as "purple."

Seeds and seed potatoes were sowed directly in the pots of soil and tomato and pepper seedlings were transplanted in pots of soil at the UWM greenhouse. Plants were grown to

maturity in a dedicated area outside of the UWM greenhouse to represent atmospheric stress normally experienced by produce grown in backyard gardens. Each pot was mulched with a commercial blend of shredded hardwood mulch to control dust. Plants were watered as necessary during the growing season and fertilized with Miracle-Gro® Water Soluble All Purpose Plant Food Topsoil (The Scotts Company LLC; Marysville, Ohio) at approximately 15 d and 45 d after seed germination per manufacturer recommendations as would be expected in backyard gardens.

**Acquisition of Commercial Produce.** The most common alternative to urban produce cultivation is to purchase produce from a commercial grocer; therefore, the concentration of Pb in purchased produce will serve as the control for this study. Produce grown in this study was purchased from local grocery stores periodically during the study and processed and analyzed identical to sample tissues. Although data for all crops grown in this study are not available, Pb concentrations in raw produce reported in the United States Food and Drug Administration Total Diet Study (USFDA TDS) serves as an additional control for this study (USFDA 2018).

**Preparation of Produce Samples.** At maturity, produce was harvested and processed according to tissue using methods common in a residential kitchen, as described by Attanayake et al. (2014, 2015). Leaves, stems, and fruits were cut from the plant with scissors, rinsed in fast running tap water, scrubbed by hand, chopped, and placed in labeled Ziploc bags for freezing/storage. Belowground tissues of beetroots, carrots, radishes, turnips, and potatoes were pulled from the pots, scrubbed with plastic scrub brush under fast running tap water, peeled, washed a second time to remove latent dust, chopped, and placed in in labeled Ziploc bags for freezing/storage. Skins were chopped and placed in labeled Ziploc bags for freezing/storage; however, due to the quantity of material needed for quantification with WD-XRF, skins were often composited within soil group for analysis.

**Quantification of Heavy Metals in Produce with WD-XRF.** Heavy metals were quantified as described in Byers et al. (2019). In short, plant tissues were dried at 60 ºC for 48 h, milled in a tungsten carbide shatterbox for 30 s, and 3.20 g of powdered sample was pressed at 25-T for 60s in a 40 mm diameter hydraulic die press to create a pressed pellet 1.9 mm thick. The intensities of characteristic secondary X-rays were measured with WD-XRF and concentrations determined using custom measurement and calibration routines described in Byers et al. (2019). Concentrations of heavy metals in produce discussed in this study are expressed as dry-weight (dw), except where explicitly noted. The limits of detection for Pb, Cr, and Ni were 0.3, 0.6, and 0.4 μg g-1 (dw), respectively.

**Characterization of Soil Chemistry.** The characterization of soil chemistry and fertility of soils used in this study included determining the bioavailable (plant-available) concentrations of Pb, Ca, Cu, Fe, K, Mn, Na, Ni, P, S, and Zn in soil following digestion/extraction using the Mehlich-3 method (Mehlich 1984); soil pH, and the Cation Exchange Capacity (CEC). Soil analytical work was completed by the University of Georgia Soil, Plant and Water Laboratory (Athens, GA).

A representative sample of each soil was analyzed using X-Ray Diffraction (XRD) to determine primary mineralogy of the soils. Samples were prepared and analyzed using procedures and equipment described by McHenry (2009). In summary, samples were dried, powdered in a tungsten-carbide mill, and analyzed with a Bruker D8 Focus X-Ray Diffractometer.

**Statistical Analysis – Urban Soil Quality.** Analysis of Variance models for soil CEC and soil bioavailable Pb, Cd, Cr, Mg, and Zn were developed in SAS (SAS Institute; Cary, NC) to determine if significant differences exist between the mean values of each parameter between

the soils used in this study. A post-hoc Tukey analysis was completed to determine which corresponding mean values are significantly different from each other.

**Statistical Analysis – Consumable Produce.** A general linear model (GLM) was developed in SAS (SAS Institute; Cary, NC) to predict the concentration of Pb in produce based on categorical (crop tissue and soil origin) and continuous (soil bioavailable Pb, Cd, Cr, Mg, and Zn and soil CEC) predictors. A description of the model is provided in Appendix A of this Dissertation. The model was refined to eliminate predictors with potential multicollinearity and an evaluation completed to confirm remaining predictors did not mediate the influence of bioavailable Pb in soil on the concentration of Pb in produce. The model includes the interaction between bioavailable Pb in the soil and crop tissue; therefore, to give meaning to the parameter estimate slopes, the bioavailable Pb in soil was mean-centered.

**Human Health Risk Evaluation**. In late September 2018, the USFDA established an IRL for the quantity of Pb considered safe for a child or an adult to consume daily in food (USFDA 2019). However, the IRL is not based on concentration of Pb in produce; therefore, using the IRL as a surrogate for an oral reference dose, the maximum daily ingestion rate ($IR_{food}$) in grams of food per day on a dry-weight basis that could be consumed by children and adults so as not to exceed a Target Health Quotient (THQ) can be described by:

$$IR_{food} = \frac{THQ * IRL}{C_{food}} \qquad \text{Equation 1}$$

The maximum daily ingestion rate (g d$^{-1}$, dw) for children and adults for each crop grown in this study in soil from Residence 1 was calculated based on a THQ = 1; the mean concentration of Pb (µg g$^{-1}$ dry weight) in each consumable produce ($C_{food}$); and the USFDA Pb IRL for children and adults (3 and 12.5 µg d$^{-1}$, respectively). For ease of comparison, cultivars were lumped together based on the produce type.

In the context of daily Pb ingestion, Equation 1 only considers ingestion of food. The total daily Pb body burden (BPb) in children is the sum of Pb ingested from food, water, and soil+dust as follows:

$$B_{Pb} = (C_{food} * IR_{food}) + (C_{water} * IR_{water}) + (C_{soil+dust} * IR_{soil+dust}) \quad \text{Equation 2}$$

The total daily Pb body burden was calculated for 10 exposure scenarios likely to be encountered by children by varying the concentration of Pb in each of the three terms on the right side of equation 2 (Table 4.4). The concentration of Pb in food ($C_{food}$) was represented by the Pb concentrations in produce, and includes the mean Pb in raw produce from the FDA TDS (USFDA 2018), the mean Pb in produce grown in Commercial Topsoil, the mean Pb in produce grown in soil from Residence 1, the mean Pb in taproots of root crops grown in soil from Residence 1, the mean Pb in leaves of root crops grown in soil from Residence 1, and the mean Pb in non-root crops grown in soil from Residence 1. The concentration of Pb in water ($C_{water}$) was represented by the mean Pb in household tap water samples collected in the City of Milwaukee (Milwaukee Water Works 2017), the United States Environmental Protection Agency (USEPA) Action Level for Pb in drinking water (USEPA 2019), or the concentration of Pb in drinking water in Flint, Michigan (Pieper et al. 2018). The concentration of Pb in soil+dust ($C_{soil+dust}$) was represented by the mean Pb in Commercial Topsoil, mean Pb in soil from Residence 1, or the WDNR Residual Contaminant Level for Direct Contact at residential properties (WDNR 2018), which is also equal to the USEPA regional screening level for direct contact at residential properties (USEPA 2019b). The ingestion rate for food ($IR_{food}$) assumes a child eats the recommended 2 cups of produce (wet weight) per day. The mass is converted to dry weight for use in Equation 3 assuming 85% water. The ingestion rate for water and soil+dust is calculated per Moya et al. (2011).

## 4.3    RESULTS

**Urban Soil Quality.** Bioavailable Pb, Cd, Cr, Zn, and Mg in soil and the CEC in soil contribute significantly to the prediction of Pb in produce and will be discussed. The quality of urban soils in this study is reflective of the soil origin and sources of heavy metals released to soils. The mean bioavailable Pb concentrations in soil from Residence 1, Residence 2, the Former Foundry, and in the Commercial Topsoil are $394 \pm 125$, $564 \pm 169$, $121 \pm 74$, and $6 \pm 12$ $\mu g\ g^{-1}$, respectively, which are all significantly different from each other (p<0.001; Figure 4.1). Although the data set is limited (n=14), the bioavailable concentration of Pb represented between 3% and 36% of the total Pb in metals-rich soil from the two residential properties and the Former Foundry. The mean CEC in the two residential soils are not significantly different from each other (Figure 4.1); however, the mean CEC in the Commercial Topsoil of $55 \pm 5$ meq $100g^{-1}$ is significantly greater than the Former Foundry and the two residential soils (p < 0.001). The mean bioavailable concentrations of Cd, Cr, and Zn in soil from the Former Foundry are each significantly greater compared to the other three soils, which is not surprising considering the soil source (Figure 4.1S). The mean bioavailable concentration of Mg in the Commercial Topsoil is $2184 \pm 229$ $\mu g\ g^{-1}$, which is significantly (p < 0.001) greater than the mean Mg concentrations in soil from the two residences and the Former Foundry.

The means of soil pH ranged from 7.73 to 7.43. Additional soil quality parameters are summarized on Table 4.1S. No crystalline Pb-bearing phases were identified in XRD patterns, though this technique (as applied in this study) is only capable of identifying phases at the percent level or higher. The XRD patterns confirm the presence of quartz in soil from the Former Foundry and confirms the presence of quartz and/or dolomite in residential soils and the Commercial Topsoil (Figures 4.2Sa-4.2Sd).

**Concentrations of Pb in Produce.** The mean concentration of Pb accumulated in aboveground tissues is less than the mean concentration of Pb in below ground taproot crops grown in metals-rich soils (Figure 2), with the largest Pb concentration noted in peeled carrots ($15.2 \pm 14.2$ µg g-1). Although grown belowground, the smallest mean concentration of Pb in produce was noted in peeled potatoes ($0.7 \pm 1.1$ µg g-1).

Pb was detected in nearly every crop tissue grown in metals-rich soils collected from Residence 1, Residence 2, and the Former Foundry, with the overall greatest mean concentrations noted in produce grown in residential garden soils (Table 4.2). Conversely, Pb was rarely detected in crop tissues grown in Commercial Topsoil, and when detected, the concentration of Pb was just slightly greater than the WD-XRF limit of detection ($0.3$ µg g$^{-1}$).

Radishes accumulated the greatest amount of Pb in consumable tissues, especially in residential soils, followed by carrots, turnips, and beetroots (Table 4.2). Fruits accumulated the least amount of Pb, and although potatoes are found belowground, they accumulated significantly less Pb than other belowground tissues. Between the carrot cultivars, white carrots accumulated more Pb compared to pigment-rich orange and purple cultivars. The mean concentrations of Pb in beetroot bulbs did not vary greatly, though the concentrations of Pb tended to follow the opposite trend noted in carrots, with the greatest amount of Pb accumulating in pigment-rich beetroots (Table 4.2).

The mean concentration of Pb in carrot skins was less than the Pb concentration in the corresponding consumable root, and in addition, the accumulation of Pb in carrot skins is not cultivar-specific (Table 4.2S). The mean Pb concentration in carrot leaves was greatest in the orange cultivar compared to the purple or white cultivar, with the greatest accumulation of Pb in carrot leaves grown in the two residential soils.

The concentrations of Pb in produce purchased from local grocery stores (n=19) were all less than the WD-XRF limit of detection (0.3 μg g$^{-1}$), except for one turnip bulb purchased from one grocery store with a measured Pb concentration of 0.6 μg g$^{-1}$. The wet weight concentration of Pb in raw produce from the USFDA TDS is 5.5 ± 2.6 μg kg$^{-1}$, (n=472; Figure 4.3S), which is less than the concentrations of Pb in similar vegetables purchased from markets and characterized by Hadayat et al. (2018).

The continuous (soil bioavailable Pb, Cd, Cr, Mg, and Zn and soil CEC) and categorical (crop tissue and soil origin) predictors in the GLM predicts 65% of the variability of Pb in consumable plant tissues in vegetables grown in evaluated soils (F=7.99, DF=39,166, p< 0.001). After controlling for these predictors, adding the interaction between bioavailable Pb in soil and crop tissue increases the predictability of Pb in consumable tissues (t=4.20, DF=166; p<0.001).

Cd and Ni accumulated in consumable produce tissues; however, the mean concentrations of these metals were significantly less than Pb (Table 4.3S and Table 4.4S). Additional accumulation data is provided in Appendix B, Appendix C, and Appendix D of this Dissertation. The raw data for this study is provided in Appendix E.

**Evaluation of Risk Due to Consumption of Produce.** The acceptable dry weight mass of produce grown in soil from Residence 1 that could be consumed by a child such that the USFDA IRL is not exceeded ranges from 0.1 g d$^{-1}$ of radishes to 3.0 g d$^{-1}$ of potatoes (Figure 4.3). Similarly, in adults, the maximum dry weight mass of produce grown in this study in soil from Residence 1 that could be consumed per day on a dry weight ranges from 0.4 g$^{-1}$ of radishes to 12.5 g$^{-1}$ of potatoes.

However, the total daily ingestion of Pb by a child depends on the concentrations of Pb ingested through a summation of water, food, and soil+dust (Equation 2). The total daily

ingestion of Pb by children was further evaluated by modeling the total daily intake of Pb under 10 plausible scenarios. Model scenarios are explained in Table 4.3 and model factors further explained on Figures 4.3S, S4, and S5 and Tables 4.5S and 4.6S. Scenario 1 and 2 represent a child consuming commercial produce, drinking tap water in the City of Milwaukee, and living in an area with minimum Pb in soil (Scenario 1) or Pb-rich soil (Scenario 2). Scenario 3 and 4 represent cases where a child lives in an area with Pb-rich residential soil, drinks tap water in the City of Milwaukee, and eats produce grown in commercial topsoil (Scenario 3) or metals-rich residential soil (Scenario 4). Scenarios 5, 6, and 7 compare the differences in exposure to a child from Scenario 4 who is eating different produce types grown in Pb-rich residential soil. Scenarios 8, 9, and 10 represent cases where a child drinks water with varying Pb concentrations, eats produce grown in commercial topsoil, and lives in an area where the Pb concentration is not considered by USEPA or the state regulatory agency to pose a threat to human health. The total Pb intake for each scenario varied between 3 $\mu$g d$^{-1}$ and 1,100 mg d$^{-1}$ (Figure 4.4). In the control (Scenario 1), food contributed 60% and water contributed 40% to the daily Pb ingestion (Figure 4.5). Water consistently contributes the least amount of Pb ingested per day, contributing <1% or less to the daily Pb load, except in the control (Scenario 1) and in two scenarios with significantly compromised water quality (Scenario 9 and Scenario 10), and even then, water contributes <15% of the total Pb ingestion load (Figure 4.5).

## 4.4    DISCUSSION

This study validates that custom WD-XRF routines controlling for matrix effects can be created to quantify Pb in prepared produce at concentrations as low as 0.3 $\mu$g g$^{-1}$ (dw), with slightly higher limits of detection for Ni and Cr. Significant variation is present in the quality of urban soils and in the corresponding concentration of Pb accumulated in consumable crop

tissues. The accumulation of Pb in produce is related not only to the bioavailability of Pb in soil, but also to crop type. Replacement of metals-rich urban soils with commercial topsoil of better quality or growing non-root crops in metals rich soil are acceptable as best management practices to reduce the risk of Pb exposure. Children consuming vegetables grown in metals-rich urban soil and in replacement topsoil could be at increased risk for Pb exposure; however, the risk of Pb exposure from consuming commercial produce from a grocery store cannot be ignored.

**Quantification of Pb in Prepared Produce.** The accumulation of Pb in produce has been previously documented; however, by controlling for matrix effects and controlling significant potential sources of bias in quantification of Pb with WD-XRF, this study shows that the analytical tool can detect Pb in prepared produce samples as low as 0.3 $\mu g\ g^{-1}$ and can quantify Pb in prepared samples as low as 1 $\mu g\ g^{-1}$. Central to the quantification routine was the development of custom reference materials with commutability to produce; selecting secondary characteristic X-rays to eliminate peak overlaps and possible bias from spectrometer shielding/housing; and confirming the viability of the measurement routine (Byers et al. 2019).

**Urban Soil Quality.** The concentrations of bioavailable Pb in the four soils are reflective of soil origins and anthropogenic inputs. Numerous studies have suggested a primary source of Pb in soil is weathering paint (e.g. Clark et al. 2006, 2008; Laidlaw et al. 2018). Pb paint primarily enters the soil system through weathering (e.g. chipping, peeling) or by mechanical disturbance. The Manufacture's House Paint Reference Collection database (Hall and Tinklenberg 2003) indicates Pb in historic house paint is primarily Pb-carbonate (~61% by weight) and pigments used in Pb paint are Pb-sulfate ($PbOPbSO_4$), leaded-zinc oxide ($(ZnO+Pb)PbSO_4$), leaded titanite ($PbTiO_3$), and Phoenicochroite ($Pb_2O(CrO_4)$). Paint chips were visually apparent in soil from Residence 1 and Residence 2. The bivariate relationship between

112

bioavailable Pb and bioavailable concentrations of common Pb-ligand associated elements in residential soils was the strongest with Cr ($r^2$=0.64).

The Pb source in soil from the Former Foundry is not visually apparent and the XRD diffraction pattern suggests the predominant minerology of the soil is quartz. The bioavailable concentrations of heavy metals associated with metal works (Cd, Cr, Cu, Fe, Ni, and Zn) are all significantly greater (p < 0.001) in soil from the Former Foundry compared to the soil from the residential properties. These results indicate the soils collected from the Former Foundry were involved in industrial processes and support the XRD data suggesting the soil contains mostly foundry sand. The pH of the Former Foundry soil (7.43 ± 0.2; Table 4.1S) does not suggest the Pb is associated with a spill of metals-rich acidic solution.

Additional sources of Pb in urban residential soils are associated with transportation (e.g. weathering tires and worn engine components and historic uses of Pb to enhance the octane of gasoline (Clark et al. 2006); leaching from weathered plastics; use of Pb-rich urban stormwater for irrigation purposes (Tom et al. 2014) or urban runoff; use of municipal compost as a soil amendment (Murray et al. 2011a); historic use of Pb-bearing herbicides (Yokel and Delistraty 2003); and anthropogenic fill) cannot be eliminated, but are considered minor compared to the presumed sources.

The CEC is a common soil fertility parameter used to describe the amount of exchangeable cation sites in soil. The mean CEC values are not significantly different between the two residential soils; however, the mean CEC of the Topsoil is significantly greater than the CEC of the residential soils and soil from the Former Foundry. Soils with a greater CEC have an increased capacity to retain and exchange cations in soil solution, and in the context of urban agriculture, CEC sites have the potential to retain Pb and prevent uptake into plant roots.

**Accumulation and Distribution of Pb in Produce.**The accumulation of Pb in produce varies widely in the literature and the most likely explanation for the large variability is the heterogenous and anisotropic nature of soil quality. The concentrations of Pb accumulated in produce in this study is within the ranges previously documented for target crops. The mean concentrations of Pb in carrots grown in this study range from less than 0.3 $\mu$g g$^{-1}$ to 20 $\mu$g g$^{-1}$, which is within ranges of Pb concentrations in carrots noted by others (Antoniadis et al. 2017; Attanayake et al. 2014; Ding et al. 2015; Finster et al. 2004; Jolly et al. 2013; Lima et al. 2009b; Murray et al. 2011a; Zwolak et al. 2019). Previous accumulation studies involving beetroot are limited; however, Chopra and Pathak (2015) noted the mean Pb concentration in beetroot grown in fields irrigated with wastewater was 50 $\mu$g g$^{-1}$ and Lima et al. (2009b) noted the mean concentration of Pb in beetroot grown in soil contaminated with battery residues was 108 $\mu$g g$^{-1}$. Accumulation of Pb in radishes in the literature ranges from less than 1 $\mu$g g$^{-1}$ upwards to 154 $\mu$g g$^{-1}$ (Anjos et al. 2002; Jolly et al. 2013). Concentrations of Pb in non-root crops (tomatoes and potatoes) are significantly less than concentrations found in root crops which agrees with the previous literature (e.g. Attanayake et al. 2014; Augustsson et al. 2015; Finster et al. 2004; Jolly et al. 2013; McBride et al. 2014; Rodriguez-Iruretagoiena et al. 2015; Zwolak et al. 2019).

The trend in accumulation of Pb in produce follows a recognizable pattern, with the greatest Pb accumulation in modified taproot tissues and decreasing Pb concentrations in tissues associated with aboveground biomass, similar to observation made by Finster et al. (2004). The primary entryway of Pb$^{+2}$ into the plant root is through bulk water flow by the apoplast pathway (Bovenkamp et al. 2013; Sancho et al. 2005) through a root hair. The general consensus in the literature is that Pb predominantly moves into and through the root cortex in the apoplast pathway by root pressure and bulk flow of water through transpiration from aboveground

biomass (Bhargava et al. 2012; Bovenkamp et al. 2013). As Pb has no known biological function, the working assumption is that Pb enters the symplast pathway through a protein designed for another divalent cation such as ATP-ase proteins AtHMA2 and AtHMA4, which are associated with the transport of Cd and Zn (Verret et al. 2004). During transport in the apoplast pathway, Pb could enter the symplast pathway through a membrane protein or could continue in the apoplast pathway towards the stele until the Casparian strip, at which point Pb must enter the symplast pathway. The Casparian strip is described in the literature as a "poorly ion-permeable secondary thickening in the cell" (Tester and Leigh 2001) that serves as "a partial barrier" (Peralta-Videa et al. 2009; Sharma et al. 2015) for "Pb movement into the central cylinder tissue" (Peralta-Videa et al. 2009). Scanning electron microscopy images have shown that the Casparian strip plays a significant role in restricting transport of Pb into the stele (Meyers et al. 2008; Pierart et al. 2018). By restricting Pb transport into the xylem, the Casparian strip effectively concentrates Pb in the root cortex, possibly as insoluble precipitates. Therefore, vegetables with modified taproots (e.g. radish, turnip, beetroot, carrot) accumulated more Pb compared to their corresponding aboveground tissues.

Although grown underground, a potato tuber forms on the tip of a stolon, which is morphologically a modified stem (Struik 2007). Although more work on this is needed, Pb accumulating in a potato tuber likely passes into and through the plant root, crosses the Casparian strip, enters the phloem, and then must be transported through the vascular plant tissue to the tuber. Several defense/sequestration methods are known to be used by plants in to restrict the transport of metals through the apoplast pathway [e.g. binding with pectin or hemicellulose (KrzesBowska et al. 2013; Ovečka and Takáč 2014) or cysteine-rich proteins in cell walls (Jiang and Liu 2010) or by forming precipitates with carbonate, sulfate, or phosphate (Edelstein and

Ben-Hur 2018; Jiang and Liu 2010; Meyers et al. 2008; Peralta-Videa et al. 2009)] or through the symplast pathway [e.g. sequestration in the cytoplasm by thiol-rich peptides for transport, storage, and precipitation as phosphohedyphane ($Pb_3Ca_2(PO_4)_3Cl$) or chlorophyromorphile ($Pb_5(PO_4)_3Cl$) in a vacuole (Cobbett 2000; Jiang and Liu 2010; Meyers et al. 2009; Ovečka and Takáč 2014; Peralta-Videa et al. 2009)]. Heavy metals in the symplast pathway can continue to be transported until the pericycle at which point they could be loaded into the xylem for transport to aboveground tissues. Xylem loading serves as an additional restriction on the transport of Pb into aboveground tissues. If loaded in the Xylem, Pb could move via xylem sap associated with a ligand similar to acetate, nitrate, and sulfide (Peralta-Videa et al. 2009) and distributed to aboveground tissues. In addition, further sequestration of Pb in the chloroplast is also known to occur (Sharma and Dubey 2005) and certain plant genera may use trichomes as preferential storage areas for Pb (Clemens et al. 2002). One final defense mechanism to alleviate Pb by plants is sequestering heavy metals in leaf tissues that are then eliminated from the plant through senescence (Sharma and Dubey 2005). Because of the multitude of defense mechanisms used by plants to prevent accumulation of Pb, the concentration of the Pb in potato tubers is significantly less than concentrations in modified taproots. This data supports prior work suggesting limited mobility of Pb in the phloem (Peralta-Videa et al. 2009; Sharma and Dubey 2005) although fibrous roots can form on stolons and sometimes on tubers of potatoes (Struik 2007). These roots are thought to be critical in nutrient transport during the later stages of tuber growth; therefore, if these roots are in contact with metals-rich soil solution, accumulation of Pb in potatoes could occur later in tuber growth.

As suggested by others in the literature, tomatoes and peppers can accumulate Pb in the consumable fruits; however, the concentrations are much less compared to modified taproot vegetables grown in this study.

The difference in the accumulation of Pb across morphologically different tissues suggests selection of crop type is critical in minimizing Pb exposure in consuming urban-grown produce. However, little is known about the difference in Pb accumulation in different root crop cultivars. Toxicity in plants due to Pb uptake comes in the form of oxidative stress. by formation of $H_2O_2$. To alleviate stress from Pb exposure, plants upregulate approximately 20 classes of functional genes; the primary genes upregulated are involved in antioxidant defense (e.g. upregulation of superoxide dismutase, peroxidase, and gluthione reductase; Ovečka and Takáč, 2014). In addition, Plants increase carotenoid and anthocyanin pigments to scavenge reactive oxygen species and mitigate stress in leaf tissues (Kumar et al. 2012). Betalains are nitrogen-based pigments uniquely present in the beetroot family and have been shown to be positively correlated with Pb accumulation in beetroots (Száková et al. 2010). Use of pigments to alleviate stress suggests that root crop cultivars rich in these compounds grown in metals rich soil could tolerate more Pb and therefore accumulate more Pb in tissues compared to corresponding white (albino) cultivars. However, across metals-rich soils, white carrots grown in this study accumulated more Pb in peeled root tissues compared to purple or orange cultivars. The apparent sequestration of Pb in the root of white carrots may explain why the concentrations of Pb in aboveground tissues of white carrots were smaller compared to purple or orange cultivars. It is important to note that the abundance of anthocyanins in purple carrots does not decrease the abundance of carotenoids in carrots (Macura et al. 2019) which could play a significant role in the transport of Pb to aboveground tissues. The accumulation of Pb in beetroot cultivars did not

117

follow a clear trend; however, the mean Pb concentration in the highly pigmented cultivar (var. Bulls Blood) was generally greater than the mean Pb in the white beetroot (var. Albino). The concentrations of Pb in beetroot leaves were similar between cultivars, with no discernable difference due to pigmentation.

**Evaluation of Best Management Practices Through Evaluation of Factors Contributing to the Accumulation of Pb in Produce.** By setting the reference soil equal to "Residence 1" and the reference produce to "Potato", the mean-centered GLM model developed to predict the concentration of Pb in produce can predict the change in Pb accumulation if model predictors are changed. By mean-centering the concentration of bioavailable Pb in soil, predictor estimates and estimates of the interaction between soil bioavailable Pb and Pb in produce can be interpreted. The soil from Residence 1 was selected as the reference soil in the model as this soil represents typical soil quality in gardens at residential properties and therefore allows an evaluation of the change in Pb accumulation if different soils are used for growing food. Potato was selected as the reference produce as potatoes had the lowest mean Pb in consumable tissues. The GLM predicts the concentration of Pb in potatoes grown in soil from Residence 1 at the mean bioavailable Pb will be 1.0 $\mu g\ g^{-1}$, which is not statistically different than zero (t=0.16, p = 0.88). The model indicates that if the bioavailable concentration of Pb in soil increased by 100 $\mu g\ g^{-1}$, the accumulation of Pb in potatoes in the reference soil is expected to only increase by 1 $\mu g\ g^{-1}$, which the model indicates is not statistically significant (t=0.94, p=0.35). Using Potato as a reference allows an evaluation of the change in accumulated Pb if another crop is grown under similar conditions.

Crop selection is critical in reducing Pb exposure in urban agriculture and selecting non-root crops for cultivation in metals-rich urban soils is considered a best management practice

(Entwistle et al. 2019). The GLM simple slope estimates comparing produce types can be interpreted as the difference in Pb accumulation between potatoes and the other crops, if grown in soil from Residence 1 at the mean bioavailable Pb concentration in soil. The increase in Pb in other produce compared to potatoes ranges from 0.6 $\mu$g g$^{-1}$ in peppers to 16 $\mu$g g$^{-1}$ in white carrots, suggesting that white carrots are expected to accumulate 17 $\mu$g g$^{-1}$ Pb if grown in soil from Residence 1 at the mean bioavailable Pb concentration in soil, which is a statistically significant increase compared to potatoes (t=5.6, p<0.001).

Crop selection is even more important in soils with increasing bioavailable Pb. The interaction parameter estimates allow for an evaluation of the influence of increasing the mean bioavailable Pb in soil by 100 $\mu$g g$^{-1}$ on Pb accumulation in each crop, compared to potatoes. Interaction parameter estimates range from -0.2 $\mu$g g$^{-1}$ in tomatoes to 6.9 in white carrots and radishes indicating that when the mean bioavailable Pb increases by 100 $\mu$g g$^{-1}$, the expected Pb concentration in white carrots is expected to increase by 6.9 $\mu$g g$^{-1}$ (to 7.9 $\mu$g g$^{-1}$), which the model indicates is statistically significant (t=4.72, P < 0.0001). This relationship holds true across taproot crops as slopes are positive between potatoes and carrot cultivars, beetroot cultivars, radishes, and turnips indicating that if bioavailable Pb increases in the soil above the mean, more Pb will accumulate in these tissues compared to potatoes. Therefore, the accumulation of Pb in consumable tissues as bioavailable Pb increases in soil is not the same between crops. As such, growing root crops in increasingly metals-rich soils further increases the risk for Pb exposure through consumption of root crops compared to potatoes.

Replacing inground metals-rich urban soil with topsoil or constructing raised beds of commercial topsoil for crop production is considered a best management practice to reduce Pb exposure. The parameter slope estimate comparing soil from Residence 1 to Commercial Topsoil

is -2.2 indicating that if potatoes are grown in Commercial Topsoil with the mean bioavailable Pb concentration, the concentration of Pb in tissues should decrease by 2.2 $\mu g \, g^{-1}$ (t=-.033, p = 0.74). Although the statistical significance is not established in this study, it is useful to realize the slope comparing soil from Residence 1 to Commercial Topsoil is negative, thereby predicting an overall decrease in Pb accumulation if Commercial Topsoil is used as the growing media. However, the parameter slope for the Foundry Soil is 2.4 indicating that if crops are grown in soil from the Former Foundry with the mean bioavailable Pb in soil, the concentration of Pb in consumable tissues should increase (t=0.7, p=0.48) compared to crops grown in soil from Residence 1 suggesting that "guerrilla gardening" may increase risk for Pb exposure through produce consumption.

**Evaluation of Risk Due to Consumption of Produce.** Consuming even a small amount of produce grown in soil from Residence 1 could put a child or an adult at risk for Pb exposure. Using Equation 1, a child can consume no more than 0.2 g $d^{-1}$ (dw) of carrots grown in soil from Residence 1. At 85% water content, this equates to 1.3 g (ww) of carrots, or approximately one thin slice of a small-size carrot (Figure 4.3). Conversely, a child could consume no more than 1.3 g $d^{-1}$ (dw) of tomato grown in soil from Residence 1, or roughly one thin slice from a medium tomato. Although the USFDA IRL includes a safety factor of 10, this evaluation shows that although the concentration of Pb in tomatoes is comparatively minor, even consuming a small quantity of tomatoes grown in metals-rich soil could pose an exposure risk to children. The IRL of an adult is 4.3 times the value for children indicating an adult could safely eat a slightly thicker slice of carrot grown in soil from Residence 1 or slightly less than one whole small tomato grown in soil from Residence 1 (Figure 4.3).

Scenarios modeling the daily intake of Pb in a child from ingestion of water, food, and soil+dust vary significantly based on the concentrations of Pb in each vector (Figure 4.4). This evaluation suggests that although much attention has been placed on controlling drinking water quality, food quality has the potential for contributing an equal or greater proportion to the daily ingestion of Pb in children (Figure 4.5). Without changing food or water quality, simply replacing metals-rich topsoil with soil of significantly better quality is the best management practice to quickly reduce Pb exposure risk. This is quantified by the decrease in ingestion of Pb between Scenario 2 and Scenario 1 of 476 $\mu$g d$^{-1}$.

Homeowners who are unable to replace all the metals-rich topsoil at their property, but who also want to grow produce, are encouraged to grow vegetables in raised beds of replacement topsoil of significantly better quality. Without changing water quality or soil quality in the yard, growing produce in raised beds of commercial topsoil is estimated to decrease the ingestion of Pb by 462 $\mu$g d$^{-1}$, which is the difference between Scenario 3 and Scenario 4.

Crop selection is critical in lowering the risk of Pb exposure when growing produce in metals-rich soil. If water quality is the average water quality in Milwaukee and soil quality is represented by the average soil at Residence 1, a child eating 2 cups of root crops grown in soil from Residence 1 would ingest 1173 $\mu$g d$^{-1}$ (Scenario 5). Simply by eating the leaves of the root crops (Scenario 6) instead of the taproot (Scenario 5) grown in soil from Residence 1, the Pb ingestion rate of a child would decrease by 372 $\mu$g d$^{-1}$. The Pb ingestion rate would decrease by 632 $\mu$g d$^{-1}$ if a child eats a non-root crop (Scenario 7) compared to the taproot of a root crop (Scenario 5) grown in soil from Residence 1.

Scenario 8, Scenario 9, and Scenario 10 estimate the daily ingestion of Pb based on changes in drinking water quality if soil quality meets state and federal quality guidelines and

produce is grown in replacement topsoil. Water quality in Scenario 8 is represented by the mean

water quality in Milwaukee, Wisconsin, which meets the USEPA Action level for Pb. Water

quality in Scenario 9 and Scenario 10 does not meet the USEPA Action level for Pb. The

difference in Pb ingestion between Scenarios 9 and 10 and Scenario 8 suggests an average

reduction in daily ingestion of between 3 and 7 $\mu g\ d^{-1}$; however, this decrease is small compared

to the decrease in daily Pb ingestion rate by replacing metals rich topsoil with soil of better

quality or by growing vegetables in raised beds.

## 4.5 REFERENCES

Abdel-Rahman GN, Ahmed MBM, Marrez DA. 2018. Reduction of heavy metals content in contaminated vegetables due to the post-harvest treatments. Egypt J Chem 61:1031–1037; doi:10.21608/ejchem.2018.3624.1303.

Amato MS, Magzamen S, Imm P, Havlena JA, Anderson HA, Kanarek MS, et al. 2013. Early lead exposure (<3 years old) prospectively predicts fourth grade school suspension in Milwaukee, Wisconsin (USA). Environ Res 126:60–65; doi:10.1016/j.envres.2013.07.008.

Anjos MJ, Lopes RT, Jesus EFO, Simabuco SM, Cesareo R. 2002. Quantitative determination of metals in radish using x-ray fluorescence spectrometry. X-Ray Spectrom 31:120–123; doi:10.1002/xrs.567.

Antoniadis V, Shaheen SM, Boersch J, Frohne T, Du Laing G, Rinklebe J. 2017. Bioavailability and risk assessment of potentially toxic elements in garden edible vegetables and soils around a highly contaminated former mining area in Germany. J Environ Manage 186:192–200; doi:10.1016/j.jenvman.2016.04.036.

Attanayake CP, Hettiarachchi GM, Harms A, Presley DA, Martin S, Pierzynski GM. 2014. Field evaluations on soil plant transfer of lead from an urban garden soil. J Environ Qual 43:475–487; doi:10.2134/jeq2013.07.0273.

Attanayake CP, Hettiarachchi GM, Martin S, Pierzynski GM. 2015. Potential bioavailability of lead, arsenic, and polycyclic aromatic hydrocarbons in compost-amended urban soils. J Environ Qual 44:930–944; doi:10.2134/jeq2014.09.0400.

Augustsson ALM, Uddh-Söderberg TE, Hogmalm KJ, Filipsson MEM. 2015. Metal uptake by homegrown vegetables - The relative importance in human health risk assessments at contaminated sites. Environ Res 138:181–190; doi:10.1016/j.envres.2015.01.020.

122

Bhargava A, Carmona FF, Bhargava M, Srivastava S. 2012. Approaches for enhanced phytoextraction of heavy metals. J Environ Manage 105:103–120; doi:10.1016/j.jenvman.2012.04.002.

Bovenkamp GL, Prange A, Schumacher W, Ham K, Smith AP, Hormes J. 2013. Lead uptake in diverse plant families: A study applying X-ray absorption near edge spectroscopy. Environ Sci Technol 47:4375–4382; doi:10.1021/es302408m.

Brinkmann R. 1994. Lead pollution in soils in milwaukee county, wisconsin. J Environ Sci Heal Part A Environ Sci Eng Toxicol 29:909–919; doi:10.1080/10934529409376083.

Brown SL, Chaney RL, Hettiarachchi GM. 2016. Lead in urban soils: A real or perceived concern for urban agriculture? J Environ Qual 45:26–36; doi:10.2134/jeq2015.07.0376.

Byers HL, McHenry LJ, Grundl TJ. 2016. Forty-Nine Major and Trace Element Concentrations Measured in Soil Reference Materials NIST SRM 2586, 2587, 2709a, 2710a and 2711a Using ICP-MS and Wavelength Dispersive-XRF. Geostand Geoanalytical Res 40:433–445; doi:10.1111/j.1751-908X.2016.00376.x.

Byers HL, McHenry LJ, Grundl TJ. 2019. XRF techniques to quantify heavy metals in vegetables at low detection limits. Food Chem X 1:100001; doi:10.1016/J.FOCHX.2018.100001.

Chopra AK, Pathak C. 2015. Accumulation of heavy metals in the vegetables grown in wastewater irrigated areas of Dehradun, India with reference to human health risk. Environ Monit Assess 187; doi:10.1007/s10661-015-4648-6.

City of Milwaukee. 2017. Childhood Lead Poisoning Dashboard. City Milwaukee Child Lead Poisoning Data Reports. Available: https://city.milwaukee.gov/health/Lead-Poisoning-Prevention-Data/Childhood-Lead-Poisoning-Dashboard.htm [accessed 7 October 2019].

Clark HF, Brabander DJ, Erdil RM. 2006. Sources, sinks, and exposure pathways of lead in urban garden soil. J Environ Qual 35:2066–2074; doi:10.2134/jeq2005.0464.

Clark HF, Hausladen DM, Brabander DJ. 2008. Urban gardens: Lead exposure, recontamination mechanisms, and implications for remediation design. Environ Res 107:312–319; doi:10.1016/j.envres.2008.03.003.

Clemens S, Palmgren MG, Krämer U. 2002. A long way ahead: Understanding and engineering plant metal accumulation. Trends Plant Sci 7:309–315; doi:10.1016/S1360-1385(02)02295-1.

Cobbett CS. 2000. Phytochelatins and their roles in heavy metal detoxification. Plant Physiol 123:825–832; doi:10.1104/pp.123.3.825.

Defoe PP, Hettiarachchi GM, Benedict C, Martin S. 2014. Safety of gardening on lead- and arsenic-contaminated urban brownfields. J Environ Qual 43:2064–2078; doi:10.2134/jeq2014.03.0099.

123

Dignam T, Kaufmann RB, Lestourgeon L, Brown MJ. 2019. Control of Lead Sources in the United States, 1970-2017: Public Health Progress and Current Challenges to Eliminating Lead Exposure. J Public Heal Manag Pract 25:S13–S22; doi:10.1097/PHH.0000000000000889.

Ding C, Li X, Zhang T, Wang X. 2015. Transfer model of lead in soil-carrot (Daucus carota L.) system and food safety thresholds in soil. Environ Toxicol Chem 34:2078–2086; doi:10.1002/etc.3031.

Edelstein M, Ben-Hur M. 2018. Heavy metals and metalloids: Sources, risks and strategies to reduce their accumulation in horticultural crops. Sci Hortic (Amsterdam) 234:431–444; doi:10.1016/j.scienta.2017.12.039.

Entwistle JA, Amaibi PM, Dean JR, Deary ME, Medock D, Morton J, et al. 2019. An apple a day? Assessing gardeners' lead exposure in urban agriculture sites to improve the derivation of soil assessment criteria. Environ Int 122:130–141; doi:10.1016/j.envint.2018.10.054.

Ferri R, Hashim D, Smith DR, Guazzetti S, Donna F, Ferretti E, et al. 2015. Metal contamination of home garden soils and cultivated vegetables in the province of Brescia, Italy: Implications for human exposure. Sci Total Environ 518–519:507–517; doi:10.1016/j.scitotenv.2015.02.072.

Finster ME, Gray KA, Binns HJ. 2004. Lead levels of edibles grown in contaminated residential soils: A field survey. Sci Total Environ 320:245–257; doi:10.1016/j.scitotenv.2003.08.009.

Ghose R, Pettygrove M. 2014. Urban Community Gardens as Spaces of Citizenship. Antipode 46:1092–1112; doi:10.1111/anti.12077.

Hadayat N, De Oliveira LM, Da Silva E, Han L, Hussain M, Liu X, et al. 2018. Assessment of trace metals in five most-consumed vegetables in the US: Conventional vs. organic. Environ Pollut 243:292–300; doi:10.1016/j.envpol.2018.08.065.

Hall GS, Tinklenberg J. 2003. Determination of Ti, Zn, and Pb in lead-based house paints by EDXRF. J Anal At Spectrom 18:775–778; doi:10.1039/b300597f.

Hore P, Alex-Oni K, Sedlar S, Nagin D. 2019. A Spoonful of Lead: A 10-Year Look at Spices as a Potential Source of Lead Exposure. J Public Heal Manag Pract 25:S63–S70; doi:10.1097/PHH.0000000000000876.

Huang ZY, Chen T, Yu J, Qin DP, Chen L. 2012. Lead contamination and its potential sources in vegetables and soils of Fujian, China. Environ Geochem Health 34:55–65; doi:10.1007/s10653-011-9390-6.

Jiang W, Liu D. 2010. Pb-induced cellular defense system in the root meristematic cells of Allium sativum L. BMC Plant Biol 10:40; doi:10.1186/1471-2229-10-40.

Jolly YN, Islam A, Akbar S. 2013. Transfer of metals from soil to vegetables and possible health risk assessment. Springerplus 2:1–8; doi:10.1186/2193-1801-2-385.

Keller B, Faciano A, Tsega A, Ehrlich J. 2017. Epidemiologic Characteristics of Children with Blood Lead Levels ≥45 μg/dL. J Pediatr 180:229–234; doi:10.1016/j.jpeds.2016.09.017.

KrzesBowska M, Rabęda I, Lewandowski M, Samardakiewicz S, Basińska A, Napieralska A, et al. 2013. Pb induces plant cell wall modifications - in particular - the increase of pectins able to bind metal ions level. N. Pirrone, ed E3S Web Conf 1:26008; doi:10.1051/e3sconf/20130126008.

Kumar A, Prasad MNV, Sytar O. 2012. Lead toxicity, defense strategies and associated indicative biomarkers in Talinum triangulare grown hydroponically. Chemosphere 89:1056–1065; doi:10.1016/j.chemosphere.2012.05.070.

Laidlaw MAS, Alankarage DH, Reichman SM, Taylor MP, Ball AS. 2018. Assessment of soil metal concentrations in residential and community vegetable gardens in Melbourne, Australia. Chemosphere 199:303–311; doi:10.1016/j.chemosphere.2018.02.044.

Laidlaw MAS, Filippelli GM, Sadler RC, Gonzales CR, Ball AS, Mielke HW. 2016. Children's blood lead seasonality in flint, Michigan (USA), and soil-sourced lead hazard risks. Int J Environ Res Public Health 13:358; doi:10.3390/ijerph13040358.

Lane SD, Webster NJ, Levandowski BA, Rubinstein RA, Keefe RH, Wojtowycz MA, et al. 2008. Environmental Injustice: Childhood Lead Poisoning, Teen Pregnancy, and Tobacco. J Adolesc Heal 42:43–49; doi:10.1016/j.jadohealth.2007.06.017.

Lima F de S, do Nascimento CWA, da Silva FBV, de Carvalho VGB, Ribeiro Filho MR. 2009a. Lead concentration and allocation in vegetable crops grown in a soil contaminated by battery residues. Hortic Bras 27: 362–365.

Lima F, Nascimento C, Silva F, Carvalho V, Filho M. 2009b. Lead concentration and allocation in vegetables grown in a soil contaminated by battery residues. Hortic Bras 27: 362–365.

Macura R, Michalczyk M, Fiutak G, Maciejaszek I. 2019. Effect of freeze-drying and air-drying on the content of carotenoids and anthocyanins in stored purple carrot. Acta Sci Pol Technol Aliment 18:135–142; doi:10.17306/J.AFS.2019.0637.

Magzamen S, Amato MS, Imm P, Havlena JA, Coons MJ, Anderson HA, et al. 2015. Quantile regression in environmental health: Early life lead exposure and end-of-grade exams. Environ Res 137:108–119; doi:10.1016/j.envres.2014.12.004.

Marguí E, Queralt I, Hidalgo M. 2009. Application of X-ray fluorescence spectrometry to determination and quantitation of metals in vegetal material. TrAC - Trends Anal Chem 28:362–372; doi:10.1016/j.trac.2008.11.011.

McBride MB, Shayler HA, Spliethoff HM, Mitchell RG, Marquez-Bravo LG, Ferenz GS, et al. 2014. Concentrations of lead, cadmium and barium in urban garden-grown vegetables: The impact of soil variables. Environ Pollut 194:254–261; doi:10.1016/j.envpol.2014.07.036.

McHenry LJ. 2009. Element mobility during zeolitic and argillic alteration of volcanic ash in a closed-basin lacustrine environment: Case study Olduvai Gorge, Tanzania. Chem Geol 265:540–552; doi:10.1016/j.chemgeo.2009.05.019.

Mehlich A. 1984. Mehlich 3 soil test extractant: A modification of Mehlich 2 extractant. Commun Soil Sci Plant Anal 15:1409–1416; doi:10.1080/00103628409367568.

Meyers DER, Auchterlonie GJ, Webb RI, Wood B. 2008. Uptake and localisation of lead in the root system of Brassica juncea. Environ Pollut 153:323–332; doi:10.1016/j.envpol.2007.08.029.

Meyers DER, Kopittke PM, Auchterlonie GJ, Webb RI. 2009. Characterization of lead precipitate following uptake by roots of brassica juncea. Environ Toxicol Chem 28:2250–2254; doi:10.1897/09-131.1.

Milwaukee Water Works. 2017. Water Quality. Available: https://city.milwaukee.gov/water/WaterQuality [accessed 19 October 2019].

Mombo S, Foucault Y, Deola F, Gaillard I, Goix S, Shahid M, et al. 2016. Management of human health risk in the context of kitchen gardens polluted by lead and cadmium near a lead recycling company. J Soils Sediments 16:1214–1224; doi:10.1007/s11368-015-1069-7.

Moya J, Phillips L, Schuda L. 2011. Exposure Factors Handbook. 2019th ed. USEPA Office of Research and Development:Washington, DC.

Murray H, Pinchin T, Macfie S. 2011a. Compost application affects metal uptake in plants grown in urban garden soils and potential human health risk. J Soils Sediments 11:815–829; doi:10.1007/s11368-011-0359-y.

Murray H, Pinchin T, Macfie S. 2011b. compost application affects update in plants grown in urban garden soils and potential human health risks. J Soils Sediments 11: 815–829.

Nabulo G, Black CR, Young SD. 2011. Trace metal uptake by tropical vegetables grown on soil amended with urban sewage sludge. Environ Pollut 159:368–376; doi:10.1016/j.envpol.2010.11.007.

Obrycki JF, Basta NT, Culman SW. 2017. Management options for contaminated urban soils to reduce public exposure and maintain soil health. J Environ Qual 46:420–430; doi:10.2134/jeq2016.07.0275.

ODA. 2019. Search Registered Fertilizer, Ag Mineral, Ag Amendment, and Lime Products. Available: http://oda.state.or.us/dbs/heavy_metal/detail.lasso?-op=eq&product_id=14846 [accessed 13 October 2019].

Ovečka M, Takáč T. 2014. Managing heavy metal toxicity stress in plants: Biological and biotechnological tools. Biotechnol Adv 32:73–86; doi:10.1016/j.biotechadv.2013.11.011.

Palmer PT, Jacobs R, Baker PE, Ferguson K, Webber S. 2009. Use of field-portable XRF analyzers for rapid screening of toxic elements in fda-regulated products. J Agric Food Chem 57:2605–2613; doi:10.1021/jf803285h.

Peralta-Videa JR, Lopez ML, Narayan M, Saupe G, Gardea-Torresdey J. 2009. The biochemistry of environmental heavy metal uptake by plants: Implications for the food chain. Int J Biochem Cell Biol 41:1665–1677; doi:10.1016/j.biocel.2009.03.005.

Perroy RL, Belby CS, Mertens CJ. 2014. Mapping and modeling three dimensional lead contamination in the wetland sediments of a former trap-shooting range. Sci Total Environ 487:72–81; doi:10.1016/j.scitotenv.2014.03.102.

Pettygrove M, Ghose R. 2018. From "Rust Belt" to "Fresh Coast": Remaking the City through Food Justice and Urban Agriculture. Ann Am Assoc Geogr 108:591–603; doi:10.1080/24694452.2017.1402672.

Pieper KJ, Martin R, Tang M, Walters L, Parks J, Roy S, et al. 2018. Evaluating Water Lead Levels during the Flint Water Crisis. Environ Sci Technol 52:8124–8132; doi:10.1021/acs.est.8b00791.

Pierart A, Dumat C, Maes AQM, Roux C, Sejalon-Delmas N. 2018. Opportunities and risks of biofertilization for leek production in urban areas: Influence on both fungal diversity and human bioaccessibility of inorganic pollutants. Sci Total Environ 624:1140–1151; doi:10.1016/j.scitotenv.2017.12.100.

Pizarro I, Gómez-Gómez M, León J, Román D, Palacios MA. 2016. Bioaccessibility and arsenic speciation in carrots, beets and quinoa from a contaminated area of Chile. Sci Total Environ 565:557–563; doi:10.1016/j.scitotenv.2016.04.199.

Rai PK, Lee SS, Zhang M, Tsang YF, Kim KH. 2019. Heavy metals in food crops: Health risks, fate, mechanisms, and management. Environ Int 365–385; doi:10.1016/j.envint.2019.01.067.

Ratul AK, Hassan M, Uddin MK, Sultana MS, Akbor MA, Ahsan MA. 2018. Potential health risk of heavy metals accumulation in vegetables irrigated with polluted river water. Int Food Res J 25: 329–338.

Reboredo F, Simões M, Jorge C, Mancuso M, Martinez J, Guerra M, et al. 2019. Metal content in edible crops and agricultural soils due to intensive use of fertilizers and pesticides in Terras da Costa de Caparica (Portugal). Environ Sci Pollut Res 26:2512–2522; doi:10.1007/s11356-018-3625-3.

Rodriguez-Iruretagoiena A, Trebolazabala J, Martinez-Arkarazo I, Diego A, Madariaga JM. 2015. Metals and metalloids in fruits of tomatoes (Solanum lycopersicum) and their cultivation soils in the Basque Country: Concentrations and accumulation trends. Food Chem 173:1083–1089; doi:10.1016/j.foodchem.2014.10.133.

Sampson RJ, Winter AS. 2018. POISONED DEVELOPMENT: ASSESSING CHILDHOOD LEAD EXPOSURE AS A CAUSE OF CRIME IN A BIRTH COHORT FOLLOWED THROUGH ADOLESCENCE. Criminology 56:269–301; doi:10.1111/1745-9125.12171.

Sancho D, Deban L, Pardo R, Valladolid D. 2005. Determination of zinc, cadmium, lead and copper in pellets and pulp of sugar beet. J Sci Food Agric 85:1021–1025; doi:10.1002/jsfa.2046.

Schifferstein HNJ, Wehrle T, Carbon CC. 2019. Consumer expectations for vegetables with typical and atypical colors: The case of carrots. Food Qual Prefer 72:98–108; doi:10.1016/j.foodqual.2018.10.002.

Schnur J, John RM. 2014. Childhood lead poisoning and the new centers for disease control and prevention guidelines for lead exposure. J Am Assoc Nurse Pract; doi:10.1002/2327-6924.12112.

Sekara A, Poniedzialek M, Ciura J, Jedrszczyk E. 2005. Cadmium and lead accumulation and distribution in the tissues of nine crops: Implications for phytoremediation. Polish J Environ Stud 14: 509–516.

Sharma K, Basta NT, Grewal PS. 2015. Soil heavy metal contamination in residential neighborhoods in post-industrial cities and its potential human exposure risk. Urban Ecosyst 18:115–132; doi:10.1007/s11252-014-0395-7.

Sharma P, Dubey RS. 2005. Lead Toxicity in Plants. Brazilian J Plant Physiol 14: 35–52.

Singh VK, Rai PK, Pathak AK, Tripathi DK, Singh SC, Singh JP. 2017. Application of wavelength dispersive X ray fluorescence spectrometry to biological samples. Spectrosc (Santa Monica) 32: 41–47.

Struik PC. 2007. Above-ground and below-ground plant development. In: Potato Biology and Biotechnology: Advances and Perspectives. Elsevier. 219–236.

Száková J, Havlík J, Valterová B, Tlustoš P, Goessler W. 2010. The contents of risk elements, arsenic speciation, and possible interactions of elements and betalains in beetroot (Beta vulgaris, L.) growing in contaminated soil. Cent Eur J Biol 5:692–701; doi:10.2478/s11535-010-0050-0.

Tester M, Leigh RA. 2001. Partitioning of nutrient transport processes in roots. J Exp Bot 52:445–57; doi:10.1093/jexbot/52.suppl_1.445.

Tom M, Fletcher TD, McCarthy DT. 2014. Heavy metal contamination of vegetables irrigated by Urban stormwater: A matter of time? PLoS One 9; doi:10.1371/journal.pone.0112441.

USEPA. 2019. Control of Lead and Copper.

USFDA. 2019. Interim Reference Level. Lead Food, Foodwares, Diet Suppl. Available: https://www.fda.gov/food/metals/lead-food-foodwares-and-dietary-supplements [accessed 11 October 2019].

USFDA. 2018. Total Diet Study. Available: https://www.fda.gov/food/science-research-food/total-diet-study [accessed 17 October 2019].

Verret F, Gravot A, Auroy P, Leonhardt N, David P, Nussaume L, et al. 2004. Overexpression of AtHMA4 enhances root-to-shoot translocation of zinc and cadmium and plant metal tolerance. FEBS Lett 576:306–312; doi:10.1016/j.febslet.2004.09.023.

WDNR. 2018. Soil Cleanup Standards. Chapter NR 720 Wisconsin Administrative Code.

Whitehead LS, Buchanan SD. 2019. Childhood Lead Poisoning: A Perpetual Environmental Justice Issue? J Public Heal Manag Pract 25:S115–S120; doi:10.1097/PHH.0000000000000891.

Yokel J, Delistraty DA. 2003. Arsenic, lead, and other trace elements in soils contaminated with pesticide residues at the Hanford site (USA). Environ Toxicol 18:104–114; doi:10.1002/tox.10106.

Yousaf B, Liu G, Wang R, Imtiaz M, Zia-ur-Rehman M, Munir MAM, et al. 2016. Bioavailability evaluation, uptake of heavy metals and potential health risks via dietary exposure in urban-industrial areas. Environ Sci Pollut Res 23:22443–22453; doi:10.1007/s11356-016-7449-8.

Yuan Y, Xiang M, Liu C, Theng BKG. 2019. Chronic impact of an accidental wastewater spill from a smelter, China: A study of health risk of heavy metal(loid)s via vegetable intake. Ecotoxicol Environ Saf 182; doi:10.1016/j.ecoenv.2019.109401.

Zahran S, Laidlaw MAS, McElmurry SP, Filippelli GM, Taylor M. 2015. Linking source and effect: Resuspended soil lead, air lead, and children's blood lead levels in Detroit, Michigan. In: Everyday Environmental Toxins: Childrens Exposure Risks. Apple Academic Press. 163–179.

Zheng L, Ying B, Tongming Y. 2019. Effect of Cd on the Uptake and Translocation of Pb, Cu, Zn, and Ni in Potato and Wheat Grown in Sierozem. Soil Sediment Contam An Int J 1–20; doi:10.1080/15320383.2019.1643289.

Zwolak A, Sarzyńska M, Szpyrka E, Stawarczyk K. 2019. Sources of Soil Pollution by Heavy Metals and Their Accumulation in Vegetables: a Review. Water Air Soil Pollut 230; doi:10.1007/s11270-019-4221-y.

Figure 4.1. Distribution of bioavailable Pb ($\mu g\ g^{-1}$) and cation exchange capacity (meq $100g^{-1}$) in three urban soils (Residence 1, Residence 2, and Former Foundry) and in a Commercial Topsoil.
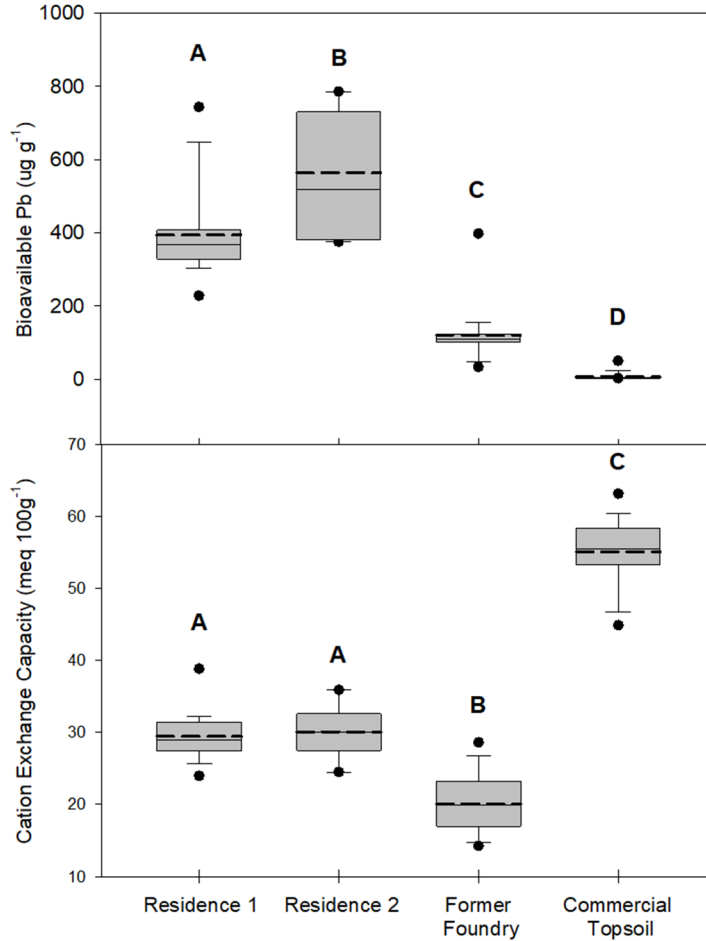


Note. The three horizontal lines of the box from the top to the bottom represent the 75th percentile, the median, and the 25th percentile. The whiskers represent the 10th and 90th percentile. Circles represent the 5th and 95th percentile. The mean is illustrated as a dashed black line. The mean values considered significantly different at an alpha value of 0.05 are denoted by a different letter above the boxplot. The number of soil samples represented by the boxplots for Residence 1, Residence 2, the Former Foundry, and the Commercial Topsoil are 29, 9, 20, and 17, respectively

Figure 4.2. Mean Pb concentrations (µg g$^{-1}$) in produce grown in three metals-rich soils.
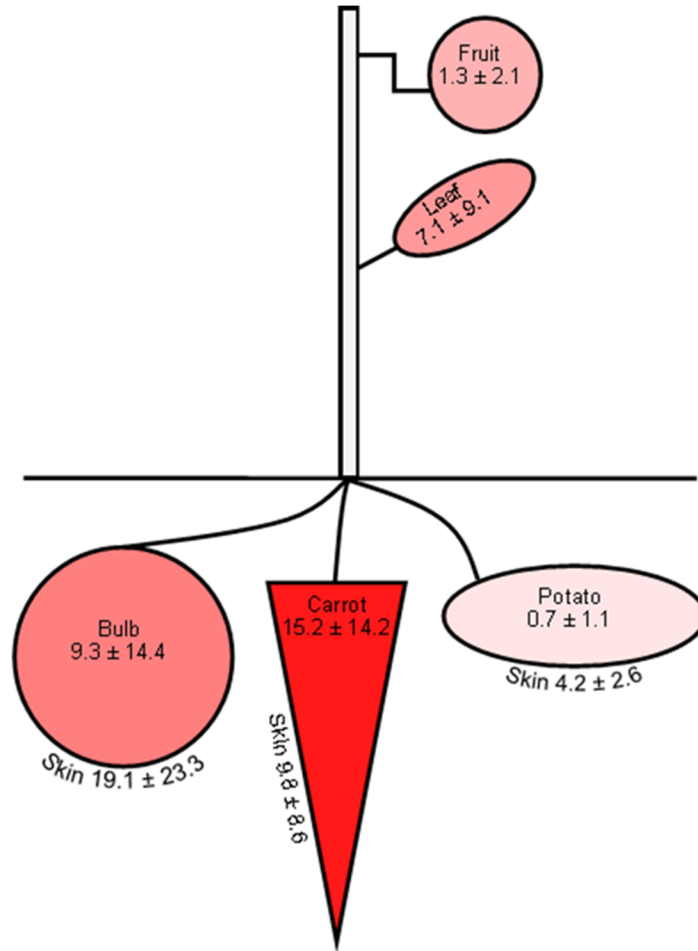


Note. Concentrations summarized above are given on a dry-weight basis and concentrations represent the mean of crop tissues grown in soils from Residence 1, Residence 2, and the Former Foundry. "Fruit" is the average Pb concentration of tomatoes and peppers (n=11); "leaf" is the average Pb concentration in all produce leaves (n=144); "Bulb" is the average Pb concentration of four beetroot cultivars, radishes, and turnips (n=76); and "carrot" is the average Pb concentration of the three cultivars of carrots (n=56). The sample size for potatoes is 20. Increasing shading intensity in the figure reflects an increase in Pb in prepared consumable tissues. The bioavailable Pb in the three soils (n=58) ranged from 32 µg g$^{-1}$ to 786 µg g$^{-1}$ with a mean of 326 ± 199 µg g$^{-1}$.

Figure 4.3. Mass of each prepared garden produce grown in soil from Residence 1 that could be consumed (g d$^{-1}$) so as not to exceed the USFDA IRL.
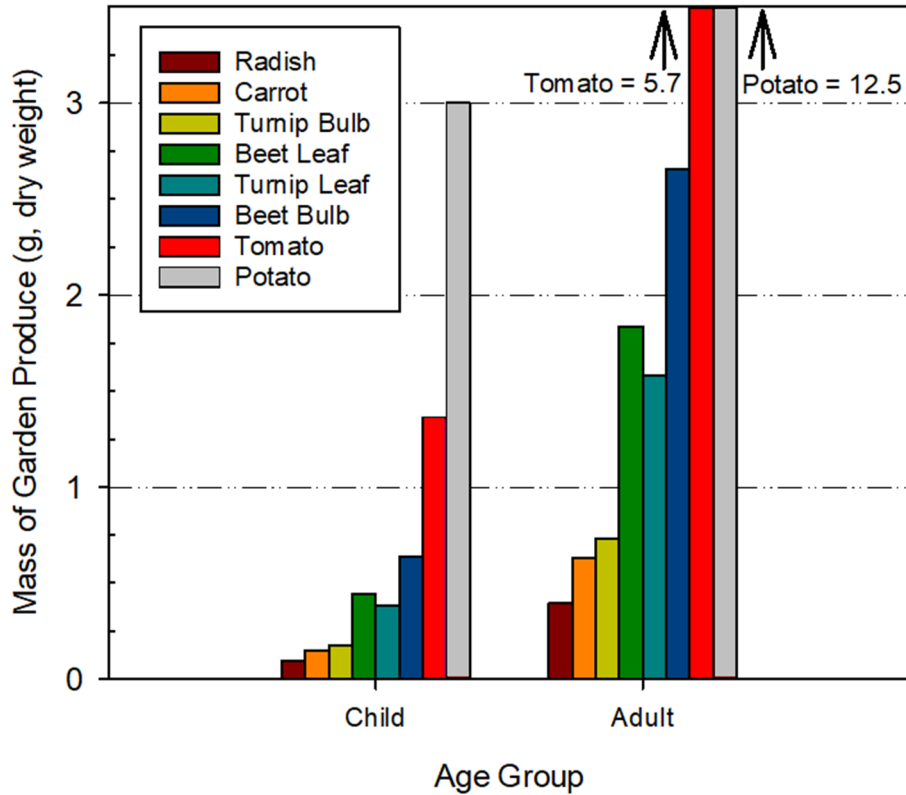


Note. The mass of vegetable is calculated based on the mean concentrations of Pb in each crop grown in soil from Residence 1. The USFDA IRL (US Food and Drug Administration 2019) is 3 μg d$^{-1}$ for children and 12.5 μg d$^{-1}$ for adults.

Figure 4.4. Estimated total Pb ingested by a child ($\mu$g d$^{-1}$) based on ten modeled exposure scenarios.
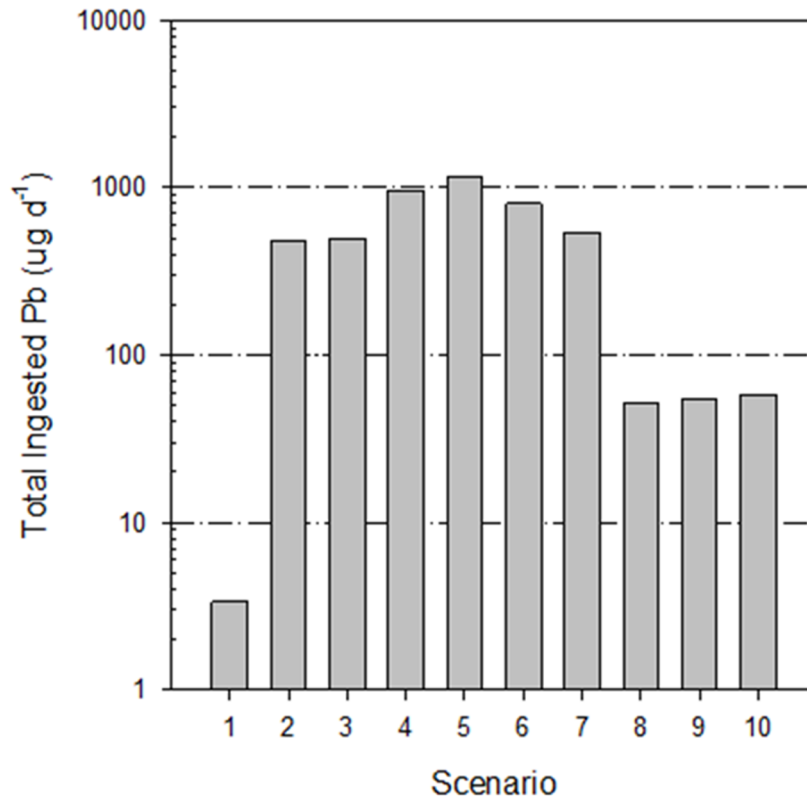


Note. Due to the difference in magnitude between scenarios, the y-axis is log-transformed. This model assumes that all Pb ingested by a child is from ingestion of water, food, and soil+dust. Model scenarios are explained on Table 4.3 and concentrations of Pb in each vector are described in Table 4.5S.

Figure 4.5. Contributions of each vector to the daily ingestion of Pb by a child based on ten exposure scenarios.
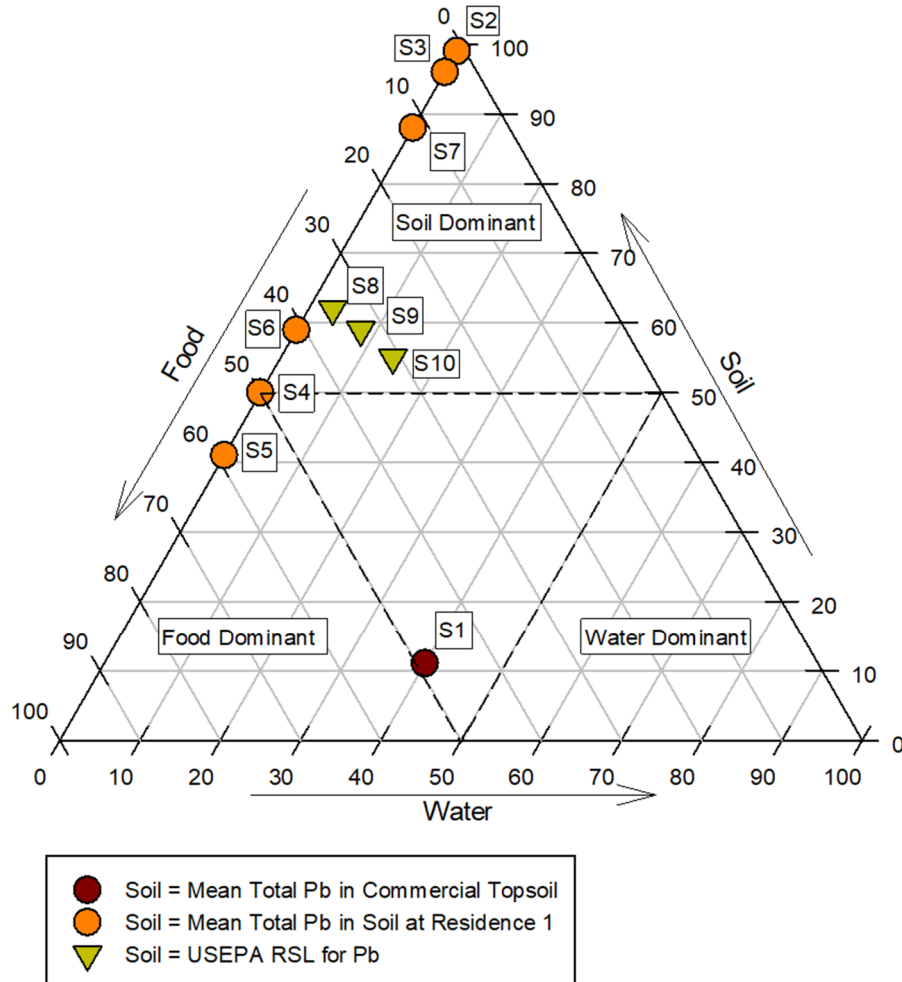


Note. USEPA RSL, USEPA regional screening level for direct contact at residential properties (USEPA 2019b). Scenarios are categorized based on the soil used to model total Pb ingestion. Model scenarios are explained on Tables 4.3 and 4.5S.

Table 4.1. Demographics of the target Census Tract compared to the City of Milwaukee,

Milwaukee County, the State of Wisconsin, and the United States.

| Population Demographic | Census Tract 90 | City of Milwaukee | Milwaukee County | State of Wisconsin | United States |
|---|---|---|---|---|---|
| Population Density | 13,314 | 6,191 | 3,943 | 107 | 92 |
| Median age | 23 | 32 | 35 | 40 | 38 |
| Percent of Population < 6 | 16% | 8% | 7% | 6% | 6% |
| Percent of Population < 9 | 26% | 15% | 14% | 12% | 13% |
| Percent of Population < 18 | 44% | 26% | 24% | 22% | 23% |
| Percent non-white | 96 % | 64 % | 49 % | 19 % | 39 % |
| Median household income | $28,113 | $39,093 | $47,591 | $59,305 | $60,336 |
| Percent poverty | 40 % | 25 % | 19 % | 11 % | 13 % |
| Percent of Homes Built Pre-1969 | 81 % | 80 % | 73 % | 46 % | 39 % |
| 2013-2016 Lead Poisoning Rate for Children (age 1-6 years) | 29 % | 12 % | 9 % | 8 % | 3% |

Note: Demographic data from the 2017 American Community Survey (US Census Bureau

2019); population density is the estimated number of people per square mile; 2013-2016 blood

lead poisoning rate is the percent of children with a blood Pb concentration greater than 5 µg dl$^{-1}$

per the number of children tested (CDC 2019; City of Milwaukee 2017; WDHS 2018).

Table 4.2. Concentration of Pb ($\mu g\ g^{-1}$) in prepared consumable garden produce grown in three urban soils and in Commercial Topsoil.

| Garden Produce | Mean ± SD (n) | | | |
| --- | --- | --- | --- | --- |
| | Residence 1 | Residence 2 | Former Foundry | Commercial Topsoil |
| Radish | 31.8 ± 23.9 (6) | 74.8* | 4.2 ± 2.9 (3) | 0.6* |
| Carrot | 19.8 ± 13.1 (29) | 19.1 ± 17.0 (12) | 3.2 ± 2.6 (15) | < 0.3 (13) |
| *White* | 26.7 ± 16.2 (5) | 28.0 ± 32.6 (3) | 6.4 ± 1.6 (4) | < 0.3 (3) |
| *Purple* | 20.1 ± 9.9 (8) | 6.2 ± 5.9 (2) | 1.2 ± 1.1 (2) | < 0.3 (3) |
| *Orange* | 17.6 ± 13.6 (16) | 19.0 ± 8.5 (7) | 2.2 ± 1.8 (9) | < 0.3 (7) |
| Turnip Bulb | 17.2 ± 9.8 (9) | 16.8 ± 21.5 (2) | 3.4 ± 1.8 (5) | < 0.3 (2) |
| Turnip Leaf | 7.9 ± 5.1 (13) | 4.2 ± 4.5 (2) | 2.2 ± 1.8 (6) | 0.7 ± 0.2 (3) |
| Beetroot Bulb | 4.7 ± 5.0 (22) | 8.3 ± 9.9 (13) | 0.8 ± 0.9 (15) | < 0.3 (11) |
| *Bulls Blood* | 5.5 ± 3.9 (4) | 16.4 ± 13.4 (4) | 0.8 ± 0.8 (3) | < 0.3* |
| *Chioggia* | 9.1 ± 7.3 (6) | NA | 1.0 ± 1.1 (4) | < 0.3 (2) |
| *Detroit* | 1.9 ± 1.6 (7) | 3.7 ± 2.3 (6) | 0.5 ± 0.5 (5) | < 0.3 (5) |
| *Albino* | 2.7 ± 1.2 (5) | 6.7 ± 10.2 (3) | 1.1 ± 1.4 (3) | < 0.3 (3) |
| Beetroot Leaf | 6.8 ± 5.5 (21) | 10.3 ± 11.4 (11) | 3.4 ± 3.2 (14) | 0.5 ± 0.2 (13) |
| *Bulls Blood* | 8.9 ± 2.2 (4) | 9.3 ± 10.8 (4) | 2.0 ± 0.9 (3) | 0.4 ± 0.2 (2) |
| *Chioggia* | 5.7 ± 7.2 (5) | NA | 2.3 ± 1.6 (5) | < 0.3 (2) |
| *Detroit* | 6.4 ± 7.1 (8) | 10.0 ± 13.4 (5) | 4.7 ± 5.1 (4) | 0.5 ± 0.3 (7) |
| *Albino* | 6.9 ± 2.7 (4) | 13.1 ± 14.3 (2) | 5.7 ± 4.3 (2) | 0.5 ± 0.2 (2) |
| Tomato | 2.2 ± 3.5 (8) | NA | 3.2* | < 0.3* |
| Pepper | < 0.3* | NA | 1.2* | 0.7* |
| Potato | 1.0 ± 1.3 (13) | < 0.3 (3) | 0.3 ± 0.1 (4) | 0.3 ± 0.1 (9) |

Note: NA; value not quantifiable as produce failed to grow to maturity in soil; SD, standard deviation. The XRF limit of detection is 0.3 $\mu g\ g^{-1}$ and mean values of "< 0.3" indicate Pb concentrations were all less than the laboratory limit of detection. The n value represents the total number of samples analyzed and a star indicates the value represents the concentration in a single sample. Concentrations are given on a dry weight basis. For ease of labeling, common produce names are used, except for denoting cultivars in italics. Beetroots are referred to by their cultivar name (var. Bulls Blood; var. Chioggia; var. Detroit; var. Albino). Carrots are referred to by pigment color where "White" corresponds to var. Lunar White, "Orange" corresponds to var. Scarlet Nantes, and "Purple" corresponds to var. Pusa Asita Black.

136

Table 4.3. Exposure scenarios used to evaluate the total daily Pb ingested by a child from three exposure vectors.

| Scenario | Vector | | |
| --- | --- | --- | --- |
| | Food | Water | Soil+Dust |
| Scenario 1 | Mean Pb in raw produce from USFDA TDS | Mean Pb in Water in City of Milwaukee | Mean Pb in Comm. Topsoil |
| Scenario 2 | | | Mean Pb in Soil at Res. 1 |
| Scenario 3 | Mean Pb in produce grown in commercial topsoil | Mean Pb in Water in City of Milwaukee | Mean Pb in Soil at Residence 1 |
| Scenario 4 | Mean Pb in produce grown in soil from Residence 1 | | |
| Scenario 5 | Mean Pb in root crops grown in soil from Residence 1 | Mean Pb in Water in City of Milwaukee | Mean Pb in Soil at Residence 1 |
| Scenario 6 | Mean Pb in root crop leaves grown in soil from Residence 1 | | |
| Scenario 7 | Mean Pb in non-root crops grown in soil from Residence 1 | | |
| Scenario 8 | Mean Pb in produce grown in commercial topsoil | Mean Pb in Water in City of Milwaukee | USEPA RCL |
| Scenario 9 | | USEPA Action Level | |
| Scenario 10 | | Flint, Michigan | |

Note: USFDA TDS, Mean Pb in 2003-2016 raw produce from Food and Drug Administration Total Diet Study (US Food and Drug Administration 2018); USEPA Action Level for Pb per (USEPA 2019); USEPA RCL, USEPA Regional Screening Level for direct contact at residential properties (USEPA 2019b). Model factors are further described in Table 4.5S.

Figure 4.1S. Bioavailable Cd, Cr, Mg, and Zn (µg g$^{-1}$) in three urban soils (Residence 1, Residence 2, Former Foundry) and in a Commercial Topsoil.
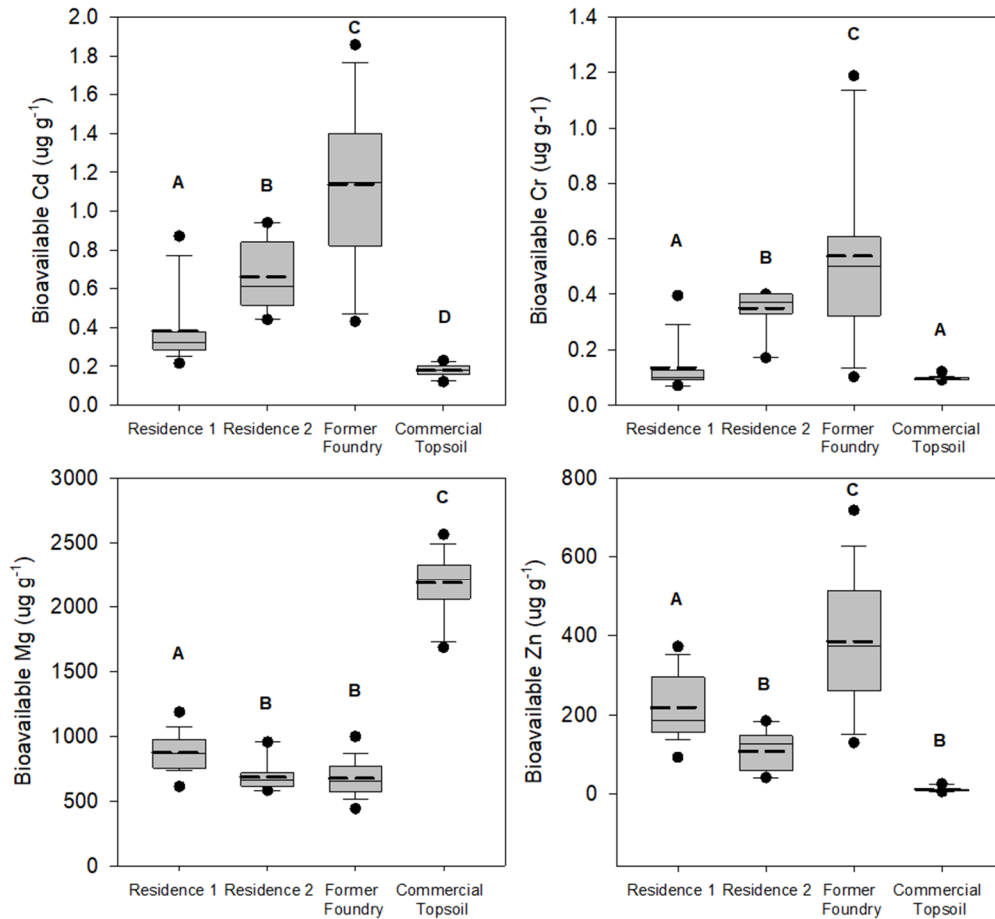


Note. The three horizontal lines of the box from the top to the bottom represent the 75$^{th}$ percentile, the median, and the 25$^{th}$ percentile. The whiskers represent the 10$^{th}$ and 90$^{th}$ percentiles. Circles represent the 5$^{th}$ and 95$^{th}$ percentiles. The mean is illustrated as a dashed black line. The mean values considered significantly different at an alpha value of 0.05 are denoted by a different letter above the boxplot. The number of soil samples represented by the boxplots for Residence 1, Residence 2, the Former Foundry, and the Commercial Topsoil are 29, 9, 20, and 17, respectively.

138

Figure 4.2S. XRD diffraction patterns of soils used in this study (A) Residence 1, (B) Residence 2, (C) Former Foundry, and (D) Commercial Topsoil.

C)



D)
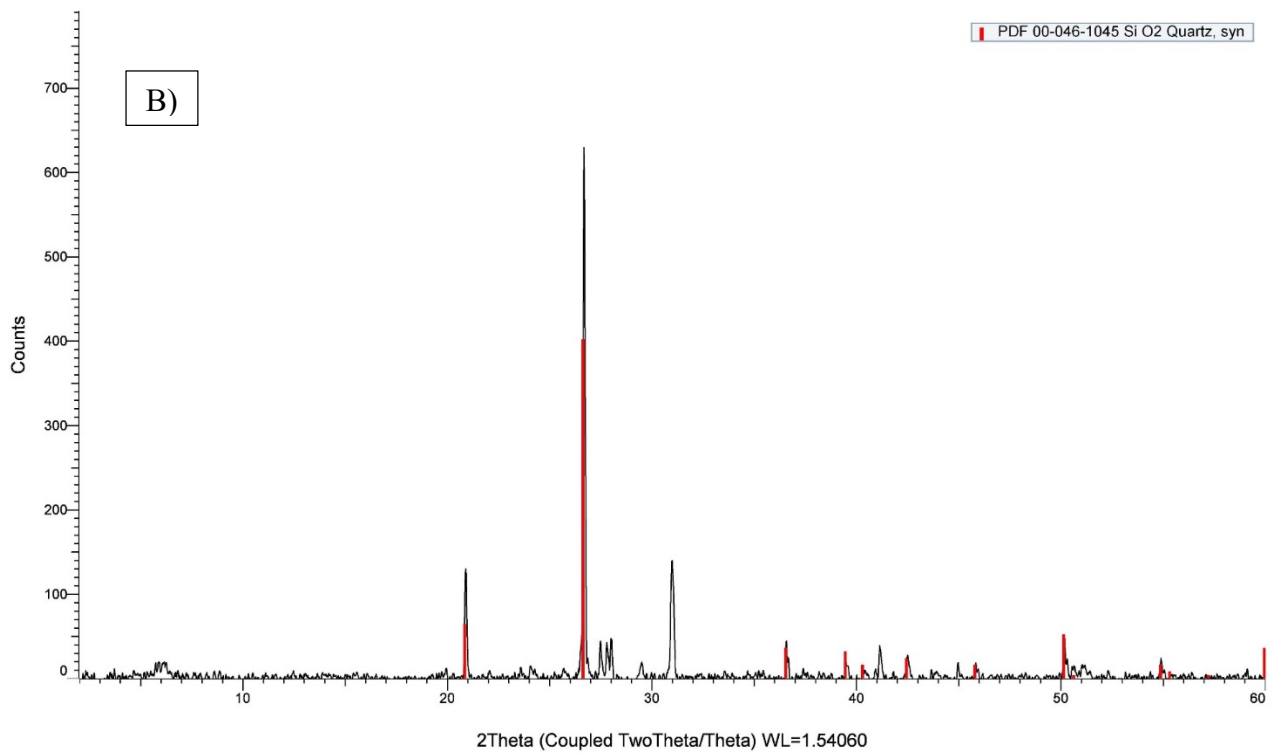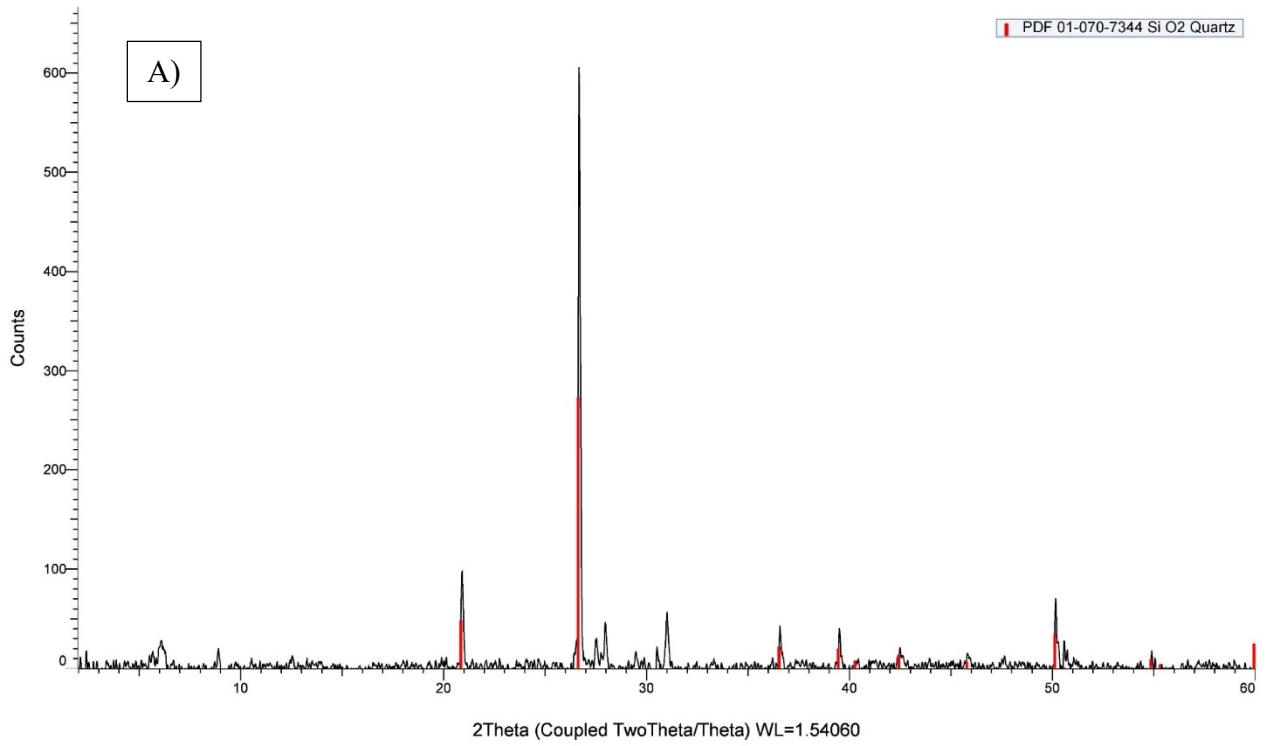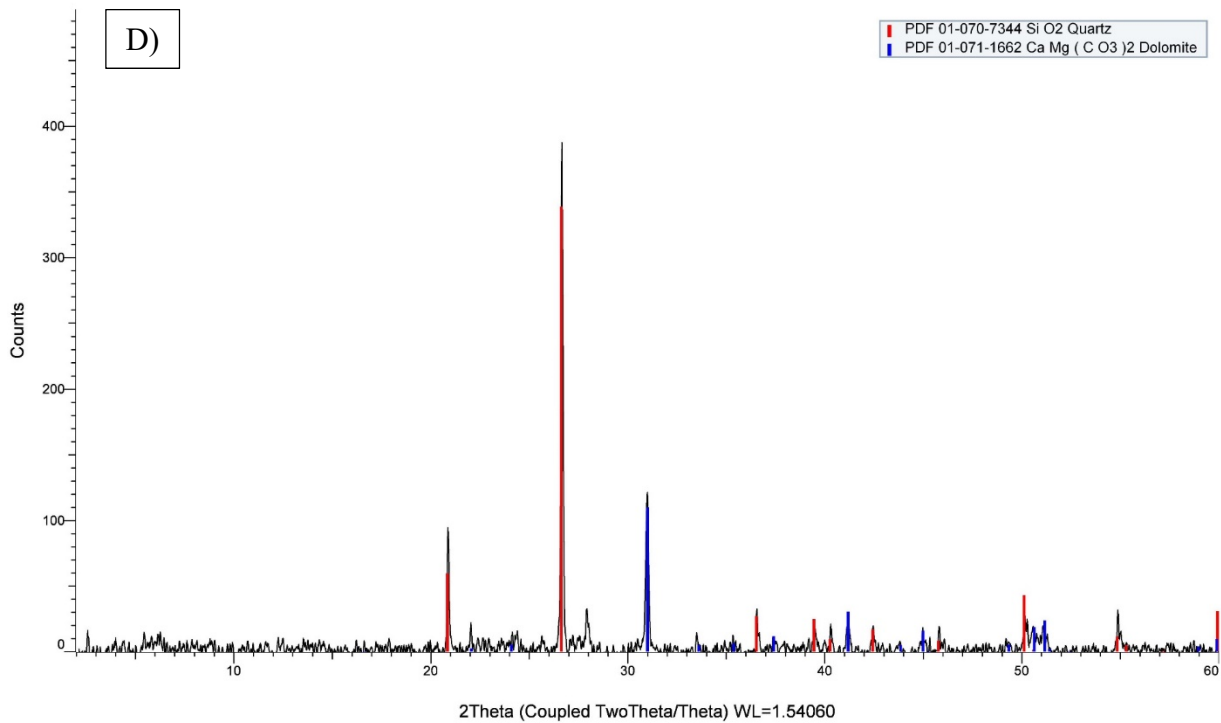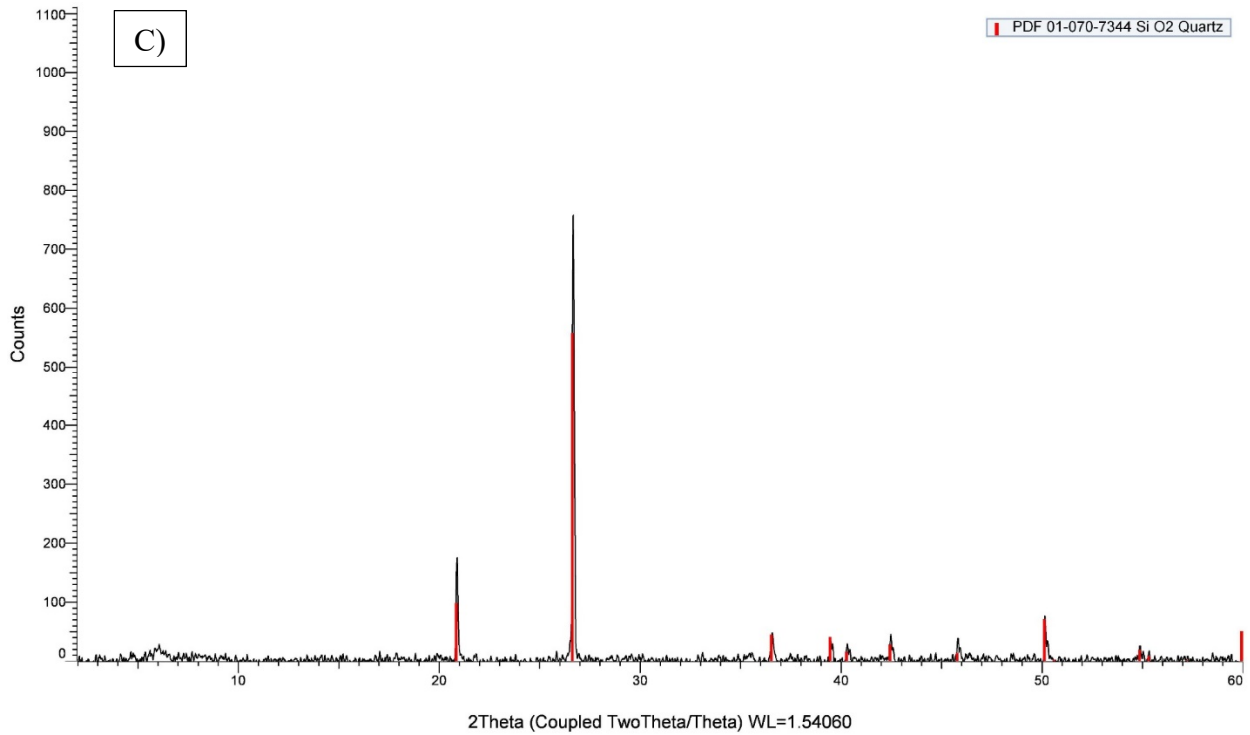
Figure 4.3S. Pb in food (μg kg$^{-1}$) from the USFDA TDS (2003-2016). The concentrations of Pb illustrated by the boxplots represent the concentration of Pb in food as consumed and are not universally corrected by USFDA to dry weight.
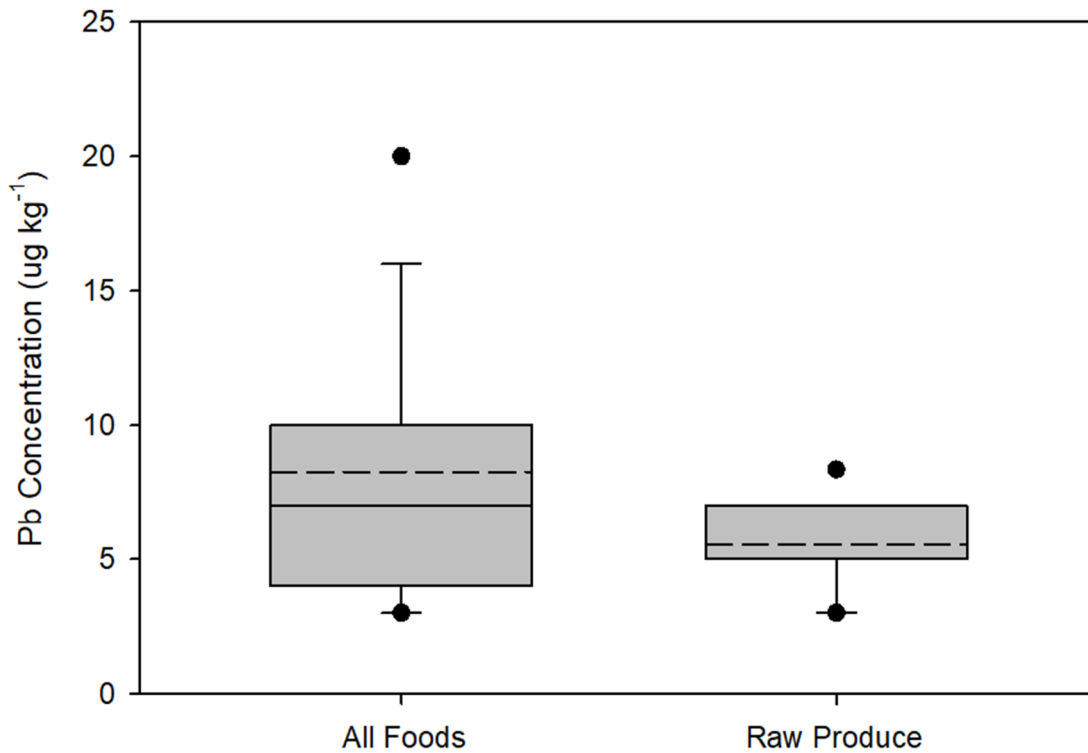


Note. The limit of detection was used when the concentration was reported as 0. The three horizontal lines of the box from the top to the bottom represent the 75th percentile, the median, and the 25th percentile. The whiskers represent the 10th and 90th percentile. Circles represent the 5th and 95th percentile. The mean is illustrated as a dashed black line. The number of samples represented by the boxplot for "All Foods" is 16,035. The number of samples represented by the boxplot for "Raw Produce" is 472. A listing of foods included in "Raw Produce" is provided in Table 4.6S.

Figure 4.4S. Pb in Produce (µg kg$^{-1}$) grown in soil from Residence 1.
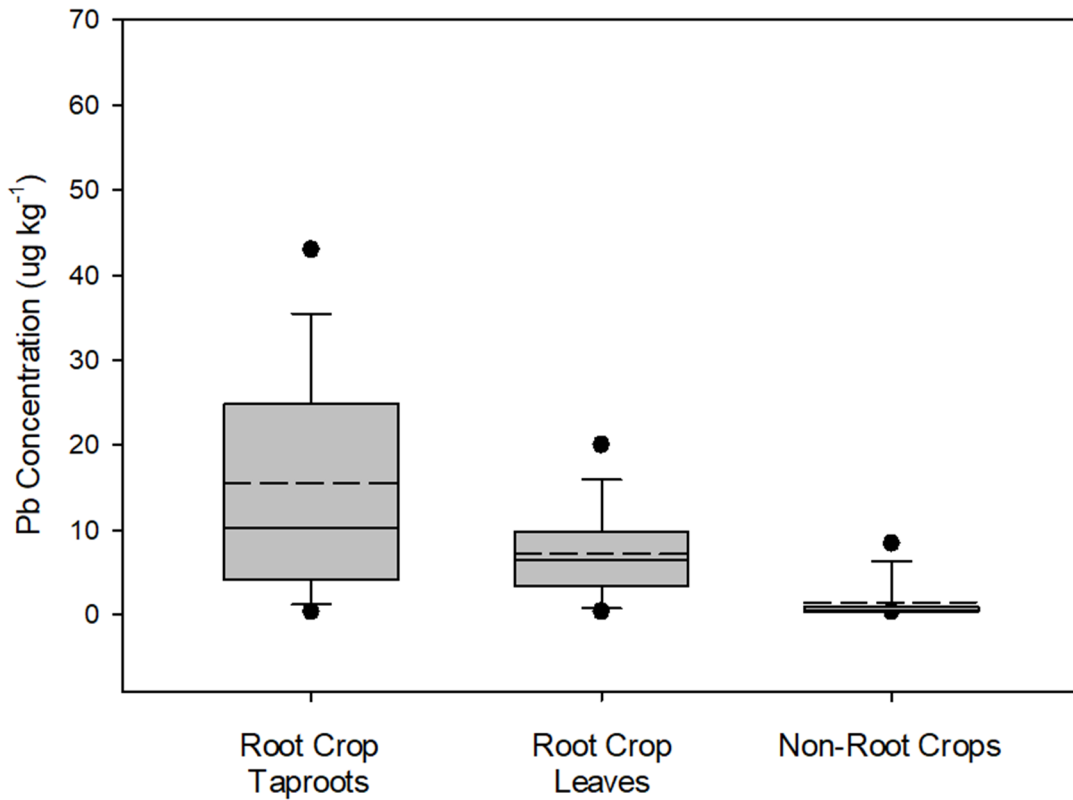


Note. The three horizontal lines of the box from the top to the bottom represent the 75th percentile, the median, and the 25th percentile. The whiskers represent the 10th and 90th percentile. Circles represent the 5th and 95th percentile. The mean is illustrated as a dashed black line. Vegetables grown in soils from Residence 1 used to calculate the average Pb concentration in: Root Crop Taproots (n=66) include radish, carrot cultivars, turnip, and beetroot cultivars; Root Crop Leaves (n=34) include turnip and beetroot cultivars; and Non-Root Crops (n=22) include tomato, pepper, potato. See Table 4.3 and Table 4.5S for a description of how this data is used.

Figure 4.5S. Pb in drinking water (µg L$^{-1}$) collected in 2014 and 2017 in the City of Milwaukee, Wisconsin, USA.
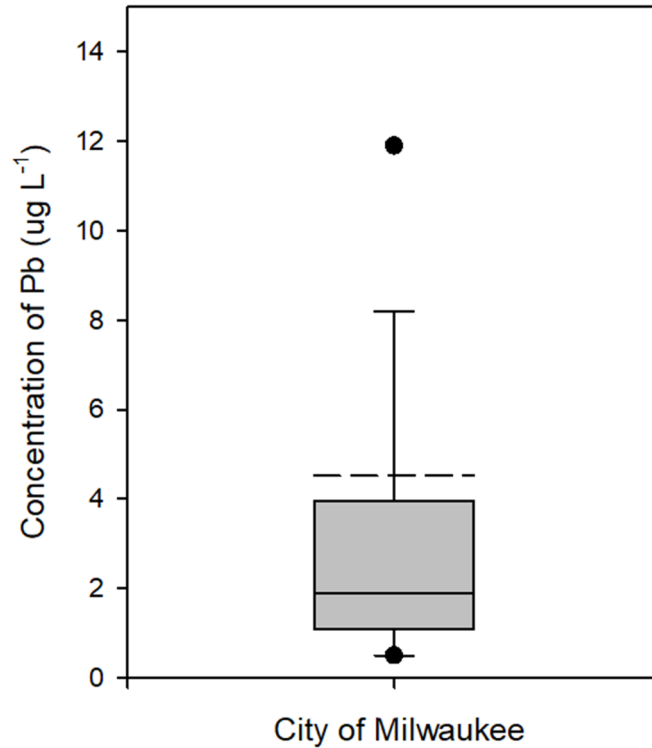


Note. Accessible 2014 and 2017 data per (Milwaukee Water Works 2017). The three horizontal lines of the box from the top to the bottom represent the 75th percentile, the median, and the 25th percentile. The whiskers represent the 10th and 90th percentiles. Circles represent the 5th and 95th percentiles. The mean is illustrated as a dashed black line. The number of samples represented by the boxplot is 101 ($n_{2014}$ = 51 and $n_{2017}$ = 50.). See Table 4.3 and Table 4.5S for a description of how this data is used.

Table 4.1S. The pH and concentrations of bioavailable elements ($\mu g\ g^{-1}$) in three urban soils and in a Commercial Topsoil.

| Soil Chemistry | | Mean ± SD (n) | | | |
|---|---|---|---|---|---|
| | | Residence 1 (n=29) | Residence 2 (n=9) | Former Foundry (n=20) | Commercial Topsoil (n=17) |
| pH | | 7.48 ± 0.2 | 7.73 ± 0.2 | 7.43 ± 0.2 | 7.54 ± 0.2 |
| Bioavailable elements | Ca | 3949 ± 566 | 4417 ± 728 | 2394 ± 594 | 6743 ± 519 |
| | Cu | 3.9 ± 2.2 | 5.3 ± 3.4 | 34.4 ± 13.2 | 3.1 ± 0.6 |
| | Fe | 29 ± 13.5 | 30.1 ± 12.5 | 87.2 ± 22.7 | 286.5 ± 30.3 |
| | K | 128.8 ± 55.1 | 104.6 ± 44.4 | 105.6 ± 52.5 | 63.5 ± 24.8 |
| | Mn | 20.6 ± 7.8 | 14.7 ± 4.8 | 33.4 ± 9.1 | 3.5 ± 0.7 |
| | Na | 484.9 ± 35.7 | 473.1 ± 23.5 | 515.5 ± 61 | 694.5 ± 34.8 |
| | Ni | 0.5 ± 0.1 | 0.4 ± 0.1 | 4.3 ± 2.1 | 0.3 ± 0.1 |
| | P | 83.1 ± 14.1 | 60.5 ± 10.8 | 19.7 ± 13.9 | 18.6 ± 9.9 |
| | S | 45.8 ± 6.8 | 46.8 ± 8.1 | 26.5 ± 5.9 | 215.3 ± 55.8 |

Note: SD, standard deviation; n, number of soil samples from each soil group.

Table 4.2S. Concentration of Pb ($\mu g\ g^{-1}$) in leaves and skins of three carrot cultivars.

| Garden Produce | Mean ± SD (n) | | |
|---|---|---|---|
| | Residence 1 | Residence 2 | Former Foundry |
| Carrot Leaf | 8.7 ± 8.7 (25) | 12.2 ± 13.8 (10) | 2.2 ± 5 (17) |
| *White* | 4.6 ± 4.4 (6) | 7.8 ± 9.3 (3) | 0.6 ± 0.4 (4) |
| *Purple* | 9.7 ± 3.7 (5) | 3.5 ± 4.1 (3) | 1 ± 0.5 (2) |
| *Orange* | 12.2 ± 12.6 (14) | 22.2 ± 16.7 (4) | 3.6 ± 6.8 (7) |
| Carrot Skin | 12 ± 9.7 (15) | 11.6 ± 6.5 (4) | 3.9 ± 3.4 (7) |
| *White* | 14.4 ± 7.3 (4) | NA | 3.2 ± 2.7 (3) |
| *Purple* | 5.8 ± 9.6 (3) | 4.0* | NA |
| *Orange* | 10 ± 6.6 (8) | 14.2 ± 5 (3) | 4.5 ± 4.1 (4) |
| Beetroot Skin | 24.6 ± 25.0 (13) | 23.0 ± 26.0 (9) | 3.6 ± 2.8 (7) |
| *Bulls Blood* | 44.1 ± 18.0 (3) | 27.5 ± 40.3 (4) | 1.4* |
| *Chioggia* | 32.5 ± 36.5 (4) | NA | 4.3 ± 3.3 (4) |
| *Detroit* | 10.0 ± 0.7 (3) | 18.6 ± 10.6 (3) | 5.2* |
| *Albino* | 9.3 ± 8.7 (3) | 20.7 ± 13.2 (2) | 1.5* |

Note: NA; value not quantifiable as not enough mass was available, or vegetable did not grow to maturity. The n value represents the total number of samples analyzed and a star indicates the value represents the concentration in a single sample. Due to small mass, skin samples could represent a composite of samples from multiple pots of the same soil, especially in the beetroot dataset. Concentrations are provided on a dry weight basis. Carrots are referred to by pigment color where "White" corresponds to var. Lunar White, "Orange" corresponds to var. Scarlet Nantes, and "Purple" corresponds to var. Pusa Asita Black. Beetroots are referred to by their cultivar name (var. Bulls Blood; var. Chioggia; var. Detroit; var. Albino).

Table 4.3S. Concentration of chromium (µg g$^{-1}$) in prepared consumable garden produce grown in three urban soils and in Commercial Topsoil.

| Garden Produce | Mean ± SD (n) | | | |
|---|---|---|---|---|
| | Residence 1 | Residence 2 | Former Foundry | Commercial Topsoil |
| Radish | 1.7 ± 1.9 (6) | < 0.6* | < 0.6 (3) | < 0.6* |
| Carrot | 1.8 ± 1.7 (29) | 1.9 ± 2.2 (12) | 11.2 ± 36.5 (15) | 2.5 ± 2.9 (13) |
| *White* | 1.8 ± 1.6 (5) | 2.0 ± 1.6 (3) | 2.0 ± 0.9 (4) | 1.1 ± 0.9 (3) |
| *Purple* | 0.9 ± 0.5 (8) | 5.0 ± 4.8 (2) | 1.0 ± 0.5 (2) | 1.0 ± 0.4 (3) |
| *Orange* | 2.3 ± 1.9 (16) | 0.9 ± 0.3 (7) | 17.5 ± 47.1 (9) | 3.7 ± 3.5 (7) |
| Turnip Bulb | < 0.6 (9) | < 0.6 (2) | 2.1 ± 2.8 (5) | 0.9 ± 0.4 (2) |
| Turnip Leaf | < 0.6 (13) | < 0.6 (2) | < 0.6 (6) | 4.4 ± 6.6 (3) |
| Beetroot Bulb | 2.7 ± 2.6 (22) | 1.9 ± 1.5 (13) | 2.3 ± 3.3 (15) | 1.4 ± 0.7 (11) |
| *Bulls Blood* | 2.4 ± 2.8 (4) | 2.4 ± 1.6 (4) | 2.2 ± 0.6 (3) | 2* |
| *Chioggia* | 2.6 ± 0.9 (6) | NA | 1.6 ± 0.7 (4) | 1.2 ± 0.9 (2) |
| *Detroit* | 3.1 ± 4.3 (7) | 2.3 ± 1.6 (6) | 3.7 ± 5.9 (5) | 1.5 ± 0.7 (5) |
| *Albino* | 2.2 ± 1.1 (5) | 0.6 ± 0.1 (3) | 1.0 ± 0.6 (3) | 1.0 ± 0.7 (3) |
| Beetroot Leaf | < 0.6 (21) | < 0.6 (11) | 0.7 ± 0.3 (14) | < 0.6 (13) |
| *Bulls Blood* | < 0.6 (4) | < 0.6 (4) | < 0.6 (3) | < 0.6 (2) |
| *Chioggia* | < 0.6 (5) | NA | < 0.6 (5) | < 0.6 (2) |
| *Detroit* | < 0.6 (8) | < 0.6 (5) | < 0.6 (4) | < 0.6 (7) |
| *Albino* | < 0.6 (4) | < 0.6 (2) | 1.1 ± 0.7 (2) | < 0.6 (2) |
| Tomato | 1.4 ± 1.1 (8) | NA | < 0.6* | < 0.6* |
| Pepper | < 0.6* | NA | < 0.6* | < 0.6* |
| Potato | 1.5 ± 0.7 (13) | 1.8 ± 2.1 (3) | 1.2 ± 0.5 (4) | 1.6 ± 1.2 (9) |

Note: NA; value not quantifiable as produce failed to grow to maturity in soil; SD, standard deviation. The XRF limit of detection is 0.6 µg g$^{-1}$ and mean values of "< 0.6" indicate chromium concentrations were all less than the laboratory limit of detection. The n value represents the total number of samples analyzed and a star indicates the value represents the concentration in a single sample. Concentrations are provided on a dry weight basis. For ease of labeling, common produce names are used, except for denoting cultivars in italics. Beetroots are referred to by their cultivar name (var. Bulls Blood; var. Chioggia; var. Detroit; var. Albino). Carrots are referred to by pigment color where "White" corresponds to var. Lunar White, "Orange" corresponds to var. Scarlet Nantes, and "Purple" corresponds to var. Pusa Asita Black.

146

Table 4.4S. Concentration of nickel ($\mu g\ g^{-1}$) in prepared consumable garden produce grown in three urban soils and in Commercial Topsoil

| Garden Produce | Mean ± SD (n) | | | |
| --- | --- | --- | --- | --- |
| | Residence 1 | Residence 2 | Former Foundry | Commercial Topsoil |
| Radish | 0.6 ± 0.5 (6) | < 0.4* | 1.0 ± 0.8 (3) | < 0.4* |
| Carrot | 1.1 ± 1.4 (29) | 1.1 ± 1 (12) | 2.5 ± 1.0 (15) | 1.0 ± 0.8 (13) |
| *White* | 0.6 ± 0.2 (5) | 1.0 ± 0.5 (3) | 3.2 ± 1.0 (4) | 0.5 ± 0.1 (3) |
| *Purple* | 1.8 ± 2.5 (8) | 2.8 ± 1.5 (2) | 1.3 ± 0.7 (2) | 0.8 ± 0.6 (3) |
| *Orange* | 0.9 ± 0.4 (16) | 0.6 ± 0.3 (7) | 2.4 ± 0.8 (9) | 1.3 ± 0.9 (7) |
| Turnip Bulb | < 0.4 (9) | 2.2 ± 2.5 (2) | 1.6 ± 1.3 (5) | < 0.4 (2) |
| Turnip Leaf | < 0.4 (13) | 1.9 ± 2.1 (2) | 1.1 ± 0.7 (6) | < 0.4 (3) |
| Beetroot Bulb | 0.9 ± 0.4 (22) | 0.7 ± 0.4 (13) | 1.9 ± 1.0 (15) | 0.8 ± 0.3 (11) |
| *Bulls Blood* | 0.9 ± 0.5 (4) | 0.9 ± 0.3 (4) | 2.2 ± 0.8 (3) | 0.6* |
| *Chioggia* | 1.1 ± 0.5 (6) | NA | 2.0 ± 0.3 (4) | 0.8 ± 0.6 (2) |
| *Detroit* | 0.8 ± 0.4 (7) | 0.8 ± 0.5 (6) | 1.8 ± 1.5 (5) | 0.8 ± 0.2 (5) |
| *Albino* | 0.7 ± 0.4 (5) | 0.6 ± 0.3 (3) | 1.6 ± 1.0 (3) | 0.9 ± 0.3 (3) |
| Beetroot Leaf | < 0.4 (21) | < 0.4 (11) | 1.4 ± 1.4 (14) | 0.4 ± 0.1 (13) |
| *Bulls Blood* | < 0.4 (4) | < 0.4 (4) | 2.5 ± 2.8 (3) | < 0.4 (2) |
| *Chioggia* | < 0.4 (5) | NA | 1.3 ± 0.6 (5) | < 0.4 (2) |
| *Detroit* | < 0.4 (8) | < 0.4 (5) | 1.0 ± 1.0 (4) | 0.4 ± 0.1 (7) |
| *Albino* | < 0.4 (4) | < 0.4 (2) | 0.7 ± 0.4 (2) | < 0.4 (2) |
| Tomato | 0.5 ± 0.3 (8) | NA | 2.3* | < 0.4* |
| Pepper | < 0.4* | NA | < 0.4* | < 0.4* |
| Potato | 0.6 ± 0.2 (13) | 0.5 ± 0.1 (3) | 1.2 ± 0.4 (4) | 0.8 ± 0.3 (9) |

Note: NA; value not quantifiable as garden produce failed to grow to maturity in soil; SD, standard deviation. The XRF limit of detection is 0.4 $\mu g\ g^{-1}$ and mean values of "< 0.4" indicate chromium concentrations were all less than the laboratory limit of detection. The n value represents the total number of samples analyzed and a star indicates the value represents the concentration in a single sample. Concentrations are provided on a dry weight basis. For ease of labeling, common produce names are used, except for denoting cultivars in italics. Beetroots are referred to by their cultivar name (var. Bulls Blood; var. Chioggia; var. Detroit; var. Albino). Carrots are referred to by pigment color where "White" corresponds to var. Lunar White, "Orange" corresponds to var. Scarlet Nantes, and "Purple" corresponds to var. Pusa Asita Black.

Table 4.5S. Definitions and model parameters for calculating the daily Pb ingestion rate of a child from consuming food, water, and soil+dust.

<u>$IR_i$ = Ingestion rate for each vector for a child</u>

| Vector | Value | Source |
|---|---|---|
| Food | 45 g d$^{-1}$ | The food vector assumes that a child only ingests Pb in produce. The ingestion rate for this vector was estimated by assuming a child eats the USDA recommended 2c of produce per day. The average mass of 2c of produce represented by chopped carrots, tomatoes, beetroots, turnip, and potato was calculated based on tabulated data (Aqua-Calc 2019), which were in general agreement with measurements made in this study. The mass of 2c of vegetables was converted to dry weight based on an assumed 85% water content. |
| Water | 0.305 L d$^{-1}$ | Average daily intake rate of each vector for children age 1 to 6 years calculated based on data by (Moya, Phillips, and Schuda 2011). |
| Soil+Dust | 80 mg d$^{-1}$ | |

Note: the mass ingested per day of soil and food is provided in dry weight.

<u>$C_i$ = Concentration of Pb in each vector</u>

| Scenario | Vector | | |
|---|---|---|---|
| | $C_{food}$ (µg g$^{-1}$, dw) | $C_{water}$ (µg L$^{-1}$) | $C_{soil+dust}$ (µg g$^{-1}$, dw) |
| Scenario 1 | 0.037 | 4.5 | 4.5 |
| Scenario 2 | | | 5,950 |
| Scenario 3 | 0.4 | 4.5 | 5,950 |
| Scenario 4 | 10.7 | | |
| Scenario 5 | 15.5 | | |
| Scenario 6 | 7.2 | 4.5 | 5,950 |
| Scenario 7 | 1.4 | | |
| Scenario 8 | | 15 | |
| Scenario 9 | 0.4 | 15 | 400 |
| Scenario 10 | | 26.8 | |

Note: dw, the concentration of Pb is expressed on a dry weight basis.

**$C_{food}$.** The mean concentration of Pb (5.5 ± 2.6 ug kg-1; n=472) in raw commercial produce (see Figure 4.3S and Table 4.6S) was calculated on a wet-weight basis using data from (US Food and Drug Administration 2018) where the limit of detection was used when the

concentration was reported as zero. The mean concentration was converted to dry weight by assuming a water content of 85% and the value is used as Cfood in Scenarios 1 and 2. The mean Pb concentration in produce grown in commercial topsoil was calculated and used as Cfood in Scenarios 3 and 8-10. The mean Pb concentration in produce grown in soil from Residence 1 was calculated and used as Cfood in Scenarios 4. Vegetables grown in soils from Residence 1 used to calculate the average Pb concentration in root crops (Scenario 5) include radish, carrot cultivars, turnip, and beetroot cultivars; vegetables used to calculate the average Pb concentration in root crop leaves (Scenario 6) include turnip and beetroot cultivars; and vegetables used to calculate the average Pb concentration in non-root crops (Scenario 7; see Figure 4.4S) include tomato, pepper, potato.

$C_{water}$. Mean concentration of Pb in tap water as measured by Milwaukee Water Works (2017) (see Figure 4.5S) and calculated for this study based on accessible data from 2014 and 2017 (Scenarios 1-8). USEPA Action Level for Pb in Scenario 9 per (USEPA 2019). Water quality from Flint, Michigan in Scenario 10 is the reported 90th percentile (n=268) of samples collected in August 2015 per (Pieper et al. 2018).

$C_{soil+dust}$. Mean concentration of Pb in soil at Residence 1 and Commercial Topsoil per Figure 4.1. USEPA regional screening level for direct contact at residential properties (USEPA 2019b).

Table 4.6S. Foods included in the "Raw Produce" classification from the USFDA TDS used to model Pb exposure in children.

| Food Name | (n) |
|---|---|
| Carrot, baby, raw | 59 |
| Celery, raw | 59 |
| Cucumber, peeled, raw | 59 |
| Lettuce, iceberg, raw | 59 |
| Lettuce, leaf, raw | 59 |
| Onion, mature, raw | 59 |
| Pepper, sweet, green, raw | 59 |
| Tomato, raw | 59 |

Note. Data from 2003-2016 USFDA TDS (US Food and Drug Administration 2018). The mean concentration of Pb in raw commercial produce ($5.5 \pm 2.6$ μg kg$^{-1}$; n=472) was calculated on a wet-weight basis using data from (US Food and Drug Administration 2018) where the limit of detection was used when the concentration was reported as zero. The mean concentration was converted to dry weight by assuming a water content of 85% and the value is used as $C_{food}$ in Scenarios 1 and 2 (see Table 4.3 and Table 4.5S).

# 5.0  DISCUSSION

## 5.1  EVALUATION OF PROJECT OBJECTIVES

**Objective 1.** As expected, 85 percent of measurements made in Chapter 2 when compared to NIST certified, reference, and information values were within a control limit of ± 20 % RD. Further, Chapter 2 describes the variability in concentrations of up to 49 elements (plus LOI) and provides values for up to 21 elements previously uncharacterized by NIST in these soil SRMs. The additional characterization provided in this investigation was used to reduce the measurement uncertainty in custom calibration routines and improve the quality of control checks developed using these NIST SRMs. Using the characterized SRMs, measurement and calibration routines for quantification of heavy metals with XRF were built.

**Objective 2.** By managing matrix effects, XRF is shown in Chapter 3 to be a useful tool in quantification of Pb and other heavy metals in produce. In addition to measuring samples and reference materials under the same conditions (e.g. energy, current, filter, count time, atmosphere), the most critical factors to be managed in developing measurement routines for quantification of heavy metals in plant tissues with WD-XRF and portable ED-XRF are:

1.  Developing reference materials with commutability to samples and maintaining consistency with sample preparation/handling (e.g. drying time, milling time, sample mass),

2.  Selecting proper wavelengths to eliminate peak overlaps and controlling for possible enhancement from within the matrix or from characteristic X-rays generated by the shielding/housing,

3.  Irradiating samples for long enough to maximize accuracy and precision, and

4.      Confirming the viability of new routines for actual samples through paired analysis of samples with another quantification technology to provide additional assurance in the measurement and calibration routines.

**Objective 3.** This study described in Chapter 4 confirms significant variation in the quality of urban soils and in the corresponding concentration of Pb accumulated in consumable crop tissues. Produce grown in metals-rich soil accumulated Pb in consumable tissues at concentrations significantly greater than identical fresh produce purchased from commercial sources. Pb concentrations were the greatest in taproot vegetables, with decreasing trends in aboveground biomass. Pb concentrations in primary consumable tissues followed this trend: radish > carrots > turnip > beetroot > tomato > pepper > potato. Pb accumulation in pigment rich cultivars did not follow the expected trend, with the greatest Pb concentrations in white carrots, with lesser concentrations in orange carrots.

The accumulation of Pb in produce is related to the bioavailability of Pb in soil; however, the relationship between bioavailable Pb in soil and Pb accumulated in consumable produce varies by crop type. Therefore, it is critical to measure Pb directly in consumable tissues for an accurate estimation of child Pb exposure.

Replacement of metals-rich urban soils with commercial topsoil of better quality or growing non-root crops in metals rich soil are confirmed as best management practices to reduce the risk of Pb exposure. Additionally, peeling vegetables grown belowground in metals-rich soil will further reduce Pb exposure risk; however, the reduction in risk depends on produce type. Children consuming produce grown in metals-rich urban soil and in replacement topsoil could be at increased risk for Pb exposure; however, children are also possibly at a risk of Pb exposure from consuming commercial produce from a grocery store.

**Objective 4.** As described in the study in Chapter 4, the concentrations of Pb in domestically-grown vegetables was less than the XRF detection limit. Concentrations of Pb in internationally-sourced foods were greater than the XRF detection limit; however, concentrations could not be confirmed suggesting the possibility of significant variability of Pb in commercially sourced foods.

## 5.2 FUTURE WORK

**Future Work on Compartmentalization of Pb with Micro-XRF**

The vast majority of studies contributing to the current understanding of Pb uptake/transport/accumulation at the cellular level grew plants in hydroponic solutions with Pb-nitrate. These laboratory studies, though useful, do not necessarily represent realistic growing conditions and therefore much remains unknown as to the basic physiology of Pb accumulation in crops grown in metals-rich soils. With the recent advancements in micro-XRF, the potential now exists to measure Pb in specific regions of plant tissues at the cellular-level at single-digit concentrations. Future work with micro-XRF could be useful in confirming if the accumulation of Pb in crops occurs more prominently in specific areas of plant tissues, or if accumulation is more homogenous. For example, if plants are accumulating Pb in tissues that are indigestible and therefore Pb passes through the digestive system unaltered, then the risk to children from consuming produce described in this study may be overly conservative.

The pilot study described in Appendix B suggests the Casparian strip may be especially critical in Pb accumulation in taproot crops. Micro-XRF would be particularly useful in further evaluating the role of the Casparian strip in tap-root crops grown in realistic scenarios.

153

**Use of ED-XRF and TR-XRF in Food Security Applications**

Although this study is able to predict 65% of the variability of Pb accumulated in produce grown in metals-rich soils, directly measuring Pb in produce is the most accurate way to assess the risk to children form consumption of foods. This study shows that portable ED-XRF instrumentation is capable of achieving limits of detection in the ranges of health-based food standards. More recent ED-XRF and Total Reflection XRF (TR-XRF) advancements have addressed many of the initial instrumentation issues limiting the limits of detection. As these techniques are further developed, the applicability of these measurement methods in food security will only increase.

This study attempted to use ED-XRF to directly measure Pb in produce coarsely homogenized with a commercial hand-held food processor. As noted in Chapter 3, the study was successful in developing measurement and calibration routines using a library of reference materials containing 85% water. However, this study faced several significant obstacles when trying to use the measurement routine on actual produce samples. Most root-crop and fruit samples could be successfully homogenized; however, the water content of the samples diluted the concentration of Pb atoms per unit volume to the point the limit of detection became an issue. To overcome this challenge in the future, one possibility would be to spin the homogenized sample in a portable centrifuge after homogenization to concentrate the solid phase of the sample which could then be packed in an ED-XRF capsule for analysis. This approach would require a pilot study to quantify if significant concentrations of Pb are present in the liquid phase.

**Best Management Practices to Lower Child Exposure to Pb**

One of the more fascinating observations from this study is the proportion of Pb ingested by children per day from food. Initial work by others suggested ingestion of Pb from food was

not a pathway of significant concern. Our work suggests that for an average child, after addressing significant soil impacts at residential properties, water quality should not be addressed until food quality is maximized. This is opposite of recent trends where communities are under increasing pressure to replace Pb water laterals. Further study on the cost/benefit from community-initiated projects is warranted so the greatest positive health outcomes are realized.

APPENDICES

# Appendix A: Development of a GLM to Predict Pb in Produce

**Background**

  Prior work has attempted to predict the concentration of Pb in produce from the concentration of Pb in soil. However, due to the heterogenous and anisotropic nature of urban soils, prior models have failed to accurately predict Pb accumulated in produce.

**Methods**

  Using model factors in this study, a GLM was developed to predict accumulation of Pb. The following model factors were initially included, then the model revised as summarized in the following.

1.   Categorical = Vegetable (Carrot-Orange; Carrot-Purple ; Carrot-Orange ; Beet-Bulls Blood; Beet-Chioggia; Beet-White; Beet-Detroit; Pepper; radish; Potato; Tomato; Turnip-Bulb; Turnip-Leaf; Beet-Bulls Blood-Leaf; Beet-Chioggia-Leaf; Beet-White-Leaf; Beet-Detroit-Leaf)

2.   Categorical = Soil Source (Site 8, Site 11, Foundry, Home Depot)

3.   Continuous = several soil chemistry parameters (pH, CEC, Bioavailable Elements [Ca, Cd, Cr, K, Mg, Mn, Ni, P, Pb, S, Zn, Cu, Fe, P, Zn])

  **Preprocessing.** Preprocessing included letting the LOD represent cases where the measured Pb concentration was less than the LOD ($0.3$ $\mu g$ $g^{-1}$, dw). Three outliers were removed.

  **Mediation.** The first refinement of the model was to determine if mediation was possible between bioavailable Cd and bioavailable Pb in the soil (Table A.1) or between bioavailable Zn and bioavailable Pb in the soil (Table A.2).

157

| SAS Code | Result |
|---|---|
| model1: model Plant_pb=pb | p< 0.001 |
| model2: model cd=pb | P=0.89 |
| model3: model Plant_pb=cd pb | p< 0.01 cd = 0.4450 |

Table A.1. SAS model to determine if Mediation was possible between Cd and Pb

Use Sobel bootstrap = 1,000

| | | bt | | | | |
|---|---|---|---|---|---|---|
| | Mean | s.e. | LL 95 CI | UL 95 CI | LL 99 CI | UL 99 CI |
| Effect | 0.0000 | 0.0001 | -0.0003 | 0.0003 | -0.0004 | 0.0005 |

As zero is within the Upper and Lower 95% CI, you can say with 95% CONFIDENCE that mediation is **not** considered significant between Pb and Cd

| SAS Code | Result |
|---|---|
| model1: model Plant_pb=pb | p< 0.001 |
| model2: model zn=pb | P=.643 |
| model3: model Plant_pb=zn pb | p< 0.01 zn = 0.34 |

Table A.2. SAS model to determine if Mediation was possible between Zn and Pb

Use Sobel bootstrap = 1,000

| | | bt | | | | |
|---|---|---|---|---|---|---|
| | Mean | s.e. | LL 95 CI | UL 95 CI | LL 99 CI | UL 99 CI |
| Effect | 0.0001 | 0.0002 | -0.0002 | 0.0005 | -0.0004 | 0.0007 |

As zero is within the Upper and Lower 95% CI, you can say with 95% CONFIDENCE that mediation is **not** considered significant between Pb and Zn

158

**Multicollinearity.** Multicollinearity was evaluated between continuous soil predictors to determine which predictors should be removed (Table A.3). Variance inflation factors (VIF) greater than 10 suggests a predictor may have multicollinearity. The initial model suggests removing Ca, Cu, P. When done, the revised model suggests multicollinearity is no longer an issue.

| Table A.3. Evaluation of Multicollinearity |
| --- |
| model Plant_Pb=pH CEC Ca Cd Cr Cu Fe K Mg Mn Na Ni P Pb S Zn/vif tol collin scorr2 pcorr2; |
| Initial Model |

**Parameter Estimates**

| Variable | DF | Parameter Estimate | Standard Error | t Value | Pr > \|t\| | Squared Semi-partial Corr Type II | Squared Partial Corr Type II | Tolerance | Variance Inflation |
| --- | --- | --- | --- | --- | --- | --- | --- | --- | --- |
| Intercept | 1 | -32.96996 | 59.38884 | -0.56 | 0.5794 | . | . | . | 0 |
| pH | 1 | 4.01734 | 7.41378 | 0.54 | 0.5885 | 0.00112 | 0.00155 | 0.19223 | 5.20198 |
| CEC | 1 | 40.92036 | 50.65540 | 0.81 | 0.4202 | 0.00249 | 0.00344 | 0.00000457 | 218918 |
| Ca | 1 | -0.20674 | 0.25371 | -0.81 | 0.4162 | 0.00254 | 0.00350 | 0.00000631 | 158353 |
| Cd | 1 | -1.92117 | 6.23865 | -0.31 | 0.7585 | 0.00036220 | 0.00050150 | 0.05754 | 17.37835 |
| Cr | 1 | 6.10431 | 5.42962 | 1.12 | 0.2623 | 0.00483 | 0.00664 | 0.20567 | 4.86225 |
| Cu | 1 | -0.11153 | 0.18652 | -0.60 | 0.5506 | 0.00137 | 0.00189 | 0.04280 | 23.36701 |
| Fe | 1 | -0.04858 | 0.06460 | -0.75 | 0.4530 | 0.00216 | 0.00298 | 0.06333 | 15.79093 |
| K | 1 | -0.09293 | 0.13312 | -0.70 | 0.4860 | 0.00186 | 0.00257 | 0.01079 | 92.69037 |
| Mg | 1 | -0.32019 | 0.42173 | -0.76 | 0.4487 | 0.00220 | 0.00304 | 0.00007016 | 14253 |
| Mn | 1 | -0.18085 | 0.12213 | -1.48 | 0.1403 | 0.00837 | 0.01147 | 0.24963 | 4.00600 |
| Na | 1 | -0.17998 | 0.21647 | -0.83 | 0.4068 | 0.00264 | 0.00364 | 0.00350 | 285.47011 |
| Ni | 1 | 0.70478 | 0.88704 | 0.79 | 0.4279 | 0.00241 | 0.00333 | 0.11489 | 8.70407 |
| P | 1 | -0.04797 | 0.09484 | -0.51 | 0.6135 | 0.00097738 | 0.00135 | 0.04727 | 21.15698 |
| Pb | 1 | 0.02624 | 0.00931 | 2.82 | 0.0054 | 0.03032 | 0.04031 | 0.12734 | 7.85278 |
| S | 1 | -0.03838 | 0.10567 | -0.36 | 0.7168 | 0.00050391 | 0.00069757 | 0.13947 | 7.16980 |
| Zn | 1 | 0.01498 | 0.01331 | 1.13 | 0.2616 | 0.00484 | 0.00666 | 0.10511 | 9.51426 |

Revised Model

| | | | | | | | | | |
|---|---|---|---|---|---|---|---|---|---|
| **Parameter Estimates** | | | | | | | | | |
| Variable | DF | Parameter Estimate | Standard Error | t Value | Pr > \|t\| | Squared Semi-partial Corr Type II | Squared Partial Corr Type II | Tolerance | Variance Inflation |
| Intercept | 1 | -25.85531 | 42.26869 | -0.61 | 0.5415 | . | . | . | 0 |
| pH | 1 | 3.10656 | 5.16894 | 0.60 | 0.5485 | 0.00137 | 0.00188 | 0.39294 | 2.54495 |
| CEC | 1 | -0.46732 | 0.35301 | -1.32 | 0.1871 | 0.00665 | 0.00905 | 0.09346 | 10.70013 |
| Cd | 1 | -1.65385 | 4.22665 | -0.39 | 0.6960 | 0.00058105 | 0.00079681 | 0.12456 | 8.02802 |
| Cr | 1 | 3.15254 | 4.70320 | 0.67 | 0.5035 | 0.00171 | 0.00233 | 0.27235 | 3.67176 |
| Fe | 1 | -0.03238 | 0.05088 | -0.64 | 0.5253 | 0.00154 | 0.00210 | 0.10145 | 9.85664 |
| K | 1 | 0.01166 | 0.01726 | 0.68 | 0.5004 | 0.00173 | 0.00237 | 0.63732 | 1.56908 |
| Mg | 1 | 0.02154 | 0.00687 | 3.13 | 0.0020 | 0.03727 | 0.04867 | 0.26251 | 3.80937 |
| Mn | 1 | -0.16936 | 0.11554 | -1.47 | 0.1444 | 0.00815 | 0.01107 | 0.27711 | 3.60861 |
| Na | 1 | -0.00164 | 0.02900 | -0.06 | 0.9550 | 0.00001214 | 0.00001666 | 0.19397 | 5.15534 |
| Ni | 1 | 0.68323 | 0.83287 | 0.82 | 0.4130 | 0.00255 | 0.00349 | 0.12949 | 7.72284 |
| Pb | 1 | 0.02738 | 0.00745 | 3.68 | 0.0003 | 0.05130 | 0.06577 | 0.19796 | 5.05150 |
| S | 1 | -0.02209 | 0.10014 | -0.22 | 0.8256 | 0.00018467 | 0.00025337 | 0.15434 | 6.47937 |
| Zn | 1 | 0.00782 | 0.01166 | 0.67 | 0.5034 | 0.00171 | 0.00234 | 0.13603 | 7.35110 |

**Initial Bivariate Regression Model.** Similar to work attempted by others in the literature (though prior work used total Pb in soil), the initial model was a simple linear regression between plant Pb and bioavailable Pb in soil (Table A.4).

| Table A.4. Bivariate regression model between bioavailable Pb in soil and Pb in consumable produce | |
|---|---|
| proc reg data=veg; model1: model Plant_Pb=Pb; run; | **Analysis of Variance** <br><br> Source, DF, Sum of Squares, Mean Square, F Value, Pr > F <br> Model, 1, 6212.68876, 6212.68876, 82.89, <.0001 <br> Error, 255, 19112, 74.94747 <br> Corrected Total, 256, 25324 <br><br> Root MSE, 8.65722, R-Square, 0.2453 <br> Dependent Mean, 6.12187, Adj R-Sq, 0.2424 <br> Coeff Var, 141.41455 |

**Second Bivariate Regression Model.** The initial model indicates that bioavailable Pb in soil can predict 25% of the variability in Pb accumulated in produce. This suggests further revision of the model is warranted. A second model was built by adding all predictors summarized on Table A.3.

| Table A.5. Revised regression model to predict Pb in consumable produce | |
|---|---|
| proc reg data=veg;<br><br>model1: model Plant_Pb=Pb pH CEC Cd Cr Fe K Mg Mn Na Ni S Zn/solution;<br><br>run; | **Analysis of Variance**<br><br>| Source | DF | Sum of Squares | Mean Square | F Value | Pr > F |<br>|---|---|---|---|---|---|<br>| Model | 13 | 6302.39955 | 484.79997 | 5.50 | <.0001 |<br>| Error | 192 | 16923 | 88.14155 | | |<br>| Corrected Total | 205 | 23226 | | | |<br><br>| Root MSE | 9.38837 | R-Square | 0.2714 |<br>|---|---|---|---|<br>| Dependent Mean | 7.54322 | Adj R-Sq | 0.2220 |<br>| Coeff Var | 124.46107 | | | |

Some parameters have a high p-value suggesting they contribute little to the prediction of Pb in consumable plant tissues. However, this model only predicts 27% of variability in Pb in consumable tissues. Suggesting further revision of the model is necessary; regardless of the p-value of individual predictors.

**Initial GLM Model.** To add categorical predictors ("Vegetable" and "Soil") to the model, a GLM is needed (Table A.6).

Table A.6. Initial GLM to predict Pb in produce

```
proc glm data=veg;

class vegetable soil;

model1: model Plant_Pb=pb vegetable

soil pH CEC Cd Cr Fe K Mg Mn Na Ni

Zn/solution;

run;
```

| Source | DF | Sum of Squares | Mean Square | F Value | Pr > F |
|--------|-----|----------------|-------------|---------|--------|
| Model | 31 | 12530.21866 | 404.20060 | 6.58 | <.0001 |
| Error | 174 | 10695.35804 | 61.46757 | | |
| Corrected Total | 205 | 23225.57670 | | | |

| R-Square | Coeff Var | Root MSE | Plant_Pb Mean |
|----------|-----------|----------|---------------|
| 0.539501 | 103.9361 | 7.840126 | 7.543221 |

| Source | DF | Type I SS | Mean Square | F Value | Pr > F |
|--------|-----|-----------|-------------|---------|--------|
| Pb | 1 | 4119.067518 | 4119.067518 | 67.01 | <.0001 |
| Vegetable | 15 | 6503.233144 | 433.548876 | 7.05 | <.0001 |
| Soil | 3 | 191.755634 | 63.918545 | 1.04 | 0.3763 |
| pH | 1 | 17.523344 | 17.523344 | 0.29 | 0.5941 |
| CEC | 1 | 31.650387 | 31.650387 | 0.51 | 0.4740 |
| Cd | 1 | 91.031863 | 91.031863 | 1.48 | 0.2253 |
| Cr | 1 | 3.559431 | 3.559431 | 0.06 | 0.8101 |
| Fe | 1 | 646.070682 | 646.070682 | 10.51 | 0.0014 |
| K | 1 | 23.039077 | 23.039077 | 0.37 | 0.5412 |
| Mg | 1 | 825.206278 | 825.206278 | 13.43 | 0.0003 |
| Mn | 1 | 58.060332 | 58.060332 | 0.94 | 0.3325 |
| Na | 1 | 5.469383 | 5.469383 | 0.09 | 0.7658 |
| Ni | 1 | 6.258399 | 6.258399 | 0.10 | 0.7500 |
| S | 1 | 1.854266 | 1.854266 | 0.03 | 0.8623 |
| Zn | 1 | 6.438920 | 6.438920 | 0.10 | 0.7466 |

By adding the two categorical predictors, the initial GLM model predicts 54% of the variability in accumulated Pb; however, further revision is warranted.

**Revised GLM Model.** To add an interaction between predictors, and to set a reference for Soil and Vegetable, further revision of the GLM is warranted (Table A.7). To make the simple slopes valuable, the bioavailable Pb in soil was mean-centered

| Table A.7. Revised GLM | |
|---|---|
| proc glm data=vegcentered;<br><br>class vegetable (ref='Potato')<br><br>soil (ref='Site 11');<br><br>mode4: model Plant_Pb<br><br>=vegetable soil cPb<br><br>cpb*vegetable CEC Cd Cr<br><br>Mg Zn/solution;<br><br>LSmeans vegetable / Adjust<br><br>= tukey;<br><br>run; | (see tables below) |

| Source | DF | Sum of Squares | Mean Square | F Value | Pr > F |
|---|---|---|---|---|---|
| Model | 39 | 15152.21028 | 388.51821 | 7.99 | <.0001 |
| Error | 166 | 8073.36642 | 48.63474 | | |
| Corrected Total | 205 | 23225.57670 | | | |

| R-Square | Coeff Var | Root MSE | Plant_Pb Mean |
|---|---|---|---|
| 0.652393 | 92.45203 | 6.973861 | 7.543221 |

Why keep these predictors:

CEC = this represents the cation exchange potential for this soil and should account for all possible sorption sites (e.g. organic material, Fe oxides, etc.). Therefore, Fe is not needed

Cd/Zn = these are the channels that Pb uses to enter plant, so keep these

Cr = The pb in paint is often bound with $CrO_4$; therefore, Pb is inherently linked to Cr

Mg = divalent cation, not sure why significant.

163

This combination of predictors predicts 65% of variability in Pb in consumable plant tissues. Partial slopes are provided on Table A.8.

Table A.8. Slope estimates from final GLM

| | | | | | |
|---|---|---|---|---|---|
| Intercept | 1.00459091 | B | 6.38229667 | 0.16 | 0.8751 |
| Vegetable Beet - Bulls Blood | 5.48544661 | B | 2.68906493 | 2.04 | 0.0429 |
| Vegetable Beet - Chioggia | 4.62921684 | B | 3.12411064 | 1.48 | 0.1403 |
| Vegetable Beet - Chioggia-L | 4.03552806 | B | 3.08635291 | 1.31 | 0.1928 |
| Vegetable Beet - Detroit | 1.40452661 | B | 2.73525239 | 0.51 | 0.6083 |
| Vegetable Beet - Detroit-L | 3.64720615 | B | 2.80345447 | 1.30 | 0.1951 |
| Vegetable Beet - White | 1.01124467 | B | 3.20855740 | 0.32 | 0.7530 |
| Vegetable Beet - White-L | 5.35541118 | B | 3.50938755 | 1.53 | 0.1289 |
| Vegetable Carrot - Orange | 9.46555218 | B | 2.41035827 | 3.93 | 0.0001 |
| Vegetable Carrot - Purple | 11.25455384 | B | 3.05071412 | 3.69 | 0.0003 |
| Vegetable Carrot - White | 15.75778528 | B | 2.82126356 | 5.59 | <.0001 |
| Vegetable Pepper | 0.67049215 | B | 5.46324317 | 0.12 | 0.9025 |
| Vegetable Radish | 9.74583884 | B | 3.62271721 | 2.69 | 0.0079 |
| Vegetable Tomato | 1.40784517 | B | 3.74289252 | 0.38 | 0.7073 |
| Vegetable Turnip-Bulb | 11.13512981 | B | 2.61654522 | 4.26 | <.0001 |
| Vegetable Turnip-Leaf | 4.52749533 | B | 2.49720362 | 1.81 | 0.0716 |
| Vegetable Potato | 0.00000000 | B | . | . | . |
| Soil Foundry | 2.41246083 | B | 3.42417437 | 0.70 | 0.4821 |
| Soil Home De | -2.20937675 | B | 6.75814404 | -0.33 | 0.7441 |
| Soil Site 8 | 1.03502453 | B | 2.38189006 | 0.43 | 0.6645 |
| Soil Site 11 | 0.00000000 | B | . | . | . |
| Cpb | 0.00936196 | B | 0.00996862 | 0.94 | 0.3490 |
| Cpb*Vegetable Beet - Bulls Blood | 0.02516735 | B | 0.01108391 | 2.27 | 0.0245 |
| Cpb*Vegetable Beet - Chioggia | 0.02931123 | B | 0.01430972 | 2.05 | 0.0421 |
| Cpb*Vegetable Beet - Chioggia-L | 0.01611206 | B | 0.01397114 | 1.15 | 0.2505 |
| Cpb*Vegetable Beet - Detroit | 0.00579263 | B | 0.01346552 | 0.43 | 0.6676 |
| Cpb*Vegetable Beet - Detroit-L | 0.00526530 | B | 0.01367444 | 0.39 | 0.7007 |
| Cpb*Vegetable Beet - White | -0.00091282 | B | 0.01694266 | -0.05 | 0.9571 |
| Cpb*Vegetable Beet - White-L | -0.00475923 | B | 0.01774034 | -0.27 | 0.7888 |
| Cpb*Vegetable Carrot - Orange | 0.03198305 | B | 0.01107269 | 2.89 | 0.0044 |
| Cpb*Vegetable Carrot - Purple | 0.04377116 | B | 0.01868734 | 2.34 | 0.0204 |
| Cpb*Vegetable Carrot - White | 0.06879825 | B | 0.01458138 | 4.72 | <.0001 |
| Cpb*Vegetable Pepper | -0.00830689 | B | 0.03958568 | -0.21 | 0.8340 |
| Cpb*Vegetable Radish | 0.06938311 | B | 0.01590217 | 4.36 | <.0001 |
| Cpb*Vegetable Tomato | -0.00232139 | B | 0.03236333 | -0.07 | 0.9429 |
| Cpb*Vegetable Turnip-Bulb | 0.06011842 | B | 0.01500940 | 4.01 | <.0001 |
| Cpb*Vegetable Turnip-Leaf | 0.02218687 | B | 0.01431758 | 1.55 | 0.1231 |
| Cpb*Vegetable Potato | 0.00000000 | B | . | . | . |
| CEC | -0.57477231 | | 0.19927764 | -2.88 | 0.0044 |
| Cd | -3.54965759 | | 3.20925896 | -1.11 | 0.2703 |
| Cr | -2.54587638 | | 4.09558492 | -0.62 | 0.5350 |
| Mg | 0.01770003 | | 0.00577405 | 3.07 | 0.0025 |
| Zn | 0.00879673 | | 0.00675798 | 1.30 | 0.1948 |

# Appendix B: Accumulation of Pb in Carrots

## Background

Lead (as $Pb^{+2}$) is thought to primarily enter the root hair and pass through the cortex of plant roots through bulk flow of water using the apoplast pathway. Pb can continue through the apoplast pathway until it reaches the Casparian Strip, at which point, Pb must enter the symplast pathway to continue to the stele. Prior work using scanning electron microscopy has shown that plants could precipitate Pb on the cortex side of the Casparian Strip to prevent entry of Pb into the stele. However, prior work evaluating root was completed using hydroponic growing methods. Therefore, an evaluation of modified taproots grown in garden conditions is warranted to determine if Pb is concentrated in the cortex.

## Methods

Taproots of seven orange carrots grown in metals-rich soil as part of the 2016 growing season were harvested and processed as described in Chapter 4. A sharp knife was used to break the outer portion of the cortex from the inner portion of the root (assumed to be the stele). It is assumed that this break occurs at the Casparian Strip. The physiology of the carrot is illustrated on Figure B.1a.

Both the inner and outer portions of the taproot were dried and Pb concentrations determined with WD-XRF (n=14) as described in Chapter 4. The mean concentrations of Pb in each tissue group are illustrated on Figure B.1b.

<table>
<tr><td>

Figure B.1a. Physiology of carrot taproot.



</td><td>

Figure B.1b. Mean concentration of Pb ($\mu$g g$^{-1}$ dw) in carrot taproot tissues.



</td></tr>
</table>
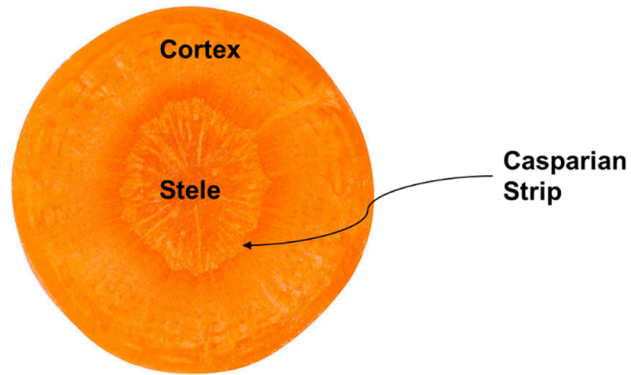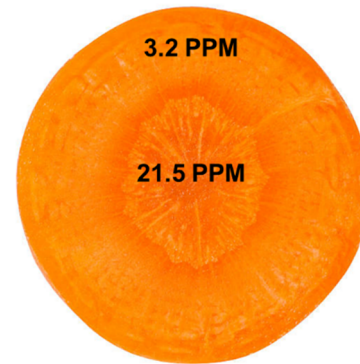
A matched-paired analysis was completed in JMP (SAS Institute; Cary, NC) to determine if the concentrations were significantly different between the tissue groups (Figure B.2).

Figure B.2. Matched-pair statistical analysis of Pb in two tissue groups



| | | | |
|---|---|---|---|
| Cortex | 3.23475 | t-Ratio | -2.87602 |
| Stele | 21.4647 | DF | 6 |
| Mean Difference | -18.23 | Prob > |t| | 0.0282* |
| Std Error | 6.3386 | Prob > t | 0.9859 |
| Upper 95% | -2.7199 | Prob < t | 0.0141* |
| Lower 95% | -33.74 | | |
| N | 7 | | |
| Correlation | 0.92089 | | |

www.manaraa.com
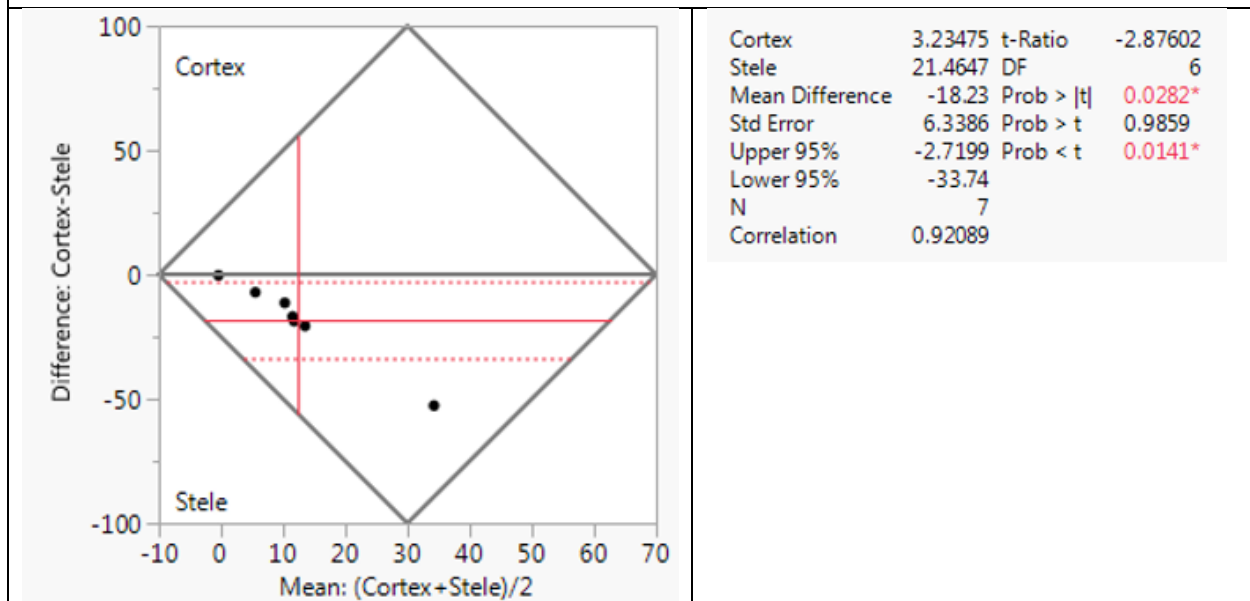
**Conclusions**

The concentration of Pb in the center tissue was greater than the concentration in the outer tissue (t = -2.87, DF=6, p < 0.01). This supports the understanding that Pb is not uniformly distributed within the taproot but appears to concentrate towards the stele. However, we had expected Pb to accumulate in the cortex and had expected the concentration of Pb in the stele to be less than detection limits. The results are backwards of the expected trend. One explanation for this is the taproot did not break cleanly at the Casparian Strip, but instead broke further into the cortex; thus not clearly separating the cortex from the stele.

Recent advances in micro-XRF spectroscopy have allowed for µm resolution on measurements. Therefore, this investigation could be repeated to determine at the cellular level if Pb-rich regions are identifiable in a carrot taproot cross-section. The difficulty in using micro-XRF is developing reference materials with enough homogeneity for quantification purposes. Specific focus should be placed in the area separating the apparent cortex from the stele.

## Appendix C: Pb Accumulation in Commercial Prepared Foods

**Background**

As a considerable amount of pre-packaged ready-to-eat foods (e.g. candy, snacks, fruit, etc.) are processed/packaged in Southeast Asia, significant concern has been expressed as to the integrity/quality of these foods. Of specific concern, prior work has identified the presence of Pb in select canned foods readily fed to children, such as Mandarin Oranges and other packaged fruits. Further, recent work has identified Pb in spices and other foods originating from Asia. Therefore a study is warranted to determine if techniques developed in Chapter 3 can be used to evaluate Pb in commercial-sourced foods.

**Methods**

A variety of pre-packaged foods were purchased from grocery stores in Milwaukee, Wisconsin and processed as follows:

- **Metal Cans.** Metal cans were opened with a stainless steel can opener and the contents drained through a kitchen strainer to remove packaging liquid.

- **Glass Jars**. Glass jars were opened and the contents drained through a kitchen strainer to remove packaging liquid.

- **Plastic Cups.** Plastic cups were opened and the contents drained through a kitchen strainer to remove packaging liquid.

- **Loose/Dried.** Foods that were dried or purchased loose (e.g. candy, sushi wrappers, spices) were removed from packaging for processing.

All food samples were processed and the concentration of Pb measured with WD-XRF as described in Chapter 4.

**Results and Conclusions**

Significant difficulty was encountered in preparing pressed pellets of samples high in fat (e.g. select snacks, chocolate). Additionally, samples high in sugar content tended to warp during analysis with WD-XRF suggesting heat generated during the measurement routine compromised the integrity of the sample. Pressed pellets of samples preserved with vinegar (e.g. pickled beets, pickled ginger) tended to be fragile and did not handle well. Pressed pellets of sushi wrappers were very fragile and often did not resist handling. Therefore, a large number of samples collected in this study could not be analyzed with WD-XRF (Table C.1).

The LOD was 0.3 ug g$^{-1}$ and the LOQ was 1 ug g$^{-1}$. Pb was identified in several commercially-sourced goods (Table C.2); however, apparent detections could not be confirmed through additional sampling of different batches of the same food. Therefore, it is possible that Pb concentrations vary widely between manufacturers and between batches/lots. The results of this work further illustrate the need for additional work in this area and further illustrate the value in the use of a quick portable quantification instrument, such as a portable ED-XRF for food security studies.

Table C.1. Samples that could not be analyzed with WD-XRF due to complications with pellet

competency.

| Store | Food | Description |
|-------|------|-------------|
| Cermak | Water Chestnut | Water Chestnut |
| | Large Root | Large Root |
| | Waxy Root | Waxy Root |
| Pick-N-Save | Hello Panda | Biscuit with milk cream |
| | Hello Panda | Biscuit with coco cream |
| | Pocky | (snack stick) |
| | Yam-Yam | Stick |
| | Yam-Yam | Chocolate Dip |
| | Yam-Yam | Stick |
| | Yam-Yam | Strawberry Dip |
| | Honey Twist | (snack stick) |
| | Hi-Chew | Strawberry |
| | Hi-Chew | Apple |
| | Mandarin Oranges (store brand can) | Fruit |
| | Mandarin Oranges (Dole Can) | Fruit |
| | Mandarin Oranges (Dole Can) | Fruit |
| | Mandarin Oranges (Delmonte Can) | Fruit |
| | Mandarin Oranges (Delmonte Can) | Fruit |
| | Citrus Salad (Delmonte can) | Fruit |
| | Citrus Salad (Delmonte can) | Fruit |
| | Mandarin Oranges (Dole-plastic jar) | Fruit |
| | Mandarin Oranges (Dole-plastic jar) | Fruit |
| Sendik's | International | Seaweed (Baycliff Nori) |
| Trader Joes | International | Okra |
| Walgreens | Gimme Goo | Candy |
| | Sour Heads | Candy |
| | Hershey's Kisses Deluxe | Candy |
| | Hershey's Kisses Deluxe (wrapper) | Candy |
| | Spongebob | Candy |
| | Finding Dory Easter Egg | Lemonheads |
| | Finding Dory Easter Egg | Bracelet (all) |
| | Finding Dory Easter Egg | Bracelet (Dory Dangle) |
| | Finding Dory Easter Egg | Bracelet wrapper |
| | Mandarin Oranges (store brand can) | Fruit |
| | Mandarin Oranges (store brand can) | Fruit |

Table C.2. Concentration of Pb in commercial foods that produced a competent pellet.

| Store | Food | Pb Concentration ($\mu g\ g^{-1}$, dw) |
|---|---|---|
| Sendik's | Crystalized Ginger | 26.5 |
| Cermak | Diced Peaches | 0.5 |
| Cermak | Diced Pears | < 0.3 |
| Cermak | Dried Ginger | 0.6 |
| Asian Market | Dried seaweed | < 0.3 |
| Asian Market | Dried seaweed | < 0.3 |
| Walgreens | Finding Dory Easter Egg | < 0.3 |
| Sendik's | Fresh Ginger | 0.9 |
| Cermak | Fresh Ginger | 6.9 |
| Cermak | Green Mukhwas | < 0.3 |
| Pick-N-Save | Hi-Chew | 2.9 |
| Asian Market | Jack fruit | < 0.3 |
| Cermak | Lychee | < 0.3 |
| Cermak | Mandarin Oranges | < 0.3 |
| Pick-N-Save | Mandarin Oranges | < 0.3 |
| Cermak | Mandarin Oranges | 33.4 |
| Asian Market | Mustard in Soy | < 0.3 |
| Cermak | Pickled Beets | < 0.3 |
| Pick-N-Save | Seaweed | 21.1 |
| Cermak | Seaweed (Dried Roland) | < 0.3 |
| Cermak | Seaweed (Roasted Roland) | < 0.3 |
| Cermak | Seaweed (Yaki Nori) | < 0.3 |
| Cermak | Sushi Ginger | 1.8 |
| Asian Market | Tamarind leaves | < 0.3 |
| Asian Market | Tamarind leaves | 1.1 |
| Sendik'sra | Tamarind Stir Fry | < 0.3 |
| Asian Market | Turmeric | 1.2 |

# Appendix D: Additional Pb Accumulation Data

**Background**

Additional vegetables were grown in this study which are not discussed in Chapter 4. The produce was either limited in sample size (e.g. okra, peanuts) or the tissue group was represented by another vegetable (e.g. rutabagas). The majority of samples were part of a pilot greenhouse study, which was limited to soils from the Former Foundry and two small buckets of soil from Residence 1.

**Methods**

Vegetables grown outside the greenhouse follow methods described in Chapter 4 and heavy metal concentrations quantified as described in Chapter 3. Vegetables grown inside the greenhouse as part of the pilot study were grown under lights in a climate-controlled environment. Produce was harvested, processed, and concentrations of metals quantified similarly to Chapter 3 using pilot WD-XRF quantification routine named "Plants Pressed."

**Results**

Pb accumulated in consumable produce grown in the pilot greenhouse study (Table D.1) and in additional vegetables grown outside as part of work described in Chapter 4 (Table D.2). This work suggests a larger variety of produce could increase Pb exposure if consumed.

Table D.1. Pb concentration in vegetables grown in greenhouse pilot study.

| Soil Source | Soil Total Pb (ug g⁻¹) | Pb in Produce (ug g⁻¹, dw) | | |
|---|---|---|---|---|
| | | Turnip Bulb | Turnip Leaf | Rutabaga Bulb |
| Former Foundry | 724 | 0.1 | – | 0.3 |
| | 753 | 0.1 | – | 0.3 |
| | 1300 | 0.2 | 0.2 | 0.3 |
| | 1500 | 0.1 | 0.3 | 0.3 |
| | 1700 | 0.3 | 0.3 | 0.3 |
| | 1800 | 5.7 | 2.8 | 0.3 |
| | 1800 | 2.1 | – | 0.3 |
| | 1800 | 2.1 | 0.3 | 2.3 |
| | 1900 | 4.4 | 1.2 | 0.3 |
| | 1900 | 0.2 | 0.3 | 0.3 |
| | 2200 | 4.4 | 1.3 | 1.2 |
| | 2400 | 3.4 | – | 0.3 |
| | 2600 | 3.4 | – | 1.2 |
| | 2900 | 3.4 | – | 1.2 |
| Residence 1 | 2100 | 12.9 | – | 1.8 |
| | 2500 | – | 3.5 | 2.8 |

Table D.2. Net intensity of secondary X-rays in additional produce samples.

| Soil | Vegetable | Tissue | Cr (Int) | Pb (Int) | Ni (Int) |
|---|---|---|---|---|---|
| Site 11 | Peanut | Nut | 1.031902 | 0.082997 | 0.983059 |
| Home Depot | Okra | Fruit | 0.362656 | 0.13434 | 0.810244 |
| Foundry | Okra | Fruit | 0.436709 | 0.336417 | 1.113889 |
| Foundry | Okra | Leaf | 0.477033 | 0.561727 | 1.166593 |
| Site 11 | Peanut | Leaf | 0.366246 | 0.69908 | 0.758822 |
| Foundry | Peanut | Leaf | 0.379745 | 1.265027 | 1.588249 |

## Appendix E: XRF Spectra and XRD Defraction Patterns

XRF spectra and XRD defraction patterns generated in this study is provided to Dr. Tim Grundl in the Department of Geosciences on a USB flash drive for archival purposes. The following folders are included on the flash drive: \\Appendix D - Raw Data

01 – WD-XRF Spectra\

02 – ED-XRF Spectra\

03 – Bruker Training PPT\

04 – Bruker Software\

05 – XRD Patterns\

The following files are included on the flash drive: \\Appendix D - Raw Data

PDZ Summary.xlsx

Pressed Pellet 2.xlsx

Pressed Pellet.xlsx

The following provides further explanation of folders and files on the flash drive.

**WD-XRF**

The WD-XRF software stores the results of the measurement routines as .ssd files that can only be read by proprietary software. A data-dump of .ssd files is provided in the folder "01 – WD-XRF Spectra" – please note this includes files not associated with this study. The names of the files correspond to the names of samples. A summary export from the Bruker software of produce samples analyzed between 8/19/14 and 2/18/19 using the "Pressed Pellet 2" routine (n=937) is provided in the Excel file "Pressed Pellet 2.xlsx". A summary export from the Bruker software of produce samples analyzed between 9/24/13 and 4/16/14 as part of the pilot greenhouse study (n=98) using the "Pressed Pellet" routine is provided in the Excel file "Pressed

www.manaraa.com

Pellet.xlsx." Both Excel files have a workbook named "Read Me," with further details on the files.

**ED-XRF**

The ED-XRF software writes the spectra to .pdz files, which can only be read by Bruker's proprietary software or by an add-on to Excel. The .pdz files associated with this study are stored in subfolders within the folder "02 – ED-XRF Spectra." These files are organized by folders describing the date the routine was completed (n=1,252 files in 18 folders). Please refer to the lab notebook for a description of each sample. Training PowerPoint slides from Bruker on using the ED-XRF and analyzing spectra are saved in the folder "03-Bruker Training PPT." Another excellent online training resource for working with these spectra is https://xrf.guru/. Software programs from Bruker used to read ED-XRF spectra are saved in the folder "04-Bruker Software." The spectra can be read by the program "S1PXRF." The spectra can be read and manipulated (e.g. basian deconvolution, peak matching, data export, etc.) in Buker's software package "Artex". The Excel add-on "S1CalProcess" reads, imports, and bins the .pdz files for development of custom calibration routines. Again, please see either the training PowerPoint slides or the online training resource for instructions on how to use S1CalProcess. Please note that more recent versions of Excel (e.g. version 365) may not be compatible with this add-on. A summary of the PDZ files with binned data is provided as "PDZ Summary.xlsx." The Excel file has a "Read Me" workbook with additional documentation.

**XRD**

The XRD software writes the diffraction patterns to .raw files which is then imported into another piece of software which is used to match peaks. After matching peaks, the file is then saved as an .eva file. The .raw and .eva files for the four soils are included in the folder "05-XRD Patterns" and can be read by the dedicated XRD computer in the geosciences X-ray lab.

Harris Byers

## Education

B.S. Science Education, University of Georgia, August 2000

M.S. Agronomy, University of Georgia, August 2004

Dissertation Title: Quantifying the variability in heavy metal concentrations in produce grown in

metals-rich soil

## Publications

Byers HL, Cabrera ML, Matthews MK, Franklin DH, Andrae JG, Radcliffe DE, et al. 2005. Phosphorus, Sediment, and Loads in Unfenced Streams of the Georgia Piedmont, USA. J Environ Qual 34:2293; doi:10.2134/jeq2004.0335.

Byers HL, McHenry LJ, Grundl TJ. 2016. Forty-Nine Major and Trace Element Concentrations Measured in Soil Reference Materials NIST SRM 2586, 2587, 2709a, 2710a and 2711a Using ICP-MS and Wavelength Dispersive-XRF. Geostand Geoanalytical Res 40:433–445; doi:10.1111/j.1751-908X.2016.00376.x.

Byers HL, McHenry LJ, Grundl TJ. 2019. XRF techniques to quantify heavy metals in vegetables at low detection limits. Food Chem X 1:100001; doi:10.1016/J.FOCHX.2018.100001.

Franklin DH, Cabrera ML, Byers HL, Matthews MK, Andrae JG, Radcliffe DE, et al. 2009. Impact of water troughs on cattle use of riparian zones in the Georgia Piedmont in the United States. J Anim Sci 87:2151–2159; doi:10.2527/jas.2008-1522.

## Certifications and Training

OSHA Hazardous 40 h Waste Site Worker Trained, National, US, 2014 (annual updates)

NIH CITI Training & NIH PHRP Training, National, US, 2014

Confined Space Entry, National, US, 2014

## Professional Memberships

National Brownfield Association

Geologic Society of America

Wisconsin Groundwater Association

Water Environment Federation

Federation of Environmental Technologists

**Professional Advisory Committees**

Wisconsin Department of Natural Resources Brownfields Advisory Committee

Wisconsin Department of Natural Resources PFAS Technical Advisory Group

**Select Professional Presentations**

"Quantifying Heavy Metals in Vegetables at Low Concentrations Using WD-XRF and ED-XRF", Denver X-Ray Conference, August 2019.

"What's in Vegetables Grown in Urban Soils?", Holistic Mothers in Milwaukee, March 2016.

"Navigating the Challenges of Brownfields Redevelopment," Federation of Environmental Technologists, Pewaukee, Wisconsin, October 2012, 2012.

"Brownfield Program Achievements Stimulated by the American Recovery and Reinvestment Act of 2009 in City of Wauwatosa, Wisconsin" USEPA National Brownfields Conference, Philadelphia, PA, April 2011, 2011.

"GIS in Identifying and Redeveloping Brownfield Properties: A Tale of Two Cities, USEPA National Brownfields Conference, Philadelphia, PA, April 2011, 2011.

"Phase I and II Environmental Site Assessments – Expectations and Limitations" Federation of Environmental Technologists, Pewaukee, Wisconsin, October 2010, 2010.

"Historic River Race Brownfield Assessment, Cleanup, and Redevelopment Planning, Goshen, Indiana" USEPA National Brownfields Conference, New Orleans, LA, November 2009, 2009.

**Professional Awards**

2013 USEPA Project Accomplishment Award, National Brownfields Conference, Tosa Yoga Studio, Wauwatosa, Wisconsin

2017 USPEA Project Accomplishment Award, National Brownfields Conference, Artist's Lofts, Manitowoc, Wisconsin

**Professional Project Narrative**

Mr. Byers has more than 15 years of professional consulting experience designing and managing investigation, remediation, and redevelopment projects at a wide variety of Brownfield properties. Harris has extensive experience in envisioning, preparing, and administering USEPA, State, Federal, and local Brownfield assessment, cleanup, planning, and research grants. Harris has prepared applications for and/or managed over $8,000,000 in Brownfield grant funded projects for a wide range of clients, including local units of government, research institutions, private developers, and local community-based non-profit organizations. As a direct result of strategic implementation of these grants, grantees have successfully leveraging over $100,000,000 in additional private redevelopment funds, local Brownfield redevelopment funds, state Brownfield redevelopment funds, and additional USEPA Brownfield grant funds. Harris has extensive experience in conducting environmental site assessments and completing environmental remediation projects at both large and small former/historic industrial properties located throughout the Midwest, including in Milwaukee. Harris has extensive experience collaborating with local, state, and federal agencies including State Departments of Natural Resources and Environmental Quality, Tribal Environmental and Natural Resource departments, Municipal Planning and Economic Development departments, USEPA, and university research faculty.